FORCED-CONVECTION SURFACE-BOILING HEAT TRANSFER

AND BURNOUT IN TUBES OF SMALL DIAMETER

by

ARTHUR EDWARD BERGLES

S.B., Massachusetts Institute of Technology
(1958)

S.M., Massachusetts Institute of Technology
(1958)

SUBMITTED IN PARTIAL FULFILLMENT

OF THE REQUIREMENTS FOR THE

DEGREE OF DOCTOR OF

PHILOSOPHY

at the

MASSACHUSETTS INSTITUTE OF TECHNOLOGY

May, 1962

Signature of Author . . . . . . . . . . . . . . . . . . .ʊ. . . . . . .
                    Department of Mechanical Engineering, May 25, 1962

Certified by  . . _ _ _ _ _ _ _ _ _ _ _ _ _ _ _ _ . . . .
                                                    Thesis Supervisor

Accepted by . . . . . . . . . . . . . . . . . . . . . . . . . . . . .
            Chairman, Departmental Committee on Graduate Students

FORCED-CONVECTION SURFACE-BOILING HEAT TRANSFER
AND BURNOUT IN TUBES OF SMALL DIAMETER

by

Arthur Edward Bergles

Submitted to the Department of Mechanical Engineering on May 25, 1962
in partial fulfillment of the requirements for the degree of Doctor
of Philosophy in Mechanical Engineering.

## ABSTRACT

A basic heat-transfer apparatus was designed and constructed for
the study of forced-convection boiling in small channels. The appara-
tus has also been used for related studies, such as burnout under stable
and unstable flow conditions and pool boiling.

The various regions of forced-convection surface boiling were stud-
ied experimentally and analytically. In the region of low wall super-
heat, the heat flux can be predicted by available correlations for
forced convection. Data indicate, however, that these correlations do
not properly account for the radial variation of properties for water
at high temperature difference. The conventional Dittus and Boelter-
McAdams relationship is recommended for design purposes on the basis
of its simplicity and conservative predictions.

An analysis for the prediction of the inception of first significant
boiling was developed. Experimental results are in good agreement with
analytical predictions. The analysis provides information necessary for
the prediction of the complete forced-convection surface-boiling curve.

The use of small-diameter tubes generally means operation at low
Reynolds numbers. It is shown that flow conditions in the transition
range of Reynolds numbers can be strongly influenced by the inception
of surface boiling. Data for a small-diameter tube indicate that the
bubbles formed at incipient boiling trip the laminar or transition
boundary layer to a fully-developed turbulent boundary layer.

The experimental results for comparison of forced-convection boil-
ing and pool boiling are inconclusive. The fully-developed region of
forced-convection surface boiling can be represented by a straight line
on the boiling plot. The effects of velocity and subcooling are negligi-
ble in this region. This region of vigorous boiling coincides approxi-
mately with the extrapolation of the pool-boiling curve in one set of
experiments. In other experiments, pool-boiling data were strongly influ-
enced by fluid and surface conditions, as well as by bubble-induced con-
vection in the pool. Due to the complexities in these pool-boiling data,
it is impossible to make a comparison with forced-convection-boiling data.

The heat flux obtained by a superposition of pool boiling and forced
convection is close to the apparent asymptote for fully-developed boiling.

For design purposes, it is concluded that fully-developed forced-convection boiling can be related to pool boiling by either direct extrapolation or superposition of forced convection.

The burnout heat flux under conditions of forced convection and surface boiling is shown to be a complicated function of subcooling at low values of subcooling. This appears to be due to the velocity increase caused by the relatively large volume fraction of vapor.

It is necessary to include geometry in the description of burnout for small channels. Burnout flux is shown to increase with decreasing tube diameter. This effect can be attributed to an increase in void fraction with decreasing tube diameter. Entrance effects are significant in forced-convection surface boiling as shown by the decrease of burnout flux with increasing length.

Flow oscillations caused by system compressibility can greatly reduce the burnout heat flux in the subcooled region. This instability is particularly difficult to avoid with tubes of very small diameter. Previously-reported studies of subcooled burnout in small channels indicated that the burnout flux decreases with decreasing channel height. However, it is believed that these data were obtained under unstable conditions. The data of the present study can be considered to indicate the actual dependence of burnout heat flux on diameter.


Thesis Supervisor:  Warren M. Rohsenow
Title:  Professor of Mechanical Engineering

# DEDICATION


To my father

EDWARD H. BERGLES

my first instructor

in mechanical engineering

# ACKNOWLEDGMENTS

This thesis was completed under the supervision of Professor Warren M. Rohsenow. His interest and encouragement have been invaluable in this work as well as in the development of my professional career. The research work was initiated by the late Professor Joseph Kaye who was an advisor and friend throughout most of my academic career.

Professor Peter Griffith served on the thesis committee and was very helpful in all phases of the investigation, especially in the analysis. Professors George A. Brown and S. William Gouse were also on the committee and gave generously of their time to discuss various aspects of the experimental program.

Mr. Lawrence Fried assisted in preliminary burnout studies. Mr. A. J. Hansen and Mr. E. B. Qvale provided capable assistance in operation and data reduction.

The personnel of the Department of Mechanical Engineering Shops and the Heat Transfer Laboratory assisted in construction details. The National Magnet Laboratory staff was especially helpful throughout the research program.

Miss Lucille Blake typed the final manuscript as well as numerous preliminary reports. Miss Nicki Nicholson took care of numerous details for the project.

My wife, Penny, has shared with understanding the daily tribulations of the project. Her encouragement and assistance have been invaluable.

This research was sponsored by the Massachusetts Institute of Technology National Magnet Laboratory. The Laboratory is sponsored by the Solid State Sciences Division of the Air Force Office of Scientific Research.

I wish to express my sincere thanks to all concerned.

TABLE OF CONTENTS

## TABLE OF CONTENTS
## (Continued)

## LIST OF FIGURES

LIST OF FIGURES
(Continued)

## SYMBOLS

$A$ = surface area

$c_p$ = specific heat

$D$ = diameter

$D_e$ = hydraulic diameter

$G$ = mass velocity

$h$ = enthalpy

$h$ = heat-transfer coefficient

$h_{fg}$ = heat of vaporization

$i$ = current

$k$ = thermal conductivity

$k'$ = thermal conductivity at $0$ $^\circ F$

$L$ = heated length

$L_p$ = pressure-tap length

$p$ = pressure

$q$ = rate of heat transfer

$q/A$ = heat flux

$(q/A)_B$ = heat flux due to bubble agitation

$(q/A)_{FC}$ = forced-convection heat flux

$(q/A)_0$ = heat flux at $(t_w - t_s) = 0$

$(q/A)_1$ = pool-boiling heat flux at incipient boiling

$(q/A)_2$ = heat flux at intersection of forced-convection and pool-boiling curves

$(q/A)_3$ = heat flux defined by Eq. (5)

$R$ = electrical resistance

$r$ = bubble radius

$T$ = absolute temperature

## SYMBOLS
## (Continued)

| | | |
|---|---|---|
| $t$ | $=$ | temperature |
| $T_g^*$ | $=$ | critical temperature defined by Eq. (15) |
| $t_{iw}$ | $=$ | measured inner-wall temperature |
| $t_{ow}$ | $=$ | measured outer-wall temperature |
| $V$ | $=$ | velocity |
| $V_s$ | $=$ | shunt voltage |
| $V_t$ | $=$ | tube voltage |
| $v$ | $=$ | specific volume |
| $w$ | $=$ | mass rate of flow |
| $y$ | $=$ | linear distance |
| $y_1$ | $=$ | laminar-sublayer thickness |
| $y'$ | $=$ | radius of bubble at incipient boiling |
| $n, C$ | $=$ | constants |
| $\alpha_k$ | $=$ | temperature coefficient of thermal conductivity |
| $\alpha_\rho$ | $=$ | temperature coefficient of resistivity |
| $\Delta t$ | $=$ | wall-minus-bulk temperature difference |
| $\Delta t_w$ | $=$ | temperature drop through tube wall |
| $\mu$ | $=$ | dynamic viscosity |
| $\nu$ | $=$ | kinematic viscosity |
| $\rho_e$ | $=$ | resistivity |
| $\rho_e'$ | $=$ | resistivity at 0 $^\circ$F |
| $\sigma$ | $=$ | surface tension |

## Dimensionless Groups

Nu     =   Nusselt number     =   $hD/k$

Pr     =   Prandtl number     =   $c_p \mu/k$

Re     =   Reynolds number     =   $GD/\mu$

St     =   Stanton number     =   $h/c_p G = Nu/PrRe$

## Subscripts

b     =   mixed-mean condition

BO     =   burnout condition

f     =   film condition

g     =   vapor condition

i     =   inlet bulk condition

$\ell$     =   liquid condition

o     =   outlet bulk condition

s     =   saturation condition

t     =   tube

w     =   condition at heat-transfer surface

# INTRODUCTION

Extensive investigations devoted to experimental and theoretical studies of boiling phenomena have been conducted during the past fifteen years. The study of boiling heat transfer has been an integral part of the development of nuclear reactors and rocket motors where exceedingly high heat fluxes are encountered. Forced convection cannot be used to obtain the high heat fluxes required due to the excessively high velocities which would be necessary. With subcooled nucleate boiling, high heat fluxes can be accommodated at much lower velocities and pressure drops.

Most research projects have concentrated on boiling at high pressures in order to meet the requirements of pressurized-water reactors and modern steam power plants. At pressures of the order of 2000 psia the wall temperature is not significantly different from the saturation temperature. Accordingly, the study of the peak heat flux in nucleate boiling has received the most attention.

With pressures near atmospheric, however, the wall-minus-saturation temperature difference with water is of the order of 100 °F, and it often becomes necessary to predict this temperature difference accurately. Such is the case, for example, in the design of high-field electromagnets utilizing boiling as the cooling mechanism. The electrical resistance of such common core materials as copper is very sensitive to temperature. Magnet power requirements are then strongly dependent on cooling-channel wall temperatures.

The efficient design of electromagnet and other high-performance cooling systems requires that channels of small cross section be used. Heat transfer and burnout for small channels have not been investigated in detail.

The first phase of this investigation is concerned with the prediction of heat transfer in small-diameter tubes under conditions of forced convection and surface boiling. The second phase is directed to the study of burnout in forced-convection surface boiling.

The construction and operation details of the experimental facility designed for this study are considered first. The data-taking and calculation procedures are also outlined.

## APPARATUS

A basic heat-transfer apparatus was designed and constructed for the study of forced-convection boiling in small channels.* The apparatus is suitable for related studies, such as pool boiling and burnout under stable and unstable flow conditions. A schematic of the system is given in Fig. 1, and a photograph of the general arrangment is presented in Fig. 2.

### Hydraulic

The piping is arranged about a test bench and tower constructed of Dexion slotted angles and plywood. All pipe and fittings are of stainless steel or copper-brass alloys for corrosion resistance. Imperial rayon-rubber hose is used for flexible connections, such as the pump inlet and outlet. High-pressure sections of the circuit are provided with thick-walled tube and pipe.

Water is circulated by a Fairbanks Morse two-stage regenerative pump providing a discharge pressure of 260 psi at 3.6 gpm. The pump is driven through a flexible coupling by a 3 HP Allis Chalmers induction motor. Special pump seals of asbestos and teflon were installed to avoid contamination of the system water. A relief valve set at 300 psi insures that the maximum-allowable pressure for the bronze casing will not be exceeded. A bypass is provided to aid in keeping sufficient flow through the pump.

---

*A preliminary apparatus was used with the power supplies and water system in the Building 4 Magnet Laboratory. Data taken with that system are not included, as tube surfaces were generally fouled due to improperly treated water. The description of the apparatus is, therefore, confined to the final apparatus constructed in the Heat Transfer Laboratory.

A 2.5 gal Greer accumulator pressurized with nitrogen serves to damp out pressure fluctuations due to the pump. A Jamesbury ball valve in the main line is used to regulate the pressure across the test-section line. A maximum pressure drop of 250 psi is available across the test-section line. A ball valve at the beginning of this line was used to further reduce the pressure fluctuations which caused the flowrater to indicate high due to float vibration. The two basic Fischer Porter flowrators are in parallel with appropriate shut-off valves.

The temperature of the water entering the test section can be controlled by a preheater consisting of a 5 KW Chromalox immersion heater in a tank fabricated of copper tube. The power to the heating element is regulated by a bank of two variacs mounted on the control-panel bench.

The fine regulation of the flow to the test section is accomplished by a Hoke metering valve. The valve requires 20 turns from open to closed position, and the position of the stem can be noted on the micrometer hand wheel. For burnout runs it was necessary to install an additional metering valve at the inlet to the test section as shown in Fig. 4.

The test sections were installed in the line by means of Conax or Swagelok fittings. Lines from the Helicoid test gauges were secured to the test-section pressure taps by Swagelok fittings. The inlet and outlet thermocouples were inserted directly into standard fittings by means of Conax adapters with lava sealants.

Another ball valve precedes the junction with the main line. This valve was used primarily to help adjust the pressure in the test section, but it was also useful in reducing back-pressure fluctuations during operation with net vapor generation. The steam would hit the cool water from the main line, causing severe cavitation as it condensed.

The heat exchanger is of the counterflow type; system water passes through the inner tube and city-water coolant flows in the annulus formed by the inner tube and a concentric outer tube. The exchanger was designed to dissipate 50 KW of heat furnished to the system water by the pump, preheater, and test section while maintaining a constant water temperature at the inlet to the preheater. During winter operation the system water could be cooled to less than 50 °F by the city water; whereas 80 °F was normal for summer operation. Except for these seasonal fluctuations, the city-water temperature and pressure were constant enough to allow steady-state operation. At high power input to the test section, a slight rise in the test-section inlet water temperature was noted.

A stainless-steel Fulflo filter was installed in the city-water line to keep impurities from reducing the performance of the heat exchanger. Periodic replacement of the filter cartridge was necessary due to the accumulation of rust. Another filter was provided at the pump intake to entrain any dirt, especially solder and pipe-joint compound, which found its way into the loop.

A stainless-steel pressure vessel fabricated for Boiling Project D.I.C. 6627[1*] was adapted for use as a degassing and expansion tank. The heaters in the tank totalling 12 KW were wired to the 110 and 220 VAC services and controlled by 5 switches on the control panel. The 4.7 gal capacity of the tank was adequate to provide make-up water for pump leakage and burnout loss for long periods of operation.

---

*Numbers denote References listed beginning on p. 88.

Distilled water was introduced into the system by using a small Hypro pump to raise the water to the 15 gal stainless-steel storage tank[1] from the standard 5 gal supply bottles. Steam heating was provided for this tank so that the water could be deaerated prior to filling. Preliminary degassing was, however, not often done as a general loop degassing was found more satisfactory after filling.

An ion exchanger[2] was adapted for the present system. Water was bypassed through a tank containing Rohm and Haas Amberlite mixed-bed resin. The distilled water was of conductivity about 0.7 ppm when added to the system but would go close to 5 ppm merely by sitting in the piping overnight. At this concentration of impurities, a heavy deposit was precipitated at the hot surface of the test section.* This condition was avoided by continuous use of the ion exchanger whereby the system water was reduced to less than 0.1 ppm as read on a conductivity meter made by Industrial Instruments, Inc.

## Power Supply

The power supply as shown in Fig. 3 consists of two 36 KW Chandeysson externally-excited generators, each rated at 12 volts and 3000 amperes. The generators are driven by 440 volt-3 phase-600 RPM synchronous motors. The M-G sets and control systems were installed for previous boiling projects, and only minor modifications were necessary to adapt them for the present operation.

A portable control console regulates generator power from zero to maximum as required. The generator outputs are connected in series, and the output from one generator is added or subtracted to the output of the second generator. Water-cooled shunts are installed in parallel

---

*The effects of such fouling are indicated in Fig. 30, where clean-tube data are compared with data for a fouled tube.

with each generator in order to take up the shock of an open circuit caused by burnout. The regulation is accomplished by a set of coarse and fine potentiometers. The control circuit was modified to increase the field strength so that a full 29 volts could be obtained as compared with the previous limit of 17 volts. A blower was also added to cool the resistors and potentiometers in the control console. A master stop button is provided for emergency use in shutting down the generator and pump. The coupling between the pump and generators can be taken out for pool-boiling experiments.

The existing buss-bar supply was extended to the test stand as shown in Fig. 4. The conductors feeding the test section consist of ten parallel braided-copper cables for each side. The use of braided cable permits considerable flexibility in installation of test sections. The cable assembly is clamped on the water-inlet side to a copper plate to which a brass test-section holder is fastened. On the outlet end, the connection to the test-section holder is made by braids with horizontal flexibility in order to allow for thermal expansion of the test section. The test-section holders were made from brass plate in two segments which clamped the test-section sleeve. The surfaces of contact were tinned with high-temperature soft solder to insure firm electrical connection from the test-section sleeves to the holders. The downstream end of the test section was connected to the main piping with rubber hose for reasons of flexibility and electrical insulation.

For pool-boiling experiments the test section was submerged in a Pyrex beaker on the bench. Copper bars secured to the power brackets

extended vertically into the pool where the test section was bolted on by means of brass fittings.

Instrumentation

Sensing devices and recording equipment are provided to monitor steady-state and transient conditions throughout the system. Pressure gages are installed as indicated in Fig. 1 to aid in adjusting the test-section pressure to desired values. A thermocouple is installed in the degassing tank to monitor water temperature during the degassing operation. A gage glass provides indication of the liquid level. A gage glass also indicates the water level in the storage tank. Replacement of the metering tubes and floats in the flowrators provides a range of test-section flows from 1.5 to 1300 $lb_m$/hr. Calibration curves giving mass flow versus scale reading are shown in Fig. 5. The units were periodically checked against the initial calibration.

The thermocouples at the test-section inlet and outlet were placed so that the water was well mixed at the point of temperature measurement. The outlet thermocouples were located sufficiently far downstream so that any steam bubbles in the liquid would have a chance to condense. In general, several outlet thermocouples were provided and the average reading taken to insure that the true mixed-mean temperature was measured. Fiberglass insulation was used from the thermocouple fittings to the test section to prevent heat loss or gain of the water.

Test-section pressures are measured by Helicoid 8-1/2 in. test gages with an accuracy of 0.25 percent of full scale. A 200 psi gage is used to measure upstream pressures, and a 100 psi gage measures downstream pressures. The gages were checked individually on a

dead-weight tester and were also compared with each other at various static pressures in the test-section line. Snubbers are provided to prevent any severe pressure oscillations from damaging the gage movements. For upstream pressure indication in cases where the bourdon-type gage caused unstable system operation, a Dynisco diaphram-type pressure transducer was used. The transducer signal was measured on the recorder.

All thermocouples were made of Leeds and Northrup 30-gage duplex copper-constantan wire. A calibration was performed; however, the deviations from the N.B.S. tables were not significant, and no correction was made to the readings. The method of installing thermocouples on the test section is described in a later section. Thermocouples are connected to a Leeds and Northrup thermocouple switch having 12 positions. The switch is in turn connected to an ice bath and to a selector switch which allows measurement of the signal on the potentiometer or recorder.

The potentiometer is a Leeds and Northrup Type K instrument with external standard cell and batteries. A Leeds and Northrup spotlight galvanometer completes the system. Signals from thermocouples, transducer, or shunt can also be indicated on a Minneapolis-Honeywell Brown recorder. This instrument is a pen-type single-channel recorder having manually-selected ranges for 0-6, 5-11, 10-16, 15-21, and 20-26 millivolts. This special design was ordered to give the best possible reading accuracy on the wide range of millivolt signals expected in this study.

The test-section current and voltage drop are measured to give the power dissipated by the test section. The current is also one of the

variables used in calculating the test-section inner-wall temperatures. Current is inferred from a reading of the voltage developed across a standard shunt. This shunt was calibrated and installed as indicated in reference 1. Spring clips were used to connect the voltage taps to the test-section bushings. A voltage-divider network was installed to scale down the voltage so that it could be read on the recorder or potentiometer. In general, however, voltage was read directly on a Weston multirange DC voltmeter as it was useful to have a visual indication of test-section power.

## Measurement of Tube-Wall Temperature

The most difficult problem in any heat-transfer experiment is the measurement of the temperature of the actual heat-transfer surface. The thermocouple cannot in any way be placed in direct contact with the tube wall. For the thin-walled tubes used in this study, the current flow would be disturbed in the vicinity of the measuring junction, and the correct surface temperature would not be recorded. Furthermore, with direct-current heating, the thermocouple would have impressed across it the voltage gradient at that point. The current would then have to be reversed to determine the thermal EMF alone.

Even if the correct surface temperature could be measured, a thermocouple at the heat-transfer surface would disturb the fluid flow, and the results would be misleading. The only solution then is to place the thermocouple wires on the wall opposite the heat-transfer surface and insulate the measuring junction from the wall. However, any electrical insulation between the thermocouple and the wall implies a thermal insulation which results in a temperature reading lower than that of the wall. A guard heater is then required to insure an adiabatic wall if the

thermocouple is located on the outside of the tube. If heat transfer takes place uniformly at the outside wall of a tube, a heater is not necessary as the thermocouple is placed at the inner surface which is adiabatic.

A heated shield was constructed from standard aluminum tubing. Threadlike grooves were cut into the outer wall of this tube. The shield sections were then black anodized to be electrically insulating. Nichrome wire was wrapped around the tube to serve as a heating element. Spacers fabricated from aluminum silicate served to hold the shield to the test section.

A layer of Scotch Electrical Tape No. 27 was wrapped around the tube at the desired location. The measuring junction was then bound radially around the tube with another layer of tape. Thermocouples were also taped to the inside of the shield. Sufficient lengths of all thermocouples were left inside the shield to avoid conduction errors. The space between the shield and tube was filled with asbestos fiber.

Power is supplied to the shields by a 110 VAC supply which is stepped down to about 25 V by a Stancor filament transformer. The power to each shield is controlled by a Powerstat. The arrangement permits fine control of each shield temperature.

Power to the shield is adjusted until the shield thermocouples and the tube-wall thermocouples within a shield section indicate approximately equal EMF. In order to reach equilibrium quickly, the variac is overshot in the direction of change and backed off quickly when the desired temperature is reached. The balancing operation can be followed easily on the recorder. There should be no temperature gradient across

the thermocouples when the two sets of readings agree. Tests performed in reference 1 indicated that outer-wall temperatures accurate to 1 °F should be obtained by this method. The use of several shield sections permits compensation for an axial temperature gradient. This gradient was, however, never found to be substantial.

The outer-wall temperature must be corrected for the gradient through the wall in order to obtain the wall temperature at the heat-transfer surface. The appropriate solution to the heat-conduction equation was given by Keith and Summerfield.[3] The tube was considered to be an infinite cylindrical resistor in which the electric power is dissipated at the inner wall and where the outer wall is adiabatic. The electrical resistivity and the thermal conductivity were considered to be linear functions of temperature. The equation solved by use of Taylor's series is given in Appendix B in its original form. The equation was put in terms of current instead of voltage gradient by Rohsenow, et al.[1] The equation was used in this form to compute the temperature drop through the tube wall for various values of outer-wall temperature and current. A check of the original solution indicated that the only modification required for the case where the power was dissipated at the outside wall was a change in sign of the second term in the series. This solution was also noted by Clark.[4]

Evaluation of the tube-wall temperature drop required accurate information on the tube dimensions, resistivity, and thermal conductivity. The dimensions of the commercially-drawn tubes used in this study are given in Appendix A. Test sections were measured in a variety of ways depending on the size. The outside diameter could, of course, be measured for all tubes. The wall could be measured with a pin

micrometer only for the nickel tubing. For the smaller tubes, a certain length of tubing was weighed and the inside diameter inferred from outside-diameter measurement and the density. Tubes were also filled with mercury, and the average inside diameter was inferred from the weight of the mercury. In general the manufacturers' mean dimensions were closely adhered to.

All necessary property and temperature-correction information was available for the nickel tube which had been used in previous boiling projects. This information was not available for the stainless-steel tubes which were used in most of the experiments. Thermal-conductivity data for 304 stainless were considered reliable and as indicated in Fig. 6 were taken from references 5 and 6. As only approximate agreement was found among available sources regarding the resistivity of 304 stainless, the temperature dependence of the resistance for a sample length of each of the several tube sizes was measured.

The resistance of the sample was compared with a standard resistance in the bridge circuit described more fully in reference 1. A small electric furnace was used to maintain the tube at uniform temperature. The resistivity was readily calculated from the relationship $\rho_e = R_t A_t / L$. No allowance for the change in dimensions due to thermal expansion was necessary. The resistivity is indicated in Fig. 7; for comparison, resistivity curves from several sources are included. It is noted that the smaller-size tube has a higher resistivity although the metallurgical composition for the two sizes is identical. The cold-drawing of small tubes from larger ones probably accounts for this effect.[9]

The temperature-correction curves for the stainless-steel tubes are indicated in Figs. 8 and 9. All computations were done with a desk

calculator. Some iteration was required as the mean resistivity $\rho_e$ is based on the temperature drop through the wall. Generally, however, the solution was obtained on the second or third iteration.

## Test Sections

Three types of test sections were fabricated in order to study forced-convection boiling and burnout. Two additional test sections were assembled for pool-boiling studies which were informative in interpreting the boiling data taken under conditions of forced convection. The tubular sections represent the geometries used in many practical applications. The various test sections used in this study are shown in Fig. 10.

### a. Tubular

The basic tubular design incorporated power-supply and pressure-tap provisions. Holes were drilled into the tubes with a 6 mil pivot drill. Jigs were provided to hold the tubes and guide the drill. Brass plugs were inserted into the tubes so that the drill would cut through the wall cleanly instead of breaking through and leaving a jagged edge. The static holes were kept as small as practically possible to avoid disturbing the flow.[10] Even the 6 mil holes would plug up with small dirt particles during fabrication or even during operation.

Brass bushings were cut from 7/16 in. round stock. Holes were drilled for the test section and for the 16 ga needle tubing which was used for the pressure taps. The tap holes in the bushings were lined up with the holes in the tube wall. The bushings were then sweated to the tube with silver solder or high-temperature soft solder. A minimum amount of solder was run into the joints to keep the static holes from

plugging up and to keep the fillets to a nominal radius. The taps were then soft soldered to the bushings by building up fillets rather than sweating which might again plug the static holes.

b. Annular

The annular test section consisted of a piece of 16 ga stainless-steel tubing centered inside a 5 mm Pyrex tube. A length of bored-out 1/8 OD copper tubing was sweated to the stainless tubing at either end. Power was supplied to brass bushings sweated to the outer ends of these copper sleeves. As the resistance of the copper sleeves was negligible compared to the stainless tubing, the heated length was defined by the length of tubing between the copper sleeves. Pyrex tubing cut approximately equal to the heated length was centered around the stainless tubing by means of clips made from copper wire. A static-pressure hole was drilled through the glass tubing at the axial position desired for local heat-transfer measurements. The holes of approximately 15 mil diameter were drilled ultrasonically by Clendenning Smith Company, Watertown.

The pressure-gage hose was then secured to the tap by means of a clamp. A thermocouple with an insulated measuring junction was inserted inside the stainless tube. The annular assembly was mounted in standard crosses by means of Conax fittings. Teflon sealants were provided at the copper sleeves to permit thermal expansion. Thermocouples and water connections completed the arrangement. The Pyrex tube made for a rather delicate assembly, and special supports were necessary for mounting in the buss-bar clamps.

c. Pool-Boiling

A pool-boiling test section was made of 16 ga stainless tubing to compliment the annular apparatus. A section was cut from the same stock

used in the annular assembly and soldered to brass blocks. A thermo-
couple with the measuring junction insulated with Teflon tape was
inserted inside the tubing. Leakage of water into the tube was pre-
vented by soldering one end and sealing the thermocouple end with epoxy.
The assembly was secured to the vertical buss-bar extensions and sub-
merged in a large beaker. An additional thermocouple was provided for
measurement of the pool bulk temperature.

Pool-boiling test sections were also prepared from tubes used in
forced-convection boiling. Tube lengths were cut down to approximately
half-cylindrical size by milling. Brass blocks for power connections
were soldered to either end. Thermocouples were bound to the insulated
outside surface by Teflon tape. This assembly was then cemented with
high-temperature epoxy to a guard heater of semi-circular form as shown
in Fig. 10. The guard heater was sealed with Dow Corning Silastic RTV
silicone-rubber insulating material. Boiling took place from the inside
surface of the cut tube, and shield power was adjusted in the usual way
to insure an adiabatic outer wall.

Only the test sections made from 0.18 in. OD nickel tubing could
be used for pool boiling at atmospheric pressure. The bubbles formed
at incipient boiling are of the order of 1/8 in. diameter at atmos-
pheric pressure. These large bubbles occupied the entire cross sec-
tion of a small tube and became attached to the edges. Instead of grow-
ing and departing, these bubbles grew axially and insulated the surface.
Burnout then ruined the test section at a very low heat flux.

### DETAILS OF OPERATION

Distilled water was pumped from the commercial 5 gal containers
into the storage tank. The system was then filled by gravity and

drained out to remove any accumulated dirt. Vents at the flowrators
and the ion exchanger as well as most valves were opened for the final
filling. The degassing-tank vent was always open. The other vents
were closed in turn as water poured out. The system was essentially
full when water poured out of the main vent. Momentary circulation
with the pump removed any remaining air pockets.

The valve to the ion exchanger was then closed, as water above
140 °F would ruin the crystals in the bed. All degassing-tank heaters
were turned on, and water was circulated through the system. Water
was bypassed into the degassing tank when the water in the tank was
near boiling. With violent boiling, considerable pressure was built up
in the tank with the result that water was pumped out. This condition
was avoided by regulating the tank heaters and the bypass valve. The
tank thermocouple and the gage glass were useful in estimating when
such control was needed. The various system valves were opened and
closed to loosen any small air pockets. The system water was effec-
tively degassed by being dumped into the vigorously boiling water
at the top of the degassing tank. About 20 minutes of degassing in
this manner was sufficient to reduce the dissolved gas to a negligible
amount. The standard Winkler analysis outlined in Appendix C indicated
air contents of approximately 1.5 cc air/liter. The tank heaters were
then shut off, and the heat exchanger turned on. The tank bypass valve
was closed as soon as steam ceased to come from the tank vent.

Degassed water was then circulated through the ion exchanger, and
the accumulator was filled. More water was then added to the system,
and the degassing procedure was repeated. The system was then ready
for operation. Degassing was performed whenever a new test section was

installed or makeup water was added from the supply tank. It was also necessary to degass periodically as the expansion tank was vented to the atmosphere, and the water in the tank would eventually become saturated with approximately 20 cc air/liter.

The system was operated for at least 30 minutes at zero power level before beginning any heat-transfer measurements. The system water was then cooled down and was thoroughly circulated through the ion exchanger. The generators were also given a chance to warm up during this period.

When using nickel test sections, one of the power leads was usually disconnected when starting the generators. This was necessary as the generators would not come up to full speed in unison, and a potential of several volts would momentarily exist across the test sections. This provided considerable power input with the low-resistance nickel sections and even caused burnout on several occasions. The original control circuit contained starting resistors set to give a zero voltage output; however, these were apparently taken out by successive users.

The only shut-down precaution was to lock out the accumulator before turning off the pump. This prevented the water from being forced out of the accumulator and eventually out of the system through the degassing-tank vent. The pump is electrically connected with the generators so that the generators are shut down if the pump power fails or is shut off. The generators can, however, be shut off separately by a switch on the control console.

The amount of data recorded varied with the type of test section. In general the flow and pressure level were established, and the power level was varied. The power to the guard heater was continually adjusted to maintain an adiabatic outer wall opposite the wall thermocouple

locations. The inlet and outlet pressures were recorded. Also recorded were the EMF's of the inlet-and outlet-water thermocouples and the wall thermocouples. The shunt voltage was recorded, and the reading of the voltage drop across the test section was taken from the voltmeter. All millivolt readings were taken on the potentiometer unless fluctuations made it necessary to average the signal from the recorder trace. Power measurements were taken before and after the wall temperatures were recorded. This was necessary due to the considerable DC ripple in the generating system. Power fluctuations were also due to turbulence in the test section, especially in the transition region. The variation of the heat-transfer coefficient caused a change in wall temperature due to the low thermal capacity of the wall. The resulting fluctuation in tube resistance caused oscillations in the power. This was especially noticeable in the low-resistance nickel tubes.

In general, data for a particular operating point could be taken within 15 minutes. Most of the time would be spent adjusting the temperature of each guard heater.

Burnout was approached by increasing the power at constant flow rate. The shunt voltage was indicated on the recorder and test-section voltage was noted on the voltmeter. The flow was adjusted as required due to changes in the hydraulic resistance of the test section.

Burnout data consist of those data recorded just subsequent to the physical destruction of the test section. When burnout occurred the generators and pump were shut off, and the test-section line was isolated from the rest of the flow system. Before securing the fittings on the replacement test section, water was allowed to leak from both directions. This insured that a minimum of air would be entrained in the system.

DATA REDUCTION

## Calculation Procedure

The calculation procedure was formalized to allow for efficient reduction of the numerous data taken during the study. Sample calculations for non-boiling and boiling runs are shown in Appendix D. In all cases the axial temperature gradient was not large enough to cause local variations in the heat flux. This was convenient as it allowed several independent measurements of the heat flux. The heat-transfer rate was calculated from

$$q = w(h_o - h_i) \tag{1}$$

where the enthalpies were evaluated from the measured inlet and outlet temperatures. The heat-transfer rate was also given by

$$q = V_t i \tag{2}$$

where the voltage across the tube was measured directly with the voltmeter, and the current was inferred from the shunt voltage. Finally, the heat-transfer rate was calculated from

$$q = i^2 R_t = i^2 \rho_e L/A_t \tag{3}$$

where the electrical resistivity was interpolated from the measured data at the mean radial wall temperature. Excellent heat balances were obtained; the values of the heat input as calculated from the above equations differed by 5 percent at most. The heat flux was obtained by averaging the three rates of heat transfer and dividing by the heat-transfer area. The heat-transfer area was defined by the section of tube between the inlet and outlet bushings. Fillets from the soldering operation were considered part of the bushings. The

heat balance verified that the bushings themselves contributed negligible heat to the water.

Due to the uniform q/A, it was possible to consider a linear increase in the bulk temperature from inlet to outlet.

The pressure was also assumed to vary linearly from inlet to outlet. The pressure taps were located close enough to the heated section so that the pressure drop in the small lengths of unheated section could be considered part of the heated-section pressure drop. This assumption is reasonable in view of the moderate pressure drop in the test sections.

No data were taken at very low values of subcooling where the void volume at the tube exit becomes significant. Under these conditions most of the pressure drop can be expected to occur over the last portion of the tube. The assumption of linear pressure drop is then obviously no longer valid. In practice a run was terminated when the pressure drop increased appreciably. This precaution also avoided premature burnout due to flow oscillations which is discussed in the section on burnout.

The temperature of the heat-transfer surface was obtained by subtracting the appropriate correction from the measured outer-wall temperature.

The values of thermal conductivity and viscosity for water were taken from McAdams,[6] and specific heat was taken from Eckert and Drake.[11] The surface tension was taken from Dorsey.[12]

## Accuracy of Results

The greatest uncertainty lies in the determination of the temperature of the heat-transfer surface. With the smaller tubes the measuring junction of the thermocouple was placed circumferentially around a

considerable portion of the tube. This tended to eliminate error due to flow stratification and wall-thickness variation. It is noted that the temperature drop given by equation (B1) is a strong function of the resistivity and thermal conductivity. As noted, the resistivity was measured for each size tube and found to be well represented by a straight line. Unfortunately the thermal conductivity could not be obtained experimentally for the various tubular sections used. Published data were, therefore, used to obtain the temperature variation of this parameter. It was noted that the resistivity depended somewhat on tube size and in all probability the thermal conductivity follows the same trend. In view of the difficulty involved in estimating the magnitude of this effect, the available data were used as is.

The geometric terms in the wall-temperature correction are less of a source of error than the items mentioned above. Even with the worst combination of nominal dimensions and tolerances listed by the manufacturer, the percentage variation in $\Delta t_w$ was found to be of the order of only one percent. Of course, actual dimensions were used; however, slight variations in outside diameter and wall thickness occurred for any piece of stock.

The larger nickel tubes were instrumented with thermocouples at the top and bottom of the tube. The readings were then averaged to get the local value of the outer-wall temperature. In general the upper-wall temperature was higher than the lower-wall temperature at the low flow rates. This temperature stratification was also noted with large tubes by Kreith and Summerfield[13] who attributed it to the effect of gravity.

In any case the estimate of error in the temperature is simply an educated guess; however, $\pm 5$ °F seems reasonable. It is noted that the

maximum error in $\triangle t_w$ will occur simultaneously with the maximum $(t_w - t_s)$ at the highest flow rate.

The heat flux as obtained from the average of three values is considered to be within $\pm$ 2 percent. The error in the increase in enthalpy of the water from inlet to outlet is then of the same order.

The local pressure should be well within one percent even if errors due to improperly-drilled pressure taps are considered.

## CHARACTERISTICS OF NUCLEATE BOILING

The study of boiling heat transfer began in 1926 when Mosciki and Broder[14] conducted experiments wi.. ε.. electrically-heated wire submerged in a tank of water. Boiling heat transfer cannot be predicted by the usual formulations derived for forced convection. In addition, it is influenced by many minor variables. As a consequence it has become customary to represent the heat transfer by the boiling curve. The heat flux is plotted versus the wall-minus-saturation temperature difference which has been found to be the governing temperature difference in boiling. The prediction of the boiling curve for a particular system has been the object of boiling researchers ever since the first boiling curve was obtained by Nukiyama[15] in 1934.

The regimes of boiling are indicated in Fig. 11 for a specified fluid-surface combination and constant pressure.

### Pool Boiling

Consider first the boiling curve for saturated pool boiling. As the wall temperature rises above the saturation temperature in the region A-B, convection currents circulate superheated liquid, and evaporation occurs at the surface of the pool. As the wall temperature is increased further to B, bubbles form at active nuclei on the heating surface. These bubbles rise through the pool transferring steam to the vapor space. The growth and departure of bubbles at the surface augments the heat transfer, and the $(q/A)$-versus-$(t_w - t_s)$ curve changes slope in the nucleate-boiling region. The slope of the curve then decreases, and the heat flux goes through a maximum as the heating surface is partially covered with vapor bubbles.

Beyond the peak of the curve in region C-D, an unstable film forms around the wire. Under the action of circulation currents, this steam film collapses and reforms rapidly. The partial vapor film provides additional resistance to heat transfer, and the heat-transfer rate decreases as the temperature difference increases. In the film-boiling region D-E, heat is transferred through the film covering the surface by conduction and radiation.

If the temperature difference is the dependent variable as with electric heating, operation at C is unstable, and the system will proceed toward region E'. The temperature at E' is generally above the melting point for most metals. For this reason point C is referred to as the burnout point.

The above description applies, with minor modifications, when the bulk liquid is subcooled. Surface or local boiling occurs when a liquid below saturation is brought into contact with a heating surface hot enough to cause boiling. The vapor bubbles collapse at the surface or break loose and condense in the cold liquid.

In the region A-B the curve for subcooled pool boiling obeys the usual law for natural convection. The behavior of the subcooled-pool-boiling curve in the nucleate-boiling region is, however, not well established. It is indicated here as simply merging with the nucleate-boiling curve for saturated pool boiling. As shown, the burnout heat flux is appreciably raised when the bulk liquid is subcooled.

Forced-Convection Surface Boiling

Numerous experiments have been performed to obtain data for surface boiling under conditions of forced convection. Flow normal or parallel

to wires or tubes has been considered as well as flow inside tubes. The general characteristics are shown in the upper portion of Fig. 11. At low $(t_w - t_s)$, where the heat transfer is governed primarily by forced-convection, the heat flux increases at constant $(t_w - t_s)$ as the velocity is increased. This effect was clearly shown by Kreith and Summerfield[13] and Rohsenow and Clark.[16] It has been argued by Rohsenow[17] that subcooling has a similar effect. In the limit at zero wall superheat, $t_w = t_s$, the heat flux should be predicted by forced convection.

$$(q/A)_0 = h \, (t_w - t_b) = h \, (t_s - t_b) \tag{4}$$

It is noted that as the subcooling increases, h decreases; however, the net effect can still be expected to increase the heat flux. It is believed that no data have been published which clearly indicate the effect of subcooling in forced-convection surface boiling. The effect of pressure and subcooling are frequently lumped together as in the presentation of Kreith and Summerfield. It is well known that the boiling curves shift to the left with increased pressure.

Considerable wall superheat is required before boiling is initiated. This has been studied quite extensively in connection with pool boiling; however, little work has been done on the prediction of incipient boiling under conditions of forced convection.

Most work in forced-convection surface boiling has concentrated on the "fully-developed" region of the boiling curves. In this region the effects of velocity and subcooling disappear and the boiling curves appear to merge into a line. The data have been shown by McAdams, et al.,[18] Buchberg, et al.,[19] and Jens and Lottes,[20] among others, to be represented by a straight line in the fully-developed-boiling region. The data from

these experiments as presented do not indicate the transition region, or knee of the boiling curve, which is always present between incipient boiling and fully-developed boiling.

The plot of McAdams et al.[6] showing the heat flux versus temperature difference has been accepted as a standard for many years. However, this plot is misleading in certain respects as it does not include all of the data taken for the pertinent runs. An effort was made to separate out the effects of velocity and subcooling using the original data. Plotted in Fig. 12 are data for 60 psia and 1, 4, and 12 ft/sec. Values of subcooling from 20-150 °F are indicated. Several test sections were used; however, they were cut from the same tube, and identical cleaning procedures were used. The trend of velocity and subcooling as discussed above appears to be indicated by the data points which were omitted from the published plot. It is also apparent that there is no significant effect of either velocity or subcooling in the fully-developed-boiling region.

## Design Procedures

Commonly used design procedures for forced-convection surface boiling are indicated in Fig. 13.

McAdams, et al.[18] considered the boiling curve to consist simply of the forced-convection curve and a fully-developed-boiling curve. A transition point was defined as the intersection of the two curves. At heat fluxes higher than the transition flux, the fully-developed-boiling curve is to be used. In a preceding publication for this project Kennel[22] noted that the transition point may not necessarily be the point at which first vapor is formed. Although the similarity between the fully-developed-boiling curve and the pool-boiling curve was mentioned,

it was not claimed that forced-convection-boiling data were directly related to pool-boiling data for a particular system.

It is generally assumed that the fully-developed region of the boiling curve coincides with the extrapolation of the pool-boiling curve.[23] This explanation is physically reasonable at least at low velocities. However, no data have been found which support this assumption. A design criterion based on this assumption was proposed by Engelberg-Forster and Greif.[24] The non-boiling forced-convection correlation and the pool-boiling correlation for the particular fluid and surface are required. The intersection of the two equations gives a heat flux $(q/A)_2$. An empirical relation is then used to locate the point where the boiling curve is essentially the same as for pool boiling.

$$(q/A)_3 = 1.4(q/A)_2 \tag{5}$$

The region between incipient boiling and $(q/A)_3$ is represented by a straight line. It is not made clear, however, how the point of incipient boiling is determined.

An alternative design procedure suggested by Rohsenow[17] is the only procedure which realistically attempts to account for the combined effects of forced convection and nucleate boiling in the transition region. Rohsenow considers the total heat flux to be given simply by a superposition of the heat flux due to bubble motion and forced convection.

$$(q/A) = (q/A)_B + (q/A)_{FC} \tag{6}$$

The forced-convection term is the heat flux that is predicted by the applicable forced-convection correlation at the particular flow conditions. The effect of bubble motion is given by the correlation for

saturated pool boiling for the particular fluid-surface combination. The influence of velocity and subcooling is included in the forced-convection term. It is seen that the velocity and subcooling curves will merge with the pool-boiling curve only at relatively high heat fluxes where the forced-convection heat flux becomes very small compared to the total heat flux. Implicit in the method is the assumption that at low values of wall superheat, the pool-boiling term is negligible, so that the total heat flux is essentially accounted for by forced convection.

Data of Rohsenow and Clark,[16] Clark and Rohsenow,[25] Kreith and Summerfield,[13] and others were analyzed to test this method. In all cases the points representing $(q/A)_B$-versus-$(t_w - t_s)$ could be approximately correlated by a straight line. The slope was approximately three for commercially-prepared surfaces, and the intercept varied with fluid and surface. Both slope and intercept compared favorably with pool-boiling data; consequently, the $(q/A)_B$-versus-$(t_w - t_s)$ plots were called the pool-boiling curves for the particular fluid-surface combinations. Actual data for saturated pool boiling were, however, never taken.

An interesting approach to the correlation of forced-convection surface boiling has been presented by Bernath and Begell.[26] These investigators analyzed data taken with annular test sections in the Columbia boiling project. Most data appear to have been taken in the transition region which was denoted as the "region of fully-developed local boiling" in that paper. In plots of wall superheat versus subcooling at constant velocity and heat flux, the data were found to lie in two regions. The first region is where wall superheat is independent of subcooling; this is apparently the region of fully-developed boiling.

The second, however, is a region where the wall superheat decreases linearly with increasing subcooling. This linear dependence is unusual and must be due, at least partially, to the variation of pressure within the data. Furthermore, it is implied that the wall superheat at fully-developed boiling is independent of pressure in the range 25-150 psia. This is at variance with the views of most investigators. One of the crossplots indicates that the wall superheat at the inception of fully-developed boiling decreases with increasing velocity. This also seems unreasonable.

In any case the design procedure developed by Bernath and Begell for predicting wall superheats is too involved to be put to practical use. It must be noted that it should be successful in predicting the Columbia data since these data were used in evaluating the various functional relationships constituting the correlation.

## Scope of Heat-Transfer Studies

The preceding discussion has indicated several areas in forced-convection surface boiling that have not been investigated in detail. The effect of subcooling has not been clearly noted in the region of low wall superheat. The point of incipient boiling has not been considered adequately. The relation of the fully-developed-boiling region to pool boiling has not been clearly established. As a result several design procedures are recommended which predict different boiling curves for the same conditions.

In addition, the study of heat transfer in subcooled boiling with forced convection has been confined to channels of relatively large hydraulic diameter. The smallest channels used for heat-transfer studies are apparently the 0.18 in. tubes of references 16 and 19. It is not

clear whether the results obtained from studies with large channels can be safely extrapolated to small channels.

These areas are considered in the following discussion of the heat-transfer experiments conducted in this study. The regions of forced-convection surface boiling are considered in the following order:  region of low wall superheat, incipient boiling, and transition and fully-developed boiling.

## THE INFLUENCE OF TEMPERATURE DIFFERENCE ON THE
## TURBULENT FORCED-CONVECTION HEATING OF WATER

### General

It has been noted that a considerable wall superheat may be required before boiling is initiated under conditions of forced convection. It follows that heat transfer at low wall superheat can be correlated by the expressions developed for non-boiling forced convection. It is apparent, however, that under these conditions the wall-minus-bulk temperature difference $\Delta t$ will be higher than that normally encountered in ordinary heat-transfer equipment. In addition, when predicting the curve for forced-convection surface boiling, the forced-convection correlation employed will be extrapolated to very high values of $\Delta t$. It is thus necessary to examine in detail the influence of $\Delta t$ on the forced-convection heating of water.

Three of the more widely accepted correlations of forced-convection turbulent flow in tubes are the following:

Colburn:[27]

$$(h/c_{p_b} G) \, (\mu_f \, c_{p_b}/k_b)^{2/3} \;=\; 0.023/(GD/\mu_f)^{0.2} \tag{7}$$

Sieder and Tate:[28]

$$(h/c_{p_b} G) \, (c_p \mu/k)_b^{2/3} \, (\mu_w/\mu_b)^{0.14} \;=\; 0.027/(GD/\mu_b)^{0.2} \tag{8}$$

McAdams:[29]

$$(h/c_{p_b} G) \, (c_p \mu/k)_b^{0.6} \;=\; 0.023/(GD/\mu_b)^{0.2} \tag{9}$$

The subscripts refer to the temperature at which the particular fluid property is evaluated; w refers to wall temperature, b to bulk or mixed-mean fluid temperature, and f to a film temperature defined by $(t_w + t_b)/2$.

These equations are for heating or cooling of various fluids and include
the effect of temperature-dependent properties. They correlate the data
for moderate $\triangle t$, Reynolds number $(GD/\mu) > 10^4$, Prandtl number
$0.5 < (c_p\mu/k) < 120$, and heated length-to-inside diameter ratio $L/D > 60$.
The form of equation (9) was first proposed for the heating of various fluids
by Dittus and Boelter.[30]

Air data at high $\triangle t$ have been correlated by a modified form of equa-
tion (9);[31] however, it appears that no systematic data have been reported
which consider the effect of $\triangle t$ on the heating of liquids. McAdams[6] recom-
mends either equation (7) or (8) for extrapolating results for liquids to
high $\triangle t$. Al-Arabi[32] examined the data of several observers for the turbu-
lent heating of water and found that the results for low $\triangle t$ and moderate
$\triangle t$ had to be treated separately for good correlation. Heat-transfer
coefficients were computed on an average basis, and the highest $\triangle t$ was
approximately 80 $^o$F. The data considered were too limited to enable a
complete study of the effect of $\triangle t$. Owens and Schrock[33] took data for
forced convection of water at the inception of surface boiling. These
investigators considered incipient boiling to be the intersection of the
forced-convection and fully-developed-boiling curves. Their data were
consistently below the values predicted by the correlations of equations
(7) to (9). Kreith and Summerfield[13] correlated non-boiling data at high
heat fluxes by equations (8) and (9). The use of a short test section
and high system pressure permitted very high $\triangle t$. The data were too few
to check the influence of $\triangle t$ on these correlations. Furthermore, the
average heat-transfer coefficients used in that study are somewhat mis-
leading as entrance effects are included.

## Experimental

As available information appeared inadequate to predict forced-convection heat transfer at high $\triangle t$, initial experiments were made in this area. Heat-transfer measurements were made for the heating of water in a smooth 0.094 in. ID stainless-steel tube. A calming section of 2.5 in. preceded the heated section. Outer-wall temperature measurements were made at an L/D of 70. Pressure measurements were taken to insure that no data were taken under conditions of surface boiling. The pressure level was approximately 75 psia.

In the experiments the heat flux was varied at constant mass velocity G to provide a considerable temperature variation. For example, for $G = 5.56 \times 10^6$ $lb_m$/hr ft$^2$, $\triangle t$ varied from 24 - 160 °F, $t_b$ from 71 - 140 °F, and $t_f$ from 83 - 221 °F. A higher pressure level as well as a lower inlet temperature would have been needed to increase the range of these variables.

The results indicated in Fig. 14 give the left-hand side of equations (7) to (9) versus the appropriate Reynolds number. All data lie within the scatter of the original correlations which is usually considered to be $\pm$ 30 percent. The values of the experimental constants differ somewhat from those in equations (7) to (9); for example, the constant based on the correlation of equation (9) is 0.026. This constant was found to change slightly with tube diameter and material indicating a probable roughness effect. The constant is substantially lowered[16] for water at high pressure indicating that the variation of fluid properties with pressure is important. The fact that the results of reference 33 have lower constants than the present data can be explained at least partially by roughness and pressure-level considerations.

The radial variation of properties causes the data to diverge with respect to the correlating line as $\triangle$t is increased. In the case of the McAdams correlation, the predicted heat-transfer coefficients would be quite conservative at high $\triangle$t. The Colburn and Sieder-Tate equations attempt to correct for radial property variation by considering the wall temperature as well as the bulk temperature in the evaluation of properties. It is seen, however, that these correlations overcorrect for the property variations, and the predicted heat-transfer coefficients are optimistic at high $\triangle$t.

A better correlation of the radial property variation could be found which would cause all points to fall in a straight line; however, the correlation would be of limited general interest as it would depend on how the properties vary with temperature. The data of this study indicate that there is no great error introduced by assuming conventional correlations valid for low-temperature water at high $\triangle$t. The relationship of equation (9), however, appears desirable as it is the simplest to use and is on the conservative side.

On the basis of this study, it was decided to use the relationship of equation (9) for the turbulent forced-convection heating of water. A further refinement was to use the exact correlating line at constant mass velocity for extrapolation into the wall superheat region.

## FORCED-CONVECTION SURFACE BOILING AT

## LOW WALL SUPERHEAT

Experiments with large L/D tubes are generally restricted to low heat fluxes if bulk boiling is to be avoided. This usually limits boiling tests to the region of low wall superheat. However, the longer tubes are better suited for investigating this region where forced convection is important. Entrance effects are reduced to a minimum, and it is also practical to monitor several axial positions to obtain data for several values of subcooling at a single power setting.

Data for a 0.0465 in. ID stainless-steel tube of heated length 5.0 in. and calming length 1.25 in. are indicated in Figs. 15 and 16. Two guard-heater segments were used, and wall-temperature measurements were taken at 50 and 80 L/D. Mass velocities of 2.46, 6.23, and 12.72 $lb_m$/hr ft$^2$ were investigated. These mass velocities correspond to inlet velocities of 11, 28, and 57 ft/sec. It is seen that forced-convection data from both stations are well correlated for $Re_b > 10^4$; however, the data for lower Reynolds numbers exhibit considerable scatter. These low-velocity data are characteristic of the transition region which is generally considered to be in the range $2300 < Re < 10,000$.

As shown on the boiling plot, data in the region of wall super-heat are very regular for the two higher velocities. As the pressure decreases and bulk temperature increases axially, the subcooling for station 2 should always be lower than that for station 1. Lines of constant subcooling are sketched in and are seen to be asymptotic to the heat flux predicted by the forced-convection correlation at zero wall superheat.

The data for the low velocity are very complicated due to the transitional character of the flow. The wall temperature at station 2 is generally higher than that at station 1 in contrast to observations at higher velocities. There is also considerable scatter, although the usual increase in slope from forced convection to fully-developed boiling is evident. Wall temperatures fluctuated considerably, and it was necessary to read most values of thermocouple EMF from the recorder rather than the potentiometer.

Similar data for a 0.094 in. ID stainless-steel tube of heated length 5.48 in. and calming length 2.5 in. are given in Figs. 17 and 18. Outer-wall temperatures were measured at 29 and 48 L/D.

In Fig. 17 it is seen that for Re $> 10^4$, data for the lower L/D lie slightly higher than the data for the higher L/D although the correlating lines have similar slopes. The higher heat transfer appears to be due to an entrance effect. An analysis by Deissler[34] and experiments by Hartnett[35] indicate that a length of 15 diameters brings the local heat-transfer coefficient approximately equal to that reached asymptotically in a long tube. However, this holds only when the flow is fully developed and turbulent at the beginning of the heated section. The calming length for this tube was probably inadequate for full development of the hydrodynamic boundary layer; thus, the hydrodynamic and thermal boundary layers both developed over a considerable portion of the tube. Linke and Kunze[36] have shown that entrance effects in this case can be noticed until approximately 70 L/D.

The data for the low flow rate are reasonably well ordered; however, they lie below values which would be predicted for turbulent flow. A diameter-Reynolds-number transition appears to be taking place similar to that noted for the low flow rate with the smaller tube.

The boiling plot compares favorably with the plot for the smaller-diameter tube. The asymptotes at zero wall superheat for equal subcooling do not coincide however, due to the influence of diameter and entrance length on the heat-transfer coefficient.

The data obtained with test sections 12 and 13 indicate clearly the characteristics of the boiling plot at low wall superheat. At constant wall superheat the heat flux increases with velocity and subcooling. The asymptotic value of the heat flux at zero wall superheat is given by Eq. (4) where the heat-transfer coefficient is obtained from the forced-convection correlation found most suitable at high radial temperature difference.

Since the effect of subcooling was clearly shown by these tests, further experiments were run simply at constant velocity and inlet temperature. The subcooling was then dependent on the heat flux.

## INCEPTION OF FIRST SIGNIFICANT BOILING

### Analysis

No analyses are known to have been reported which predict the conditions under which nucleate boiling will be initiated in a forced-convective system. As mentioned earlier the intersection of the forced-convection and fully-developed-boiling curves is velocity dependent. This does not, however, mean that the transition to fully-developed boiling begins at a wall superheat dependent on the velocity. On the contrary, Rohsenow's superposition principle suggests that the transition zone for all values of velocity and subcooling begins at a wall superheat corresponding to the inception of boiling in a saturated pool. In order to develop a criterion for incipient boiling, the conditions required for bubble nucleation will first be considered.

In an attempt to explain the basic physics of boiling, several alternative descriptions of bubble nucleation have been proposed. Theories based on the thermodynamics of pure liquids have been unsuccessful in predicting nucleation superheats except with pure degassed liquids in scrupulously-clean glass containers.[37] The more commonly accepted theory of nucleation in practical boiling systems suggests that bubbles originate at small cavities in the heating surface.[38] Bubble nuclei are formed by vapor trapped in the cavities.

Consider a segment of a spherical vapor bubble of radius r in a liquid; at equilibrium

$$\pi r^2 (p_g - p_\ell) = 2 \pi r \sigma \tag{10}$$

or

$$p_g - p_\ell = 2\sigma/r \tag{11}$$

It is noted that $T_\ell = T_g$ at equilibrium. Then, according to the Helmholtz relation for the radii of curvature of interest, $p_\ell < p_g$. Consequently, the liquid temperature must be superheated with respect to the liquid pressure.

The Clausius-Clapeyron equation relates $T$ and $p$ along the saturation line:

$$dp_g/dT_g \cong h_{fg} \rho_g/T_g = h_{fg}/v_g T_g \qquad (12)$$

It is noted that

$$(p_g - p_\ell)/(T_g - T_s) = dp_g/dT_g \qquad (13)$$

Combination of Eqs. (11) to (13) then gives

$$T_g^* - T_s \cong 2 \sigma T_g v_g/h_{fg} r \qquad (14)$$

or

$$T_g^* = T_s / \left[ 1 - 2 \sigma v_g/h_{fg} r \right] \qquad (15)$$

This final equation can readily be applied to a hemispherical bubble forming at a cavity with a mouth radius $r$. The bubble must pass through the hemispherical state before growing outside the cavity; this shape conforms to the configuration of the minimum radius of curvature. Equation (15) then represents the criterion for bubble growth. The thermal layer surrounding a bubble nucleus must attain a temperature such that there is net heat transfer to the bubble if it is to grow.

In forced convection this thermal layer is the laminar sublayer. However, the temperature gradient within the laminar sublayer makes it difficult to define the relation of local liquid temperature to the critical vapor temperature. It is postulated simply that the nucleus of

hemispherical shape with radius r will grow if the liquid temperature at a distance y = r from the wall is greater than the critical vapor temperature defined by equation (15). The liquid adjacent to the bubble is then greater than or equal to the critical bubble temperature.

In all probability, this represents an upper limit, as all of the surrounding fluid is then able to transfer heat to the bubble. In reality, if the fluid temperature at a distance somewhat less than r is equal to the critical vapor temperature, the bubble should still grow. There is then heat transfer to the base of the bubble and heat transfer from the top of the bubble, with the net heat transfer equal to zero at equilibrium. The solution for this heat transfer is complex as the liquid temperature profile is distorted near the bubble. Han and Griffith[40] present a pool-boiling analysis which uses the relationship r = 0.67y. In their analysis it was necessary to make numerous assumptions which cause considerable uncertainty in the final result. An exact solution, if it were possible, would involve labor out of all proportion to the results.

The postulate as stated above appears sound enough physically for a design approximation. Hsu and Graham[39] have used this same criterion for estimating the critical temperature profile for initiation of bubble growth in pool boiling.

The temperature profile in the laminar sublayer is given simply by

$$T_\ell = T_w - (q/A)y/k \tag{16}$$

Equations (15) and (16) together with the postulated relationship

$$T_\ell = T_g \quad \text{at} \quad y = r \tag{17}$$

represent the criterion for incipient boiling. The wall superheat at which boiling will occur is best evaluated graphically for a particular system.

Consider forced-convection heat transfer at high heat flux to a system at constant pressure. The inception of boiling is indicated schematically in Fig. 19. Equation (15) can be plotted for the system as all properties are evaluated at the saturation temperature. The liquid temperature profile is a function of the bulk temperature and velocity in addition to the heat flux. The wall temperature will increase with an increase in heat flux or with a decrease in velocity or subcooling. The heat flux can be increased to the point where the curves are tangent at a distance y'. The bubble originating from a cavity of this radius can now grow. Only a small additional increase in wall temperature is necessary to activate a considerable range of cavity sizes.

It is noted that grooves are more probable than cavities due to the nature of most metal-forming operations. It has, however, been shown by Bankoff[41] that cavities are more stable vapor traps than grooves. In most cases the smaller second-order roughnesses formed statistically by the fracture of the solid determine the superheat. In commercially-prepared surfaces a wide range of cavity sizes can be expected. Incipient boiling, then, should be independent of surface condition for most commercially-finished surfaces. The present analysis should, therefore, be valid in most practical applications. It is noted, however, that the position and slope of the remainder of the boiling curve should be dependent on the size range of active nuclei.

Experimental Verification

The data taken with test section 13 were used to check the preceding analysis for incipient boiling. Successive points at moderate wall superheat for each flow rate were checked graphically for incipient

boiling. In Eq. (16) the thermal conductivity was evaluated at the wall temperature. The variation of the thermal conductivity for water in the range of liquid temperatures encountered near the wall is so small that no error is introduced by this assumption. Figure 20 shows the results for test section 13 at the three mass velocities considered. The lines indicating the liquid-temperature variation are terminated at the end of the laminar sublayer to indicate that this analysis is confined to the laminar sublayer. The thickness of the laminar sublayer can be shown to be approximated by

$$y_1 = 5D/Re^{0.9}\sqrt{0.023} \tag{18}$$

for a smooth tube. Several $t_g^*$ curves are shown because of the axial pressure gradient in the tube at higher flow rates.

The experimental verification is indicated in Fig. 21. The relative amount of boiling for each point is indicated by

$$(q/A) - (q/A)_{FC} \ /(q/A)$$

where the forced-convection term is evaluated from an extrapolation of the appropriate correlation line from Fig. 17. When plotted versus wall superheat, this boiling proportion is seen scattering about or remaining close to the zero line, indicating that forced convection accounts for all the heat transfer. At a definite wall superheat, however, the points become positive, indicating that the heat transfer is augmented due to the boiling. This wall superheat at incipient boiling is seen to be strongly dependent on velocity. The exact transition point is a matter of judgment, as the break point can be imagined to occur over a spread of at least $5°$ of wall superheat. In any case, the experimental break points can be considered to coincide with the transition points suggested

by analysis. The same procedure was followed for test section 12 with equally good correspondence between the predicted and observed transition points.

The system water was degassed to less than 1.5 cc air/liter for all runs. Premature "boiling" due to gas release at the hot surface[18] should not occur at this low air content.

The wall superheats for incipient boiling are indicated in Fig. 18. The locus of points for incipient boiling is seen to be approximately a line on the $(q/A)$-versus-$(t_w-t_s)$ plot. It is apparent that at constant mass velocity the wall superheat required for incipient boiling increases as the subcooling is increased. The plot then illustrates the commonly-observed phenomenon of boiling starting first at the exit of a tube with uniform heat flux. The wall superheat increases axially due to the decrease in subcooling. Accordingly, the last section of the tube can have forced-convection boiling while the rest of the tube has ordinary forced convection.

The design procedure using this analysis is clear. The locus of points for incipient boiling at a given pressure can be plotted on the $(q/A)$-versus-$(t_w-t_s)$ plot since the heat flux, wall temperature, and pressure determine all quantities in Eqs. (15) and (16). The intersection of the appropriate forced-convection line with this incipient-boiling curve gives the start of the transition to fully-developed boiling. A general correlation giving critical wall superheat as a function of pressure and heat flux can readily be developed for convenience in design.

As noted in the derivation of the incipient-boiling criterion, bubbles will probably grow at lower values of the wall superheat than predicted. However, the first few bubbles are unlikely to increase the heat transfer

above what can be expected from forced convection. Even though the nucleated bubbles stick up before growth, it is doubtful if they contribute to heat transfer either. The experimental plot would then also be expected to give a transition point at wall superheats higher than where the first bubbles are actually formed. Thus both analysis and experiment are in the same direction.

All available boiling data were checked to see if more support could be gained for the present analysis. Several pertinent studies are now discussed.

An investigation of the conditions required for the inception of boiling for water at high pressures was conducted by Buchberg, et al.[19] For the particular tube size considered, the heat flux at incipient boiling was found to be a function only of mass velocity and bulk temperature at constant pressure. Axial wall-temperature variation and wall-temperature fluctuation were observed to determine the incipient-boiling point. The difference in wall temperature between a downstream location and a location near the inlet was plotted versus heat flux for constant pressure and flow. A sharp peak in the curve then defined the heat flux at incipient boiling. Oscillogram traces also indicated that wall-temperature oscillations were reduced considerably at the so-called incipient-boiling point.

It is believed, however, that this method actually indicated the start of fully-developed boiling rather than the beginning of first significant boiling. Reference to the boiling plot shows that at constant heat flux and pressure, the wall temperature must increase axially in the forced-convection and transition regions, whereas in the fully-developed region it remains constant. This effect is due to the axial

decrease in subcooling in the direction of flow for a channel. It is the sudden flattening of the axial temperature profile which gives rise to the inflection point on the crossplot noticed by Buchberg and co-workers. The inflection point must then signify the start of fully-developed boiling. However, it must be noted that a sensitive experiment of this type is almost impossible at high pressures where the wall superheat at fully-developed boiling is less than 10 $^{\circ}$F.

An attempt was made to apply the present incipient-boiling analysis to the data of Buchberg, et al. Their correlation for non-boiling convective heat transfer was used to obtain the value of $(t_w - t_b)$ at their value of incipient boiling corresponding to the particular G and $t_b$. The resulting values of $(t_w - t_s)$, however, were all approximately -20 $^{\circ}$F indicating that the forced-convection correlation must be inaccurate at high $\triangle t$. As a result there was no possiblity of checking the present analysis with those high-pressure data. In any case it is usually not necessary to determine the point of incipient boiling at high pressures, as it is separated from fully-developed boiling by only a few degrees of wall superheat.

Hsu[42] applied his pool-boiling analysis to the inception of forced-convection surface boiling as obtained by McAdams, et al.[18] The concept of a transient thermal layer was retained and the thickness of the limiting thermal layer was estimated from reference experimental points. The effect of pressure and subcooling on the wall temperature at incipient boiling was then checked and found to be approximated by the analysis. It is recalled that McAdams et al. have defined incipient boiling as the intersection of the forced-convection and fully-developed-boiling curves. Actual boiling will start at considerably lower wall temperature. In addition, the concept of a transient thermal layer

appears to be unnecessary in a forced-convective system where the temperature profile in the laminar sublayer is well defined.

Reference to experimental results of Mantzouranis[43] for incipient boiling is given in a recent article by Haselden.[44] The wall superheat at incipient boiling is shown to increase with increasing velocity and subcooling while decreasing with increasing pressure. This general relationship agrees with the results of the present study; however, a more detailed comparison is not possible until the actual data are published.

The analysis of the inception of boiling under conditions of forced convection is not limited in its application to subcooled systems. Nucleate boiling actually extends into the region of slug flow in a two-phase-flow system. It has long been recognized that strong two-phase circulation suppresses nucleation. The procedure outlined in this section should be useful in predicting the heat transfer in two-phase systems.

Tripping of Boundary Layer by Incipient Boiling

Boiling data were taken with a short 16 ga. tube with the intention of uncovering any unusual diameter effect which might be present in forced-convection surface boiling. The sought-after diameter effect turned out to be pertinent to the analysis of incipient boiling, hence the results are presented in this section.

Data taken for a 0.0465 in. ID tube at axial locations of 29 and 51 L/D are shown on the boiling plot in Fig. 23. The right-hand portions of the curves are seen to be merging and the effects of velocity and subcooling are clearly diminished.

The apparent asymptote in the fully-developed-boiling region is similar to that obtained with test section 12. For higher mass flows, the region of low wall superheat is correlated by the extrapolation of the forced-convection data given in Fig. 22. For $G = 2.46 \times 10^6$ $lb_m/hr$ $ft^2$, however, the situation is more complex.

The data for the lowest flow rate are seen to fall into regions of low and high heat flux on the boiling plot. The phenomenon is more clearly indicated in Fig. 24 where Cartesian coordinates are used. As the heat flux is increased, the wall temperature increases, and the effect of sub-cooling is as it should be. At a wall superheat of approximately 15 $^oF$, the wall temperature at station 2 suddenly becomes less than station 1. As the heat flux is further increased, the wall temperatures decrease well into the non-boiling region. A regular pattern is then evident with the usual trend of subcooling. The slope of the curve increases slightly as a wall superheat of somewhat less than 20 $^oF$ is reached.

This unusual phenomenon can be explained in terms of laminar-turbulent transition and incipient boiling. The data taken at lower heat flux as indicated in Fig. 22 lie well below the turbulent line although somewhat above values that would be predicted for laminar flow. Due to the small diameter and low bulk temperature, the Reynolds numbers lie near the beginning of the transition region. On the other hand, the data for high heat flux are definitely turbulent as indicated in Fig. 22. Something happened to suddenly change the character of the flow from transition to turbulent.

The sequence of wall-temperature variation with heat flux was perfectly reproducible with the transition always starting at about 15 degrees of wall superheat. For 38 psia and $q/A = 0.45 \times 10^6$ Btu/hr $ft^2$, the

incipient-boiling analysis predicts the start of boiling at $(t_w - t_s) \cong$ 18 $^o$F. As noted earlier the first bubbles can be expected to grow at a slightly lower wall superheat. It appears to be no coincidence that the wall temperatures behave strangely when the first bubbles grow.

The bubbles can be considered as devices which trip the boundary layer from transition to turbulent. The second station exhibits this behavior first, in accordance with the spread of boiling upstream in the tube. These data then constitute further experimental verification of the analysis for predicting incipient boiling. They also indicate the difficulty of predicting the behavior of boiling or nonboiling systems operating in the laminar-turbulent transition region.

Data for other test sections were examined to see if there were any discontinuities which would imply a change in flow character at the point of incipient boiling. None were found, as might be expected, since the other data for low wall superheat were sufficiently close to turbulent flow to start with.

TRANSITION AND FULLY-DEVELOPED SURFACE BOILING

## Discussion

The introductory section on nucleate boiling considered only the
most basic presentation of boiling data, the $(q/A)$-$(t_w - t_s)$ plot. It
is clear that this presentation lacks generality and can be very cumber-
some if a wide range of variables is to be indicated. At this point it
is appropriate to outline the attempts which have been made to correlate
the data in nucleate boiling.

In the region of strong nucleate boiling, for both pool boiling
and forced-convection surface boiling, the data of many investigators
can be expressed by

$$q/A = C(t_w - t_s)^n \tag{19}$$

In this expression n is a constant, ranging from 3 to 4 for most commer-
cially-prepared surfaces, and C a particular constant for each pressure
and fluid-surface combination. For example, Jens and Lottes[20] found
that MIT and UCLA forced-convection surface-boiling data for water could
be correlated approximately by

$$q/A = (e^{p/900}/1.9)^4 (t_w - t_s)^4 \tag{20}$$

Similar dimensional equations have been presented by many investigators.
It must be emphasized that these equations apply only to the region of
fully-developed boiling. As noted earlier, the replot of data from McAdams'
project indicates no effect of velocity or subcooling in this region.
Recent studies by Lurie and Johnson[21] of transient pool boiling lend addi-
tional support to the general observation that fully-developed nucleate-
boiling heat transfer is a weak function of the fluid circulation.

The similarity of equations for forced-convection boiling and pool boiling has led to the conclusion that the curve for fully-developed forced-convection surface boiling is simply the extrapolation of the curve for saturated pool boiling. This coincidence has not, however, been directly verified by experiment.

Generalized correlations can only be successful if they are based on an accurate physical model of boiling heat transfer. A number of proposals have been made concerning the dominant mechanism for heat transfer. Dimensionless groupings of the macroscopic variables based on the proposed mechanisms have been correlated empirically.

Correlations for saturated pool boiling have been proposed by Rohsenow[45] and Gilmour[46] among others. These correlations have been successful in predicting the heat transfer for various liquids at various system pressures. However, the position of the fully-developed-boiling curve has been found to shift with each fluid-surface system. Nominal experiments are therefore required to establish the constant for the particular system being considered.

Rohsenow[17] has p. posed that the convection effect is superimposed on the bubble-motion effect. This applies for calculation of the heat transfer under conditions of forced flow or unbounded natural convection. The superposition appears to work in spite of the fact that the convective terms are based on expressions valid for undisturbed velocity distributions. The bubbles clearly disturb this velocity distribution.

More recent correlations by Levy[47] and Engelberg-Forster and Greif[24] appear to be more general as it is claimed that they correlate data independently of fluid and surface condition. These correlations were

derived for pool boiling, but they are supposed to be applicable to the fully-developed region of forced-convection surface boiling.

All four correlations are based on different mechanisms of nucleate boiling, and yet each claims success in predicting boiling heat transfer. The success is at least partially due to the fact that vigorous-boiling data have a very steep slope on the boiling plot. As a consequence, it is possible to pass any number of correlating lines through experimental points.

It is apparent that the fluid mechanics of boiling in forced-convection are different from those in saturated pool boiling. In forced-convection subcooled boiling, for example, the bubbles grow and collapse at the surface as they are swept downstream. On the other hand, in saturated pool boiling, vapor bubbles detach from the surface and rise through the pool. It is natural, then, to question why correlations based on pool boiling should be successful in the forced-convective case. Kreith and Foust[48] looked at this problem and concluded that the correlation chosen by Rohsenow is broader in scope than the original model would indicate. They found that the agitation for detaching and non-detaching bubbles was the same order of magnitude.

Bankoff[49] recently summarized the various mechanisms which have been proposed to explain the high heat-transfer rates associated with boiling. He concluded that a single simple formulation was not adequate to describe all of the features of nucleate-boiling heat transfer. He then proposed a more complex formulation which describes subcooled nucleate boiling with convection by a threestep model:

1. The heat flows from the wall to the liquid by two paths: (a) The wall area periodically covered by bubbles is cooled by quenching

as colder liquid rushes in as the bubbles collapse, and (b) the remainder of the wall area is cooled by microconvection induced primarily by bubble growth, departure, and collapse.

2. Heat then flows through the two-phase wall layer by convection in the liquid between the bubbles and by latent-heat transport within the bubbles.

3. The heat is finally transferred by turbulent convection from the edge of the two-phase layer to the turbulent core.

An analysis for any one of these series paths is sufficient to describe the heat transfer. Bankoff derived expressions for the quenching and convection fluxes in the first and third steps. Data of Gunther[50] and Gunther and Kreith[23] on bubble parameters together with an empirical constant were used to estimate the total heat flux at the wall. Bankoff divided the turbulent convection in step three into components due to the bubble and stream motion. The bubble boundary layer was considered thin compared to the channel dimensions. The stirring action of the stream was calculated from a forced-convection correlation where the equivalent diameter was used. The stirring action of the bubbles again required bubble parameters and arbitrary constants which were evaluated from Gunther's data. It is noted that step three then is similar to the procedure of Rohsenow which is used to estimate the total heat flux by adding forced convection to pool boiling.

Bankoff has ably described the probable mechanism of forced-convection surface boiling; however, the use of local bubble parameters limits the practical application of his theory. These parameters, such as bubble frequency and lifetime, must be experimentally related to the macroscopic system variables. In short, even the most sophisticated

model leans heavily on experiments to determine the necessary constants. These constants are, however, not dependent simply on the fluid properties of the boiling system.

A general correlation of boiling data does not seem possible because of the strong influence of minor variables which are not readily controlled. Among these variables are amounts of dissolved and adsorbed gases, impurities and contamination on the surface, and differences in experimental technique. All of these variables have a pronounced effect on both the slope and position of the boiling curve. These minor variables are discussed further due to their importance in interpreting the data of this study.

In this study heat-transfer surfaces were thoroughly cleaned before installation. Trichloroethylene and acetone were used as cleaning agents. The test section was swabbed with either of these solvents and rinsed with warm water. The only possible deposit that could result from this cleaning operation would be a film of partially dissolved oil.[52] This white film, which was observed when hastily cleaning fittings, would not be left if the swabbing operation was thorough. In any case, this film was removed by water in the rinsing process.

As the system water was continually deionized, no deposits were found on the heating surfaces. The stainless-steel heaters were clean and bright after all runs. A very slight discoloration was, however, noticed on the inside surface of the nickel tubes. This film was observed with the same tubes in a previous boiling study and found to have a thickness of the order of a wave length of blue light.[16] Its effect on heat transfer is pure speculation.

Each tube size must be considered to be a different surface with regards to boiling, even though the same material is used. The stainless-steel tubes in this study are cold drawn without internal plugs; smaller size tubes being merely larger tubes drawn down. The inner surface of the tube is free to distort, and it is reasonable to assume that surface characteristics for small tubes are different from those of large tubes. The positions of the fully-developed portions of the boiling curves for the stainless test sections 12, 15, and 13 are different, although the slopes are basically the same. It is also noted that the same finishing procedure for different materials will usually result in a different surface due to the different material properties. Finishing procedure and surface conductivity are considered important factors in determining the surface characteristics.

Nucleation is generally considered to occur from pre-existing gas-filled cavities on the heater surface. The duration of boiling and the condition of the water, therefore, most certainly influences the heat transfer. The degassing procedure should remove adsorbed air from the surface as well as from the water. Boiling for a period of time before taking data should help stabilize this particular surface condition. This "aging" of the heat transfer surface is well known; however, it is not well established what length of time is required before a surface becomes stabilized. In the present experiments, surfaces were degassed for at least one hour before taking data.

The amount of degassing appears to influence the position of the boiling curve according to Kennel.[22] A $(t_w - t_s)$ shift of some 22 percent was noticed between runs where apparently the only difference was in the degassing procedure. It was suggested that the longer degassing

period, which included local boiling from the test-section surface, removed a portion of the nuclei from which boiling could occur.

Differences in experimental technique are also responsible for deviations in boiling data in the literature. As noted in a preceding section, considerable uncertainty exists in the determination of the temperature of the heat-transfer surface. As different procedures are used in most investigations, especially in flow inside tubes, it is reasonable to assume that some of the discrepancy can be traced to this measurement.

The preceding discussion has indicated the complexity of boiling heat transfer. Even if a general correlation were possible, little would be gained by attempting to generalize the boiling data which have been obtained in this study. The $(q/A)-(t_w-t_s)$ plot suffices for most aspects of this study. The one exception is where it is necessary to compare data taken at different pressures.

Data for Forced-Convection Surface Boiling at High Wall Superheat

The transition region and fully-developed-boiling region were investigated with a 0.094 in. ID tube of total heated L/D = 31. These dimensions were chosen so that local data could be taken at an L/D large enough to avoid substantial entrance effects, and yet get into the fully-developed-boiling region without going to bulk boiling.

Forced-convection data for an L/D of 14 and 24 are indicated in Fig. 25. The data indicate that heat-transfer coefficients near the entrance are larger than at downstream locations. Comparison with Fig. 17 shows that at constant G, the local heat-transfer coefficients are progressively higher as L/D goes from 48 to 14. This is in general agreement with the observations of most investigators.

The boiling data taken at an L/D of 24 are shown in Fig. 26. In the fully-developed region, the curves of different velocity appear to be merging to a single line. The subcooling varies for each velocity as noted on the plot. The effects of both velocity and subcooling, then, can be considered to be wiped out in the fully-developed-boiling region. Tests with this tube were terminated with burnout at the medium flow rate.

These data were further reduced to examine the applicability of the superposition method of Rohsenow. The forced-convection data as presented in Fig. 25 were extrapolated to obtain the hypothetical q/A due to forced convection at the local boiling conditions. This was subtracted from the total q/A and plotted in Fig. 26. The operation is a fair test of the correlation, as the pressure was constant for all runs. Superposition claims that when the effects of velocity and,

subcooling, which are incorporated in the forced-convection term, are taken away from the boiling curves, the result should be a straight line corresponding to the extrapolation of the pool-boiling curve.

It is seen that the data can be grouped into curves for each velocity rather than the single curve which would be predicted from superposition. The values of the $(q/A)_B$ go asymptotically to zero at approximately the $(t_w - t_s)$ for incipient boiling. This is according to the definition of incipient boiling; however, it means that there is a different $(q/A)_B$ curve for each velocity and subcooling. Furthermore, the curves follow no regular pattern in the transition region. They cross and each have several inflection points. Only in the fully-developed region do they become straight lines; however, it is noted that the lines are definitely separated according to velocity. In all probability, if the fully-developed region could be extended, all $(q/A)_B$ curves would appear to merge into the actual data. In short, these data demonstrate that velocity and subcooling curves appear to merge in the fully-developed-boiling region. As a consequence, the boiling portion obtained by superposition consists of different curves depending on the velocity and subcooling.

Comparison of Pool Boiling and Forced-Convection Surface Boiling

a. Tubular Geometry

It has been noted that the pool-boiling curve is essential to the construction of the forced-convection-boiling curve for a particular system. Experiments were devised with the object of directly comparing data for pool boiling and forced-convection boiling.

Since the surface condition plays such an important role in boiling, it is necessary to pool boil from exactly the same surface that

is used in forced-convection boiling tests. In general, this is a diffi-cult experimental task; however, two approaches were undertaken. In the first experiment, a tubular section was essentially sliced in half length-wise. The complete assembly, which was described earlier, included a waterproof guard heater and power connections.

Attempts were made to fabricate this pool-boiling apparatus from the stainless-steel tubes for which considerable boiling data had been taken. These efforts were unsuccessful due to the relatively large bubbles at incipient boiling. These bubbles would remain attached to the edges of the half tube and grow axially with increased heat input, causing prema-ture burnout. It was, therefore, necessary to use the larger nickel tubes for the pool-boiling tests. For purposes of comparison, data were taken over a wide range of flows with a tubular test section made from the same piece of stock.

Forced-convection-boiling data and pool-boiling data for the nickel surface are presented in Fig. 28. Fully-developed boiling could not be attained at the lowest flow rate due to bulk-flow limitations. It is noted that again the forced-convection-boiling lines appear to merge into an asymptote which can be represented by the dashed line. The pool-boiling line exhibits the usual characteristics: a region at low wall superheat where natural convection plays a part, a fully-developed portion with constant slope, and a region of decreasing slope where the bubbles begin to pack the surface. The burnout at q/A = 371,000 Btu/hr ft$^2$ compares favorably with data of other investigators for saturated pool boiling of water at one atmosphere.[6] The concave heat-transfer surface appears to have had no noticeable effect on the boiling data.

A direct comparison of pool boiling and forced-convection boiling is, however, not permitted by the raw-data plot due to the difference in pressure between the two systems. The dimensionless groups proposed by Rohsenow[45] appear to have correlated the effect of pressure from 14.7 to 2500 psia; they were, therefore, adopted for the present data reduction. The results are shown in Fig. 29. Included are several representative curves for $(q/A)_B$ which exhibit the complex behavior noted earlier. The extrapolation for the forced-convection effect is based on data given in Fig. 27.

It is seen that it is possible to consider the extrapolation of the pool-boiling curve as coincident with the curve for fully-developed forced-convection boiling. This coincidence, however, is quite speculative as any number of straight lines can be passed through the points representing the complete pool-boiling curve. The transition and bubble-packing regions as well as the fully-developed portion have often been considered in drawing a straight line through the data.[45]

It is recognized that the data for nearly-saturated pool boiling do not represent entirely the effect of bubble motion. The heat flux due to natural convection should be subtracted from the pool-boiling heat flux to obtain the heat flux due to bubble motion alone. A natural-convection correlation is, however, unavailable for the concave surface considered here. In any case, the correction due to the natural convection should be important only at low values of the pool-boiling heat flux. The slope and position of the curve would not otherwise be significantly altered.

If the fully-developed portion of the forced-convection-boiling curve is actually the region where the velocity effect is insignificant compared

to the bubble-motion effect, it should coincide with the extrapolation
of the fully-developed portion of the pool-boiling curve. The coinci-
dence of the fully-developed portions of the boiling curves clearly
does not occur, as the forced-convection-boiling curve has a smaller
slope than the pool-boiling curve. It would appear that the effect
of forced convection is to flatten the boiling curve.

It can, however, be strongly argued that the fully-developed por-
tion of the saturated pool-boiling curve at pressures near atmospheric
are not entirely representative of the bubble-motion effect. As the
heat flux was increased, a large volume of vapor was noted to depart
from the surface. The bubbles grew rapidly until they were at least
1/2 in. in diameter when they reached the surface of the pool.

The natural convection induced by the large volume flow of vapor
can be considered to augment the heat transfer and produce a steeper
boiling curve. The data of Addoms[53] indicate a decreasing slope with
increasing pressure for pool boiling. Bubble size decreases with
increasing pressure so it seems reasonable that the induced natural
convection would be reduced at higher pressure. The higher pressure
data are then more representative of the bubble-motion effect in pool
boiling.

It can be seen that the flux attributed to boiling as obtained
by superposition can also be considered the extrapolation of the pool-
boiling curve. The velocity shift at high wall superheat is not espe-
cially noticeable due to the relatively small range of velocities con-
sidered. There is some scatter at the inception of boiling. However,
a single line can be passed through the data points having a slope
similar to that of the assumed fully-developed-boiling line.

It is noted that the intercept of the fully-developed-boiling curve at $Y = 1.0$ is approximately $X = 0.009$. The approximate intercept of the points obtained by superposition is $X = 0.01$ which compares favorably with the value obtained by Walsh[54] using identically-drawn A nickel tubing.

Attention is called to an apparent discrepancy in data presented from a previous boiling project. Inspection of Fig. 9 of Clark and Rohsenow[25] indicates that the data, when correlated for pressure, fall into two distinct groups. There appears to be an asymptote with an intercept at $X = 0.006$ in addition to the one indicated at $X = 0.009$. Only the data in the left-hand grouping were reduced according to superposition as shown in Fig. 10, with the result that the intercept falls at $X = 0.006$. It is quite possible that the data from the right-hand grouping were taken with A nickel test sections instead of the L nickel tubes supposedly used throughout the study. This would explain lack of agreement between the two groups of data as well as the omission of the one group in the superposition analysis.

Figure 30 gives a clear indication of the effect of fouling on the boiling curve. Clean-tube data were taken from Fig. 28 and fouled-tube data were taken from preliminary runs where no ion exchanger was used. A heavy black deposit of carbonates precipitated at the heat-transfer surface when the water was not treated. The increased resistance to heat transfer is evident at all regions of the boiling curve.

b. Annular Geometry

An annular test section was also constructed to investigate the same problem. The annular arrangement permitted an independent check of the above conclusions with a different geometry. The dimensions of

the annulus were chosen so that a large portion of the fully-developed-boiling curve could be covered. In addition, it was hoped that a visual indication of incipient boiling could be obtained.

As described previously, the annular test section consisted essentially of 16 ga needle tubing placed inside a 5 mm Pyrex tube. A pressure tap and thermocouple were located as far as possible from the inlet in order to avoid entrance effects. Several test sections were used due to breakage of the Pyrex tubing and burnout. Careful measurements of the Pyrex tubing were made before assembly as the inside diameter varied considerably. A simple pool-boiling test section was constructed from the same length of tubing used in the annular runs.

The forced-convection and pool-boiling data are indicated in Fig. 32. It is seen that the fully-developed portion of the forced-convection-boiling curve indicates no effect of velocity or subcooling in accordance with previous results. It is noted, however, that the slope of the fully-developed portion is somewhat steeper than that obtained when boiling on the inside of the same tubing (Figs. 16 and 23). The manufacturer indicated that the outside surface of the tubing was polished whereas the inside surface was left as drawn.[9] The difference in slope is probably caused by the different surface characteristics produced by the manufacturing operations.

Due to the relatively large velocity and subcooling used in these tests, the bubble size was very small. As a consequence, it was impossible, even with magnification, to see incipient boiling. At high wall superheats the flow became cloudy and individual bubbles were discernable due to a reduced level of subcooling.

Considerable difficulty was experienced in obtaining pool-boiling data for the wire-like geometry. The two curves shown are representative

of the data obtained and indicate the sensitivity of the experiment to surface conditions, placement in the pool, and bulk temperature.

The left-hand curve for PB 3 was obtained with a surface thoroughly cleaned and rinsed with trichloroethylene. The test section was located approximately 3/16 in. from the bottom of the pool. The water was thoroughly degassed and maintained at a bulk temperature as close to saturation as possible by means of an immersion heater. The surface was also degassed by surface boiling for some time before data were taken.

The data for PB 1 were obtained with a surface that was not particularly well cleaned. The tube was placed approximately one inch from the bottom of the pool. The test section was allowed to sit in the pool for several days between taking sets of data. The bulk temperature of the pool depended on the heat input to the test section as no auxiliary heater was used.

It is noted that these data lie approximately 10 $^{O}$F to the right of the first boiling curve. This can be explained, at least partially, by the cleanliness of the surface. The prolonged soaking could also shift the boiling curve in the observed direction. The heating surface can be expected to give off adsorbed air to water degassed by previous boiling. This effect is discussed by Jakob.[55] It is probable that the soaking was more effective in degassing the surface than the aging procedure followed for PB 3.

The fully-developed portions of both boiling curves are seen to be very steep, steeper than might be expected for a commercially-prepared surface. The right-hand boiling curve actually reverses direction at higher heat fluxes. It appears that this effect is due to the large vapor volume departing from the surface in nearly-saturated pool boiling at low pressures. The net effect of this bubble motion was to violently stir the entire pool. The test section PB 1 was located

substantially farther from the bottom of the pool than was PB 3. In all probability, the convection currents in the former case were stronger at the tube than in the latter case. This could account for the bending back of the curve for PB 1.

The stronger bubble-induced convection with PB 1 also increased the peak heat flux. Neither tube was burned out, but the curves can be extra-polated to the probable burnout point.

The only known published data indicating a probable effect of bubble-induced convection were presented by Rallis, et al.[56] These data indicate that the boiling curves for subcooled pool boiling lie to the right of the curves obtained with saturated pool boiling. Ordinarily the opposite would be expected as natural convection increases with subcooling. If, however, the bubble-induced convection is larger than the natural convec-tion, the trend will be as observed.

The bending back of the boiling curve has been noted by at least one other investigator. Unpublished data of Long[57] show this effect for a boiling system using variously finished surfaces with dichlorotetrafluoroethane. Inasmuch as no satisfactory explanation has been given for the phenomenon observed by Long, the above-mentioned idea of bubble-induced convection probably explains his observations.

Forced-convection data for the annular geometry are correlated in Fig. 31 according to the equation proposed by Carpenter, et al.[58] The correlation is only one of many proposed for annuli; the main difference appears to be in a correction term which accounts for various ratios of outer-to-inner diameter. The form of the correlation is noted to be identical to that of Sieder and Tate as given in Eq. (8) although the constant is changed somewhat. The majority of the data fall close to the

original correlation. Data for the shorter tube are higher, perhaps due to entrance effects.

The forced-convection-boiling data and pool-boiling data were corrected for pressure in Fig. 33. The data given in Fig. 31 were extrapolated and used to obtain values of $(q/A)_B$ in the comparison plot. Due to the complexities of the pool-boiling curves, it appears impossible to draw any general conclusions regarding the coincidence of the pool-boiling curves and the fully-developed-boiling curve.

Pool-boiling data were not corrected for natural convection. The lower portions of the pool-boiling curves would be much steeper if this correction were applied; however, the other regions of the curves would not be significantly altered.

As a result of this study, a more accurate prediction of the forced-convection-boiling curves for a particular system is possible. Boiling curves constructed for several values of velocity and subcooling are shown in Fig. 34. These curves were obtained from the assumed line for saturated pool boiling by the two basic design methods: direct extrapolation and superposition of forced convection.

The forced-convection curves were constructed from the usual relation

$$(q/A)_{FC} = h(t_w - t_b) = h\left[(t_w - t_s) + (t_s - t_b)\right] \tag{21}$$

where h was obtained from Eq. (9). The additional variables which complicate the prediction of h, such as entrance effects, were not considered in this example. The locus of incipient boiling was obtained from Eqs. (15) to (17), and is seen to be a straight line at constant pressure.

The construction according to Engelberg-Forster and Greif consists simply of locating by Eq. (5) the point on the extrapolation of the pool-boiling line where forced convection is no longer important. A line then connects this point with the incipient-boiling point.

The curves were also constructed by the superposition method of Rohsenow for the same values of velocity and subcooling. In order to avoid the considerable discontinuity at incipient boiling, the original formulation of superposition has been modified to the following:

$$(q/A) = (q/A)_{FC} + (q/A)_B - (q/A)_1 \tag{22}$$

where $(q/A)_1$ is the pool-boiling heat flux at incipient boiling.

The boiling curves constructed by both design procedures are substantially in agreement, especially at low velocities. It is emphasized

that the independent variable in most boiling systems is the heat flux. The wall superheat predicted by either method will be within the usual uncertainties associated with boiling.

For most forced-convective systems, data for saturated pool boiling will not be readily available. The same procedures can be used to construct boiling curves if nominal data for fully-developed forced-convection surface boiling are available. These data are used to infer the saturated pool-boiling line, and the desired boiling curves are then constructed as indicated above.

In lieu of actual data for the particular boiling system, it is possible to base the design on available data for a similar system. It is emphasized that use of such data is not desirable due to the influence of minor variables on boiling heat transfer. The effects of fluid and surface condition are peculiar to a given system and influence the boiling curve rather strongly. Correlations for fully-developed boiling which are presented only in terms of fluid properties must likewise be considered as only approximate.

## SUMMARY OF HEAT-TRANSFER STUDIES

The boiling curve under conditions of subcooling and forced convection is characterized by three regions: (a) a region of low wall superheat where forced convection applies, (b) a transition region where forced convection and surface boiling are important, and (c) a fully-developed-boiling region where the effects of forced convection are unimportant.

Available correlations for forced convection can be used to predict the heat flux in the region of low wall superheat. However, it is shown that these correlations do not properly account for the radial variation of properties for water at high temperature difference. The conventional Dittus and Boelter-McAdams relationship is recommended for design purposes on the basis of its simplicity and conservative predictions.

An analysis for the prediction of the inception of first significant boiling was developed. Experimental results are in good agreement with analytical predictions. The analysis provides information necessary for the prediction of the complete forced-convection surface-boiling curve.

The use of small-diameter tubes generally means operation at low Reynolds numbers. It is shown that flow conditions in the transition range of Reynolds numbers can be strongly influenced by the inception of surface boiling. Data for a small-diameter tube indicate that the bubbles formed at incipient boiling trip the laminar or transition boundary layer to a fully-developed turbulent boundary layer.

The experimental results for comparison of forced-convection boiling and pool boiling are inconclusive. The fully-developed region of

forced-convection surface boiling can be represented by a straight line on the boiling plot. The effects of velocity and subcooling are negligible in this region. This region of vigorous boiling coincides approximately with the extrapolation of the pool-boiling curve in one set of experiments. In other experiments, pool-boiling data were strongly influenced by fluid and surface conditions, as well as by bubble-induced convection in the pool. Due to the complexities in the pool-boiling data, it is impossible to make a comparison with forced-convection-boiling data.

The heat flux obtained by a superposition of pool boiling and forced convection is close to the apparent asymptote for fully-developed boiling. For design purposes, it is concluded that fully-developed forced-convection boiling can be related to pool boiling by either direct extrapolation or superposition of forced convection.

BURNOUT

## Primary Variables

The most important information required for the successful design of a nucleate-boiling heat-transfer system concerns burnout. The burnout point usually represents the maximum heat flux which can be applied to a particular system without destruction of the heating surface. The importance of burnout was immediately recognized by early investigators of surface-boiling heat transfer.

In all probability, the first burnout investigation was carried out by Mosciki and Broder[14] in subcooled pool boiling. Burnout data for forced-convection surface boiling were presented by McAdams, et al.,[18] Kreith and Summerfield,[13] Gunther,[51] and Jens and Lottes.[20] Burnout was visualized by these investigators as a local phenomenon; at this condition the bubbles become numerous enough to coalesce and form a vapor-blanketing layer. Accordingly, the data were correlated in terms of local properties: mixed-mean temperature, pressure, and velocity. The channel dimensions were considered to have no effect on burnout. These same properties have been considered the only variables affecting burnout by more recent investigators as Mirshak, et al.[59] and Zenkevich.[60]

Data for constant pressure have often been presented on a plot of $(q/A)_{BO}$ versus $(t_s - t_b)$ and V. The burnout heat flux at constant velocity is usually linearly dependent on subcooling, suggesting that the subcooling is the driving force at burnout and that the velocity may be considered to represent a burnout heat-transfer coefficient. For example, the data of Gunther[51] were correlated by:

$$(q/A)_{BO} = const \ G^{\frac{1}{2}} (t_s - t_b)_{BO} \tag{23}$$

The same form has been used by most investigators, although a term which corrects for pressure is frequently added.

Bernath[61] has presented a method of correlating subcooled burnout which assumes that the driving force for heat transfer at burnout is $(t_w - t_b)_{BO}$. This assumption permits the evaluation of a burnout heat-transfer coefficient from burnout data where the wall temperature was recorded. Bernath used Columbia data to obtain an expression for $h_{BO}$ in terms of the velocity and the hydraulic and heated diameters of the annular test sections. Data from several burnout programs were then analyzed to arrive at an equation for the wall temperature at burnout as a function of pressure and velocity.

The final equation indicates that as the velocity increases, the wall temperature at burnout decreases for constant pressure and sub-cooling. This does not seem reasonable physically and is at variance with data of most investigators. It is also evident that the wall temperature should be a function of fluid and surface condition. In general it would appear to be rather difficult to correlate burnout in terms of the variables which Bernath has chosen.

An effect of channel length was found by Jens and Lottes.[20] When attempting to correlate data of UCLA and Purdue, they found that the burnout flux was lower for longer L/D tubes, all other conditions remaining the same. The same effect was mentioned by Green, et al.[62] It is noted, however, that neither of these studies included the length as a variable in final correlations.

The generalized burnout correlation of Griffith[63] contains hydraulic diameter in the Reynolds number. The effect of diameter was not specifically investigated, however, and Griffith mentions that the correlation is probably not valid for diameters smaller than 0.18 in.

Recent Russian studies by Chirken and Iukin[64] and Kafenhaus and Bocharov[65] have indicated a strong dependence of the burnout heat flux on channel height. In both studies the burnout heat flux was found to decrease when the channel height was reduced below 2 mm.

In contrast to these results, Aladiev, et al.[66] mentioned that $(q/A)_{BO}$ for tubes of 3 mm diameter was much higher than for tubes of 8.2 mm diameter. It is presumed that other variables were held constant in this comparison; however, the data are not presented.

At the start of the present investigation, then, the effect of primary variables in subcooled burnout appeared, at least to some extent, to have been investigated. Five dependent variables have been found to influence the burnout heat flux:

$$(q/A)_{BO} = f(p, G, t_b, L, D) \tag{24}$$

At moderate pressures $(q/A)_{BO}$ increases with increasing p and G and decreases with increasing $t_b$ and L. The effect of channel height, however, has not been systematically investigated, and there is disagreement among investigators regarding its effect. Inasmuch as this study is concerned with tubes of small diameter, it was thought appropriate to investigate in greater detail the influence of tube diameter on burnout.

Secondary Variables

The above discussion has considered the major variables which have been found to influence subcooled burnout. Other variables have been studied, and it is appropriate to consider these before discussing the present experiments.

Burnout tests were run by Jacket, et al.[67] with upflow in channels inclined 45 degrees from vertical and with vertical downflow. It was

concluded that flow direction had no significant effect on burnout. The experimental results of Zenkevich and Subbotin,[68] obtained with vertical upflow or downflow, support these conclusions.

The dissolved-gas content of the system water has been found to have no effect on the burnout flux. Experiments at high pressures by Zenkevich and Subbotin[68] and DeBortoli and Masnovi[69] with dissolved-gas concentrations up to approximately 140 cc/liter support this conclusion. Gunther[51] found no effect of dissolved-air content on the burnout limit in his low-pressure studies. It must be emphasized, however, that two-phase flow can influence system stability. This effect is discussed in a later section.

Burnout tests with tubes in crossflow by Leppert, et al.[70] indicated no significant effect of surface finish. Jacket, et al.[67] concluded that neither surface material nor surface roughness affected the burnout heat flux for rectangular channels. A more extensive investigation of surface finish by Aladiev, et al.[66] also indicated no effect of roughness of the heated surface. However, Mirshak, et al.[59] did find some increase in burnout flux when the surface was roughened.

Leppert, et al.[70] found that with small amounts of volatile organic additives, there was a slight increase in peak heat flux. This was apparently due to the decrease in bubble size caused by the additives. In these experiments the largest amount of organic fluid added was 2.65 percent by weight. This amount did not materially change the properties of the mixture from those of pure water. It is apparent, however, that a larger percentage of additive would change the properties sufficiently to require a burnout correlation which is valid for different fluids.

Dissolved and adsorbed gases, surface finish, and additives appear to have little effect on the peak heat flux. It must be emphasized,

however, that these variables will shift the boiling curve and thereby influence the critical $(t_w - t_s)$. The location of the burnout point is important; however, this information is supplied from heat-transfer measurements for the particular fluid-surface combination. It is fortunate that burnout data can be taken without consideration of these secondary variables.

The thickness of the heater appears to have a significant effect on burnout. Aladiev, et al.[66] found similar burnout points with tubes of wall thickness of 0.016 and 0.079 in. Gunther,[51] however, found that his data obtained with heating strips of 0.004 in. thickness were below results obtained with thick-walled tubes. Thin-walled heaters are unable to stand hot spots caused by temporary insulation of the surface by vapor patches. Data obtained with thin-walled heaters should be considered as premature burnout data.

Another cause of low values of the burnout flux is the use of AC heating with thin-walled heaters. Alternating current results in a uniformly-distributed but periodically-varying heat source within the heater. The peak flux being absorbed is higher than the rms values of voltage and current would indicate. In the limit, the ratio of peak heat flux using DC to that using AC approaches the ratio of maximum power to rms power, which is 2 for a single-phase power source.

The only known experimental study of this phenomenon has been performed by Szetela.[71] It was found that in pool boiling with a 10 mil nichrome wire, the DC peak flux was twice as high as AC at 10 °F subcooling and 1.3 times at 35 °F subcooling. The magnitude of the difference in burnout flux between the two forms of heating is probably a complicated function of the thermal conductivity, specific heat, and

dimensions of the heater, as well as the frequency of the power supply and the magnitude of the heat-transfer coefficient.

Experimental technique can also account for the large scatter in the data of different investigators. Griffith[63] reported that premature burnout can occur if power to the test section is increased too rapidly or too unevenly. The method of approaching burnout has also been found to influence burnout. Kreith and Summerfield[13] found that burnout fluxes were higher if the subcooling or velocity was decreased than if the heat flux was increased. This effect was believed to be due to the attainment of wall-temperature equilibrium before equilibrium surface-boiling conditions were attained.

Axial-conduction errors can be expected to cause high experimental burnout heat fluxes. Thick-walled tubes of high thermal conductivity can be expected to rupture some distance from the exit. Due to the higher subcooling, the burnout heat flux will be higher than if burnout had occurred at the exit. Local instead of exit conditions should be used to describe burnout in this case. It might be noted that this is virtually the only experimental condition which will cause high experimental burnout fluxes.

Experimental Considerations

Considerable thought has been given to the definition of burnout heat flux. In the WAPD studies, for example, burnout is not considered to be the point of transition from nucleate to film boiling, but rather the point where the departure from nucleate boiling occurs (DNB). This method of defining burnout is slightly conservative as DNB will be below the maximum heat flux by several percent. The distinction is felt to be an unnecessary refinement as the actual design would provide for operation well below either point.

Silvestri[72] mentions that tube rupture is an operational definition of burnout which can be misleading. His objections are made in reference to slow burnout, which occurs at high quality, and burnout due to flow oscillation. These conditions were avoided in obtaining the present data.

Burnout protection devices have been used in various boiling projects.[19, 73] A detection circuit and a circuit breaker are the major components of such systems. The detector relies on the fact that burnout, in all sub-cooled systems at least, occurs at the test-section exit and is charac-terized by a large temperature rise of the heater. The electrical resist-ance of the final portion of the heater is compared with that of the remaining length. A sudden change in resistance of the downstream portion unbalances a bridge circuit and ultimately interrupts power to the test section. A properly-functioning burnout detector gives an accurate indica-tion of the maximum heat flux.

Although burnout protection devices are considered unreliable by some,[61] it was decided not to use one in the present study for other reasons. A burnout detector and explosive switch were available from a previous proj-ect; however, considerable modification would have been necessary to use it with the present system. The various sizes of test sections would have required substantial adjustment of the bridge circuit for each series of runs. There is also considerable danger involved in activitating the switch with dynamite caps. In addition, time and material costs were less for fabrication and replacement of a new test section than they would have been for activitation and setting of the control circuit. Furthermore, there is no doubt that a genuine burnout has occurred when the tube ruptures.

## Flow Stability in Boiling Systems

a. Flow Excursion

Recent studies have indicated that system stability must be considered when taking burnout data. Two types of instability are recognized as causing premature burnout: flow excursion and flow oscillation.

Instability due to flow excursion was first considered by Ledinegg.[74] It can be visualized in terms of the system and tube pressure-drop-versus-flow curves as shown in Fig. 35. If the system characteristic intersects the tube characteristic with a steeper negative slope than exists anywhere along the tube curve, the system is stable. With a nearly-horizontal system characteristic, for example, operation at point (b) is unstable. A slight decrease in flow causes the operating point to move rapidly to point (a). Very often the percentage of vapor at (a) is too great and burnout occurs. Instrumentation cannot follow the rapid change in flow and apparent burnout is at (b).

As noted by Clark and Rohsenow[25] and Jens,[75] the instability may be removed by increasing available pressure drop and installing a throttle valve near the test section to effectively steepen the system characteristic. For all runs in the present study, the pressure at the inlet to the test-section line was maintained at approximately 200 psi. For an exit pressure of 15 psi, this meant that the pressure drop across the tube and throttle valve was 185 psi. Normally the pressure drop across the tube did not exceed 20 psi; therefore, it can be said that the effective system characteristic was sufficiently steep to avoid burnout due to flow excursion. In any case, burnouts due to flow excursion are easy to recognize as they exhibit characteristics of quality burnout. Subcooled burnouts caused a relatively clean rupture of the tubes, whereas the

fracture in quality burnout was large and jagged. No unusual subcooled burnouts were found.

b. Flow Oscillations

The problem of oscillations in two-phase-flow systems has become of great interest to engineers in recent years. The problem can be briefly summarized. The generation of steam in either subcooled or bulk boiling can give rise to periodic perturbations, followed by corresponding changes in the hydraulic resistance of the heated channel. The magnitude of these fluctuations depends on characteristics of the system preceding the heated section. A compressible volume, consisting of a bourdon gage, flexible hose, air pocket, etc., can exist in this preceding section. The resistance fluctuations in the heated channel cause periodic compressions of the medium in the preceding section and temporary decrease of the flow in the heated tube. These oscillations can be stable if the amplitude is such that the tube does not pass into the burnout condition. Even if the burnout condition is reached, the period of oscillation may be so short that physical destruction of the tube does not occur.

Oscillating conditions were observed in the Laboratory with a stainless-steel test section where the flow discharged to the atmosphere. At a certain heat flux where the exit subcooling was 30 $^{o}$F, the discharge practically ceased, and film boiling began at the downstream end of the tube and moved upstream. The glowing then suddenly receded, and a mixture of steam and water was discharged from the tube. This sequence of events proceeded at an almost constant period of 5 sec. until the tube failed after 20 min. from the thermal fatigue. The necessary compressible volume was believed to have been supplied by an air pocket, or perhaps merely the mass of water between the test section and the flow-control

valve. It is emphasized that these oscillations took place with a sub-cooled system.

Flow oscillations can be caused by the compressibility of the fluid in the heated tube itself as shown in the analytical and experimental investigation of Quandt.[76] Aladiev, et al.[66] obtained burnout under pulsating conditions where the compressibility was provided by an expander filled with superheated steam, water heated to the saturation temperature, or nitrogen. The same results were obtained when a two-phase mixture entered the test section. The data obtained under the latter condition are similar to those presented by Silvestri[72] for burnout in a steam-water system.

Lowdermilk, et al.[77] determined the effect of a flow restriction preceding the heated section on burnout heat flux. It was found that a definite pressure drop across the throttle valve was necessary to achieve non-oscillating conditions, and thereby stable burnout. In this case, the valve served to isolate the test section from the remainder of the system, which due to its large mass was compressible to some extent. A system of infinite stiffness or zero compressibility is certainly not possible; however, the results of Lowdermilk, et al. indicate that the stiffness need be only above a certain critical value for the burnout to be stable. It is noted that instability due to both flow excursion and flow oscillation can be eliminated by installation of a throttle valve near the test section. For this reason the two phenomena are often confused.

It is important to mention that data obtained under conditions of flow oscillation are reproducible for a given system. This accounts for the fact that data are often not questioned for possible error due to

system oscillations. The fact remains, however, that the highest burnout flux obtained for a given system will represent the true value.

## Experimental Procedures

The procedures followed in this study with respect to the secondary variables are now summarized:

1. All experiments were run with the test sections in the horizontal position.

2. System water was degassed only periodically; care was taken, however, not to trap air in the line when installing new test sections.

3. Tubes were used as manufactured except for a thorough cleaning of the inside surface with acetone. System water was continually deionized during operation to avoid fouling.

4. No additives were introduced into the system.

5. The tube wall thickness varied from 0.00625 in. for 23 ga stainless tubing to 0.015 in. for nickel tubing.

6. Direct-current heating was used for all runs.

7. The power was increased as gradually as the control circuit would allow.

8. Burnout was approached in all cases by increasing the heat flux at constant flow rate. Simultaneously, the subcooling was regulated by means of the preheater and, if necessary, with the heat exchanger.

9. Burnout occurred in virtually all cases at the tube exit; accordingly, exit conditions were considered burnout conditions.

Inlet and outlet temperatures were monitored with the usual thermocouple arrangements. At low flow rates there was considerable heat loss from the water between the thermocouples and the tube. A calibration procedure was developed to correct the measured temperatures to actual values at the tube inlet and exit.

A pressure tap was located in the piping somewhat downstream of the tube exit. It was assumed that the rapid expansion of the flow into the exit fittings consumed all of the velocity head. As the velocity head at the pressure tap was negligible due to the large-diameter fitting, the pressure gage then indicated the approximate static pressure at the tube exit. It was necessary to extend each tube approximately 1/8 in. into the current bushings in order to have a good solder connection. However, the pressure drop in this unheated section was not considered to have caused significant error in the evaluation of the exit pressure.

A multi-channel recorder would have been necessary to record all pertinent variables directly at burnout. Without this equipment, it was necessary to estimate certain quantities at the burnout point. Complete data for the inlet and outlet temperatures, flow rate, tube voltage, pressure, and shunt reading were recorded periodically as the power was increased. At burnout, however, only the voltmeter reading and a recorder indication of one temperature or shunt voltage could be obtained. Sufficiently small increments of power were taken so that missing information could be readily inferred from previous data.

Experimental Results

An experimental program was undertaken to investigate the effect of velocity, subcooling, length, and diameter on burnout in tubes under conditions of forced convection. As the system is limited to relatively low pressures, no attempt was made to ascertain the effect of pressure variation, and the outlet pressure was maintained at approximately 15.5 psi for all runs.

The effect of quality was investigated as shown in the raw-data plot of Fig. 36. At high subcooling the burnout heat flux decreases

monatonically as the subcooling is decreased. The data are then seen to
pass through a minimum at low subcooling and finally increase in the bulk-
boiling region. The range of quality covered represents the maximum possi-
ble on the system with velocity, pressure, and geometry fixed as shown.

The variation of burnout flux in the quality region has been shown
to be extremely complicated.[78] Quality burnout will be investigated at
a later phase of this project; it was not considered in detail in the
present study.

The relation of burnout flux to quality in the subcooled region can
be explained in terms of two-phase-flow considerations. At low values of
subcooling the void fraction, or volume fraction occupied by steam, becomes
appreciable. This causes an increase in the average velocity with the
result that the burnout limit is raised. In the quality region the velocity
increases with increasing quality, and the burnout limit continues to
increase. The increased velocity apparently aids in removing the bubbles
from the wall, thus preventing the formation of vapor patches which cause
burnout.

A correlation of subcooled burnout data was proposed recently by
Zenkevich:[60]

$$(q/A)_{BO} = h_{fg} \sqrt{\frac{\sigma_s g_o G}{\nu_b}} \left[ 2.5 + 184 \left(\frac{h_g - h_o}{h_{fg}}\right) \right] \times 10^{-5} \qquad (25)$$

The primary variables are seen to be mass velocity and subcooling. The
other variables are included mainly to form dimensionless groups.
Zenkevich checked the existing data and concluded that the burnout flux
was essentially independent of pressure between 1 and 20 atm. According
to Zenkevich the effects of changes in the physical parameters $h_{fg}$, $\sigma_s$,

and $V_b$ mutually cancel for changes in water pressure between 1 and 20 atm. Therefore, the inclusion of these parameters should introduce no extraneous pressure effect when the data are reduced.

Burnout limits predicted by the Zenkevich correlation are indicated in Fig. 36. It is seen that the present data lie substantially above this prediction. It seems appropriate to look to geometrical considerations to explain the deviation. A summary of the channel dimensions included in the Zenkevich correlation follows:

McAdams, et al.[18]                     Annulus, $D_e$ = 0.52 in.

Gunther[51]                             Rectangular Channel, $D_e$ = 0.189

Chirkin - Iukin[64]                     Annulus, $D_e$ = 0.158 - 0.44

Kutateladze - Borishanskii[79]          Pipe with heater inserts, $D_e$ = 0.45 - 0.65

It is seen that the channel sizes considered are relatively large compared to the 0.094 in. ID tube used in this study.

In order to investigate the influence of diameter on burnout, tests were run at two velocities for all tube sizes considered in this study: 0.1805, 0.094, 0.0465, and 0.023 in. ID. The results as shown in Fig. 37 indicate a strong inverse dependence of the burnout flux on diameter. The Zenkevich prediction is shown as a possible asymptote at each of the velocities. It appears that if the present study were extended to larger tube sizes, the burnout data would agree with the predictions of Zenkevich.

Several points are also indicated showing the effect of system compressibility on burnout. For D = 0.023 in., the burnout flux was relatively low when the upstream flow-control valve was used. When the throttle valve was located near the test section, the peak fluxes were much higher. Apparently the mass of water between the valve and test section in the first case was sufficient to cause flow oscillation and

premature burnout. The volume of these smallest tubes was so small that only a very little compressible volume was needed to cause a large temporary decrease in flow through the test section. With the larger-diameter tubes, the data were generally independent of valve placement. Premature burnouts were, however, observed with large-diameter tubes with the upstream valve placement if the inlet-water temperature was sufficiently high.

The diameter effect on stable burnout does not agree with the results of Chirkin and Iukin[64] and Kafenhaus and Bocharov.[65] The only explanation for this seems to be that these investigators had premature burnout due to flow oscillations. Valve locations are not clearly indicated in these papers; however, manometers were installed near the entrance to the test sections. The pressure instrumentation alone could have provided enough compressible volume to cause flow oscillations. The observed decrease in burnout flux with decreasing channel height is quite reasonable in a soft system. As the channel volume is decreased, a given compressible volume will exert a greater influence on the flow. The greater the amplitude of flow oscillation, the lower the burnout flux will be.

The increase of burnout heat flux with decreasing diameter suggests that the void fraction also increases with decreasing diameter. It is probable that the burnout heat flux can be directly related to the void fraction. However, the void fraction itself is a complex function of the same variables which determine burnout.[80] Due to the complexity of the boiling process, the approach to the prediction of void fractions must be almost completely empirical. Limited research has been carried out in this area, and no data are available for low pressures. Even if such data were available, it would seem rather superfluous to include

void fraction among the variables influencing burnout. The same information is already contained in the major burnout variables discussed earlier.

The results of an investigation of the dependence of burnout on L/D are shown in Fig. 39. The burnout flux is seen to be inversely dependent on the L/D ratio. This result concurs with observations of other investigators noted previously. The behavior is very similar to that observed with non-boiling forced-convection systems, suggesting that the bubble boundary layer also requires a certain length to become fully developed. No change in burnout heat flux was noted when the calming length was changed from 0.16 to 1.6 in.

Burnout data obtained in this study are presented in Appendix E. No attempt was made to correlate the burnout data obtained in this study. A more complete systematic variation of the pertinent variables will be required before a general correlation can be attempted. It has been shown that such a correlation must include terms accounting for the influence of tube diameter and length on the burnout heat flux.

## Summary of Burnout Studies

The burnout heat flux under conditions of forced convection and subcooling is shown to be a complicated function of subcooling at low values of subcooling. This appears to be due to the velocity increase caused by the relatively large volume fraction of vapor.

It is necessary to include geometry in the description of burnout for small channels. Burnout flux is shown to increase with decreasing tube diameter. This effect can be attributed to an increase in void fraction with decreasing tube diameter. Entrance effects are significant in forced-convection surface boiling as shown by the decrease of burnout flux with increasing length.

Flow oscillations caused by system compressibility can greatly reduce the burnout heat flux in the subcooled region. This instability is particularly difficult to avoid with tubes of very small diameter. Previously-reported studies of subcooled burnout in small channels indicated that the burnout flux decreases with decreasing channel height. However, it is believed that these data were obtained under unstable conditions. The data of the present study can be considered to indicate the actual dependence of burnout flux on diameter.

# REFERENCES

1  Rohsenow, W. M., Somma, E. H., and Osborn, P. V., "Construction and Operation of Apparatus for Study of Heat Transfer with Surface Boiling," M.I.T. Heat Transfer Lab. Technical Report No. 2, D.I.C. 6627, July 1, 1950.

2  Clark, J. A. and Rohsenow, W. M., "Local Boiling Heat Transfer to Water at Low Reynolds Numbers and High Pressure," M.I.T. Heat Transfer Lab. Technical Report No. 4, D.I.C. 6627, July 1, 1952.

3  Kreith, F. and Summerfield, M., "Investigation of Heat Transfer at High Heat Flux Densities: Experimental Study with Water of Friction Drop with and without Surface Boiling in Tubes," Jet Propulsion Lab. C.I.T., Progress Report No. 4-68, 1948.

4  Clark, J. A., Discussion in Trans. ASME, October, 1958, pp. 1402-1403.

5  Hoyt, S. L., ed., "Metals Properties," ASME Handbook, McGraw-Hill, 1953.

6  McAdams, W. H., "Heat Transmission," Third Edition, McGraw-Hill, 1954.

7  Driver-Harris Co., "Nichrome and Other High Nickel Electrical Alloys," Catalog R-46, 1947.

8  Miner, D. F., ed., "Handbook of Engineering Materials," Wiley, 1955.

9  Mathews, R., Personal communication from Superior Tube Co., January 18, 1962.

10  Rayle, R. E., "Influence of Orifice Geometry on Static Pressure Measurements," ASME Paper No. 59-A-234, 1959.

11  Eckert, E. R. G. and Drake, R. M., Jr., "Heat and Mass Transfer," McGraw-Hill, 1959.

12  Dorsey, N. E., "Properties of Ordinary Water-Substance," Reinhold, 1953.

13  Kreith, F. and Summerfield, M., "Heat Transfer to Water at High Flux Densities With and Without Surface Boiling," Trans. ASME, October, 1949.

14  Mosciki, I. and Broder, J., "Discussion of Heat Transfer from a Platinum Wire Submerged in Water," Rocznicki Chemje, Vol. 6, 1926. (English translation on file at Engineering Research Laboratory Experimental Station, E. I. DuPont de Nemours and Company, Wilmington, Del.)

15 Nukiyama, S., "The Maximum and Minimum Values of Heat q Transmitted from Metal Surface to Boiling Water Under Atmospheric Pressure," J. Society of Mechanical Engineers (Japan), Vol. 37, 1934. (Translation given in Appendix K of Reference 53)

16 Rohsenow, W. M. and Clark, J. A., "Heat Transfer and Pressure Drop Data for High Heat Flux Densities to Water at High Subcritical Pressures," 1951 Heat Transfer and Fluid Mechanics Institute Preprints, Stanford University Press, 1951.

17 Rohsenow, W. M., "Heat Transfer with Evaporation," Chapter in "Heat Transfer," University of Michigan Press, 1953.

18 McAdams, W. H., et al., "Heat Transfer at High Rates to Water with Surface Boiling," Industrial and Engineering Chemistry, September, 1949.

19 Buchberg, H., et al., "Studies in Boiling Heat Transfer," Final Report AEC Research Contract No. AT-11-1-Gen 9, Department of Engineering, University of California, March 1951.

20 Jens, W. H. and Lottes, P. A., "Analysis of Heat Transfer, Burnout, Pressure Drop and Density Data for High-Pressure Water," Argonne National Laboratory Report 4627, May 1, 1951.

21 Lurie, H. and Johnson, H. A., "Transient Pool Boiling of Water on a Vertical Surface With a Step in Heat Generation," ASME Paper No. 61-WA-161, 1961.

22 Kennel, W. E., "Local Boiling of Water and Superheating of High Pressure Steam in Annuli," Sc.D. Thesis in Chemical Engineering, Massachusetts Institute of Technology, 1948.

23 Gunther, F. C. and Kreith, F., "Photographic Study of Bubble Formation in Heat Transfer to Subcooled Water," Jet Propulsion Laboratory, California Institute of Technology, Progress Report No. 4-120, March 9, 1950.

24 Engelberg-Forster, K. and Greif, R., "Heat Transfer to a Boiling Liquid - Mechanism and Correlations," Trans. ASME Journal of Heat Transfer, February, 1959.

25 Clark, J. A. and Rohsenow, W. M., "Local Boiling Heat Transfer to Water at Low Reynolds Numbers and High Pressures," Trans. ASME, Vol. 76, No. 4, May, 1954.

26 Bernath, L. and Begell, W., "Forced-Convection, Local-Boiling Heat Transfer in Narrow Annuli," Chemical Engineering Progress Symposium Series, Vol. 55, No. 29, 1959.

27 Colburn, A. P., "A Method of Correlating Forced Convection Heat Transfer Data and a Comparison with Fluid Friction," Trans. AIChE, Vol. 29, 1933, pp. 174-220.

28  Sieder, E. N. and Tate, G. E., "Heat Transfer and Pressure Drop of Liquids in Tubes," Ind. Eng. Chem., Vol. 28, 1936, pp. 1429-1436.

29  McAdams, W. H., "Heat Transmission," Second Edition, McGraw-Hill, 1942, p. 168.

30  Dittus, F. W. and Boelter, L. M. K., "Heat Transfer in Automobile Radiators of the Tubular Type," University of California Publications in Engineering, Vol. 2, 1930, p. 443.

31  Desmon, L. G. and Sams, E. W., "Correlation of Forced-Convection Heat-Transfer Data for Air Flowing in Smooth Platinum Tube with Long-Approach Entrance at High Surface and Inlet-Air Temperatures," NACA RM E50H23, 1950.

32  Al-Arabi, M., "Study of Existing Data for Heating of Air and Water in Turbulent Flow in Inside Tubes," ASME Paper No. 58-A-298, 1958.

33  Owens, W. L. and Schrock, V. E., "Pressure Gradients and Heat Transfer in Forced Convection Boiling of Subcooled Water," Univ. of Calif., Berkeley, Inst. of Engr. Res. Report Ser. 73308-UCX2182, June, 1959.

34  Deissler, R. G., "Turbulent Heat Transfer and Friction in the Entrance Region of Smooth Passages," Trans. ASME, Vol. 77, November, 1955, p. 1221-1233.

35  Hartnett, J. P., "Experimental Determination of the Thermal Entrance Length for the Flow of Water and of Oil in Circular Pipes," Trans. ASME, Vol. 77, November, 1955, p. 1211-1220.

36  Linke, W. and Kunze, H., Allgemeine Waermetechnik, Vol. 4, 1953.

37  Rohsenow, W. M., "Heat Transfer with Boiling," Notes for Modern Developments in Heat Transfer, M.I.T. Summer Session, 1960.

38  Bankoff, S. G., "Ebulliton from Solid Surfaces in Absence of Pre-existing Gaseous Phase," Heat Transfer and Fluid Mech. Inst., Stanford University Press, 1956.

39  Hsu, Y. Y. and Graham, R. W., "An Analytical and Experimental Study of the Thermal Boundary Layer and Ebullition Cycle in Nucleate Boiling," NASA TN D-594, May, 1961.

40  Han, C. Y. and Griffith, P., "The Mechanism of Heat Transfer in Nucleate Pool Boiling," Technical Report No. 7673-19, Department of Mechanical Engineering, M.I.T., March 30, 1962.

41  Bankoff, S. G., "The Prediction of Surface Temperatures at Incipient Boiling," Chem. Eng. Prog. Symposium Series, Vol. 55, No. 29, 1959.

42  Hsu, Y. Y., "On the Size Range of Active Nucleation Cavities on a Heating Surface," ASME Paper No. 61-WA-177, 1961.

43  Mantzouranis, B. G., Ph.D. Thesis, University of London, 1959.

44  Haselden, G. G., "The Problem of Predicting Heat Transfer to Two-Phase (Vapour-Liquid) Fluids at Moderate Pressures," Paper presented at the Institution of Mechanical Engineers Symposium on Two-Phase Fluid Flow, London, February 7, 1962.

45  Rohsenow, W. M., "A Method of Correlating Heat-Transfer Data for Surface Boiling of Liquids," Trans. ASME, August, 1952.

46  Gilmour, C. H., "Nucleate Boiling - a Correlation," Chem. Eng. Prog. Vol. 54, No. 10, 1958.

47  Levy, S., "Generalized Correlation of Boiling Heat Transfer," Trans. ASME, Journal of Heat Transfer, February, 1959.

48  Kreith, F. and Foust, A. S., "Remarks on the Mechanism and Stability of Surface-Boiling Heat Transfer," ASME Paper No. 54-A-146, 1954.

49  Bankoff, S. G., "On the Mechanism of Subcooled Nucleate Boiling; Part I: Preliminary Considerations, Part II: Sequential Rate Process Model," AIChE Preprints 19 and 20 for Fourth National Heat Transfer Conference, August, 1960.

50  Gunther, F. C., "Photographic Study of Surface-Boiling Heat Transfer to Water with Forced Convection," Progress Report No. 4-75, C.I.T. Jet Propulsion Laboratory, June 28, 1950.

51  Gunther, F. C., "Photographic Study of Surface-Boiling Heat Transfer to Water with Forced Convection," Trans. ASME, February, 1951.

52  Rears, G., Jr., Personal communication from E. I. duPont deNemours & Company, March 9, 1962.

53  Addoms, J. N., "Heat Transfer at High Rates to Water Boiling Outside Cylinders," Sc.D. Thesis in Chemical Engineering, M.I.T., May, 1948.

54  Walsh, J. B., "Forced Convective Heat Transfer with Surface Boiling," S. M. Thesis in Mechanical Engineering, M.I.T., May, 1954.

55  Jakob, M., "Heat Transfer," Volume I, John Wiley & Sons, 1949.

56  Rallis, C. J., Greenland, R. V., and Kok, A., "Stagnant Pool Boiling From Horizontal Wires Under Saturated and Sub-Cooled Conditions," The South African Mechanical Engineer, January, 1961.

57  Long, R. A. K., "Personal communication to W. M. Rohsenow, August, 1959.

58  Carpenter, F. G., Colburn, A. P., Schoenborn, E. M., and Wurster, A., Trans. AIChE, Vol. 42, 1946, pp. 165-187.

59  Mirshak, S., Durant, W. S., and Towell, R. H., "Heat Flux at Burnout," DP-355, February, 1959.

60  Zenkevich, B. A., "The Generalization of Experimental Data on Criti-
cal Heat Fluxes in Forced Convection of Sub-Cooled Water," J. Nucl.
Energy, Part B:  Reactor Technology, Vol. 1, 1959, pp. 130-133.

61  Bernath, L., "A Theory of Local Boiling Burnout and Its Application
to Existing Data," AIChE Preprint 110 for Third National Heat Trans-
fer Conference, August, 1959.

62  Green, S. J., Le Tourneau, B. W., and Troy, M., "Forced Circulation
Uniform Flux Burnout Studies for High-Pressure Water," ASME Paper
No. 59-HT-25, 1959.

63  Griffith, P., "The Correlation of Nucleate Boiling Burnout Data,"
ASME Paper No. 57-HT-21, 1957.

64  Chirkin, V. A. and Iukin, V. P., "Critical Point in Heat Removal
From Boiling Water Flowing Through an Annular Gap," J. Tech. Physics
U.S.S.R., Vol. 26, 1956, pp. 1503-1515.

65  Kafenhaus, H. L. and Bocharov, I. D., "The Influence of Annular Gap
Width on Heat Transfer to Water," Teploenergetica, Vol. 3, 1959,
pp. 76-78.

66  Aladiev, I. T., Miropolsky, Z. L., Doroshchuk, V. E., and Styrikovich,
M. A., "Boiling Crisis in Tubes," International Heat Transfer Confer-
ence, Published by ASME, 1961.

67  Jacket, H. S., Roarty, J. D., and Zerbe, J. E., "Investigation of
Burnout Heat Flux in Rectangular Channels at 2000 psia," Trans. ASME,
Vol. 80, 1958.

68  Zenkevich, B. A. and Subbotin, B. I., "Critical Heat Fluxes in Sub-
Cooled Water with Forced Circulation," J. Nucl. Energy, Part B:
Reactor Technology, Vol. 1, 1959, pp. 134-140.

69  DeBortoli, R. A. and Masnovi, R., "Effect of Dissolved Hydrogen on
Burnout for Water Flowing Vertically Upward in Round Tubes at
2000 psia," WAPD-TH-318, April, 1957.

70  Leppert, G., Costello, C. P., and Hoglund, B. M., "Boiling Heat
Transfer to Water Containing a Volatile Additive," Trans. ASME,
October, 1958, pp. 1395-1404.

71  Szetela, E. J., "Peak Heat Flux for Water Using Direct and Alternat-
ing Electrical Power," Unpublished Paper, Pratt and Whitney Aircraft,
Division of United Aircraft.

72  Silvestri, M., "Two-Phase (Steam and Water) Flow and Heat Transfer,"
International Heat Transfer Conference, Published by ASME, 1961.

73  Raymond, M. W. and Reynolds, J. M., "Description of Boiling Project
Burnout Detector," M.I.T. Heat Transfer Lab. Technical Report No. 11,
D.S.R. 7673, July 1, 1957.

74  Ledinegg, M., "Unstabilitaet der Stroemung bei Natuerlichem und Zwangumlauf," Die Waerme, Vol. 61, No. 48, 1938, pp. 891-898.

75  Jens, W. H., "Boiling Heat Transfer:  What Is Known About It," Mechanical Engineering, December, 1954, pp. 981-986.

76  Quandt, E. R., "Analysis and Measurement of Flow Oscillations," AIChE Preprint 27 for Fourth National Heat Transfer Conference, August, 1960.

77  Lowdermilk, W. H., Lanzo, C. D., and Siegel, B. L., "Investigation of Boiling Burnout and Flow Stability for Water Flowing in Tubes," NACA TN 4382, September, 1958.

78  Collier, J. G., "The Problem of Burnout in Liquid Cooled Nuclear Reactors," AERE - R 3698, 1961.

79  Kutateladze, S. S. and Borishanskii, V. M., Energomashinostroenie, No. 2, 1957, p. 10.

80  Lottes, P. A., Petrick, M., and Marchaterre, J. F., "Lecture Notes on Heat Extraction From Boiling Water Power Reactors," ANL-6063, October, 1959.

## APPENDIX A

### PROPERTIES OF TUBING USED IN TEST-SECTION ASSEMBLIES

| Type | | Manufacturer | Material | Dimensions (measured) | | Process |
|---|---|---|---|---|---|---|
| | | | | OD | ID | |
| 20 gage | Hypoflex hypodermic needle tubing | Superior Tube Co. Norristown, Pa. | AISI Type 304 stainless steel | 0.035 in. | 0.023 in. | Cold drawn, no inside plug, outside polished |
| 16 gage | = | = | = | 0.0645 | 0.0465 | = |
| 11 gage | = | = | = | 0.120 | 0.094 | = |
| Special | | Int'l. Nickel Co. Drawn by D. E. Makepeace Attleboro, Mass. | A nickel | 0.2105 | 0.1805 | Cold drawn, inside plug |

## APPENDIX B

## TEMPERATURE DROP THROUGH TUBE WALL

The solution for the inner-wall temperature as obtained by Kreith and Summerfield[3] is given below:

$$t_w = t_{ow} - \Delta t_w$$

$$= t_{ow} - \frac{m(D_o - D_i)^2}{4(1 + \alpha_\rho t_{ow})(1 + \alpha_k t_{ow})} - \frac{m(D_o - D_i)^3}{12 D_o(1 + \alpha_\rho t_{ow})(1 + \alpha_k t_{ow})}$$

$$- \left[ \frac{m^2(3\alpha_k + 4\alpha_\rho\alpha_k t_{ow} + \alpha_\rho)}{6(1 + \alpha_\rho t_{ow})^3(1 + \alpha_k t_{ow})^3} + \frac{m}{D_o^2(1 + \alpha_\rho t_{ow})(1 + \alpha_k t_{ow})} \right] \times$$

$$\frac{(D_o - D_i)^4}{16} \tag{B1}$$

where

$$m = 3.413 \, (de/dx)^2 / 2 \, \rho_e' \, k' \tag{B2}$$

As shown by reference 1, Eq. (B2) can be expressed in terms of current as follows:

$$m = 8 \times 3.413 \, \bar{\rho}_e^2 \, i^2 / \rho_e' \, k' \, \pi^2 (D_o^2 - D_i^2)^2 \tag{B3}$$

where the mean resistivity is evaluated at the average wall temperature. The average wall temperature is given to sufficient accuracy by

$$\bar{t}_t = (t_{ow} + t_w)/2 \tag{B4}$$

If heat is transferred instead through the outside surface of the tube, it can be shown that Eq. (B1) is valid if $t_{ow}$ is replaced by $t_{iw}$ and the sign of the third term on the right is made positive.

# APPENDIX C

## AIR-CONTENT ANALYSIS

A standard Winkler technique was used to determine the quantity of dissolved oxygen in the system water. Henry's Law, which relates dissolved air to dissolved oxygen, was then used to calculate the quantity of dissolved air.

A 250 cc glass-stoppered bottle was filled with water from the test loop. The filling tube was withdrawn only after the water overflowed for several minutes. Most of the water which had come in contact with air should have been removed by this procedure.

The following reagents were used in the analysis:

1. 480 gm $MnSO_4$ in one liter water.

2. 100 gm NaOH and 360 gm KI in one liter water.

3. Concentrated $H_2SO_4$ diluted 1:1 with distilled water.

4. 5 gm starch in 100 cc water.

5. 0.01 normal solution $Na_2S_2O_3$

Two cc of reagents 1, 2, and 3 were added to the sample in order. Several cc of starch solution were added, turning the sample blue, and 100 cc of this solution were titrated with reagent 5.

Chemical reagents were introduced at the bottom of the sample through graduated pipettes. It was assumed that the dissolved air in the water displaced by the reagents was the same order of magnitude as the air which dissolved at the water surface. After the $H_2SO_4$ addition, any oxygen going into solution had no effect on the titration. More consistent results were obtained by running in a fixed amount of $Na_2S_2O_3$, shaking the solution, and slowly titrating to a colorless end point, rather than slowly titrating throughout.

The following equation relates the amount of oxygen to sample size
and cc and normality of the thiosulfate solution:

$$\text{cc } O_2/\text{liter} = 5600 \text{ (N thio) (cc thio)}/(\text{cc sample}) \tag{C1}$$

From Henry's Law,

$$\text{cc air/liter} = 2.9(\text{cc } O_2/\text{liter}) \tag{C2}$$

# APPENDIX D

## SAMPLE CALCULATION SHEET

TEST SECTION 14

D = 0.094 in.
Heated L = 2.93 in.

Calming L = 2.55 in.
Thermocouples at L = 1.35, 2.25 in.

Pressure taps 0.065 in. either side of heated section, $L_p$ = 3.06 in.

| | ① | ② | ③ | ④ | ⑤ | ⑥ | ⑦ | ⑧ | ⑨ | ⑩ | ⑪ | ⑫ | ⑬ | ⑭ |
|---|---|---|---|---|---|---|---|---|---|---|---|---|---|---|
| TEST NO. | SCALE* | $w$ | $P_i$* | $P_o$* | $P_i - P_o$ | $\frac{\Delta P}{L_p}$ | $P_1$ | $P_2$ | $P$ | $t_s$ | $t_i$* | $t_i$ | $t_o$* | $t_o$ |
| | | lbm/hr | psi | | | psi/in | | | psia | °F | mv | °F | mv | °F |
| | | from Fig. 5 | | | ④ − ③ | ⑤/3.06 | ③ − 1.42⑥ | ③ − 2.52⑥ | ⑦ + 14.7<br>⑧ + 14.7 | | | | | |
| 14-1-1-1 | 0.28 | 300.5 | 24.6 | 21.0 | 3.6 | 1.18 | 22.9 | | 57.6 | 268.5 | .521 | 46.9 | .966 | 67.0 |
| 14-1-1-2 | | | | | | | | 21.9 | 56.6 | 261.9 | | | | |
| 14-1-2-1 | 0.25 | 300.5 | 24.6 | 21.0 | 3.6 | 1.18 | 22.9 | | 57.6 | 268.5 | .524 | 47.0 | .872 | 71.8 |
| 14-1-2-2 | | | | | | | | 21.9 | 56.6 | 261.9 | | | | |
| 14-1-7-1 | 0.25 | 300.5 | 26.5 | 21.9 | 3.6 | 1.18 | 23.8 | | 58.5 | 264.9 | .541 | 47.8 | 1.213 | 86.8 |
| 14-1-7-2 | | | | | | | | 22.8 | 57.5 | 263.4 | | | | |
| 14-1-8-1 | 0.28 | 300.5 | 26.0 | 21.8 | 4.2 | 1.37 | 24.1 | | 58.8 | 265.4 | .551 | 48.2 | 1.466 | 97.8 |
| 14-1-8-2 | | | | | | | | 22.8 | 57.5 | 263.4 | | | | |

| | ⑮ | ⑯ | ⑰ | ⑱ | ⑲ | ⑳ | ㉑ | ㉒ | ㉓ | ㉔ | ㉕ | ㉖ | ㉗ | ㉘ |
|---|---|---|---|---|---|---|---|---|---|---|---|---|---|---|
| TEST NO. | $h_o$ | $h_i$ | $h_o - h_i$ | | $V_s$* | $i$ | $V_t$* | | $t_{ow}$* | $t_{ow}$ | $\overline{\Delta t_w}$ | $t_w$ | $\bar{t}_t$ | |
| | Btu/lbm | | | Btu/hr | mv | amps | volts | Btu/hr | mv | °F | | | | |
| | | | ⑮ − ⑯ | ⑰ × ② | | ⑲ × 60.17 | | ⑳ · ㉑ × 3.415 | | | from Fig. 8 | ㉔ − ㉕ | ㉔ − ㉖/2 | ㉗ × [illegible] |
| 14-1-1-1 | 35.05 | 14.96 | 20.09 | 6037 | 4.820 | 290.0 | 6.27 | 6206 | 5.669 | 264.4 | 51.7 | 212.7 | 238.8 | .165 |
| 14-1-1-2 | | | | | | | | | 5.682 | 264.9 | | 213.2 | | |
| 14-1-2-1 | 39.84 | 15.07 | 24.77 | 7445 | 5.282 | 317.8 | 6.98 | 7571 | 6.816 | 306.1 | 65.1 | 243.0 | 274.7 | .188 |
| 14-1-2-2 | | | | | | | | | 6.825 | 306.4 | | 243.3 | | |
| 14-1-7-1 | 54.80 | 15.87 | 38.93 | 11,700 | 6.535 | 393.2 | 8.96 | 12,020 | 9.568 | 394.7 | 95.4 | 299.5 | 346.9 | .237 |
| 14-1-7-2 | | | | | | | | | 9.561 | 394.5 | | 299.1 | | |
| 14-1-8-1 | 65.77 | 16.27 | 49.50 | 14,880 | 7.518 | 440.3 | 10.13 | 15,220 | 10.449 | 450.9 | 119.4 | 311.5 | 371.1 | .254 |
| 14-1-8-2 | | | | | | | | | 10.441 | 450.6 | | 311.2 | | |

| | ㉙ | ㉚ | ㉛ | ㉜ | ㉝ | ㉞ | ㉟ | ㊱ | ㊲ | ㊳ | ㊴ | ㊵ | ㊶ | ㊷ |
|---|---|---|---|---|---|---|---|---|---|---|---|---|---|---|
| TEST NO. | | $\rho_e$ | $i^2$ | $\rho_e i^2$ | | $q$ | $\frac{q}{A}$ | $\frac{\Delta h}{L}$ | $h_1$ | $h_2$ | $t_b$ | $t_w - t_b$ | $t_w - t_s$ | $t_s - t_b$ |
| | | ohm-ft | | | Btu/hr. | | Btu/hr ft² | Btu/lbm in | Btu/lbm | | | | | |
| | 1 + ㉘ | ㉙ × 2.26×10 | ⑳² | ㉚ × ㉛ | ㉜ × 27,800 | [⑱ + ㉒ + ㉝]/3 | ㉞ × 166.5 | ㉞/2.93·② | ㊱ × 1.35 + ⑯ | ㊱ × 2.25 + ⑯ | | ㉖ − ㊴ | ㉖ − ⑩ | ⑩ − ㊴ |
| 14-1-1-1 | 1.163 | 2.576 | 84,100 | .2166 | 5957 | 6067 | 1.010 | 6.89 | 24.26 | | 56.2 | 156.5 | N.B. | |
| 14-1-1-2 | | | | | | | | | | 50.46 | 62.4 | 150.8 | N.B. | |
| 14-1-2-1 | 1.188 | 2.631 | 101,000 | .2657 | 7307 | 7440 | 1.239 | 8.15 | 26.48 | | 58.4 | 184.6 | N.B. | |
| 14-1-2-2 | | | | | | | | | | 54.08 | 66.0 | 177.3 | N.B. | |
| 14-1-7-1 | 1.237 | 2.740 | 154,600 | .4236 | 11,650 | 11,790 | 1.963 | 13.59 | 33.95 | | 65.9 | 233.4 | 34.4 | 199.0 |
| 14-1-7-2 | | | | | | | | | | 46.00 | 78.0 | 224.1 | 35.7 | 185.4 |
| 14-1-8-1 | 1.254 | 2.778 | 193,900 | .5387 | 14,810 | 14,970 | 2.493 | 17.00 | 39.22 | | 71.2 | 240.3 | 46.1 | 194.2 |
| 14-1-8-2 | | | | | | | | | | 54.52 | 86.5 | 224.7 | 47.8 | 176.9 |

| | ㊸ | ㊹ | ㊺ | ㊻ | ㊼ | ㊽ | ㊾ | ㊿ | (51) | (52) | (53) | (54) | (55) | (56) |
|---|---|---|---|---|---|---|---|---|---|---|---|---|---|---|
| TEST NO. | $h$ | $G$ | $\mu_b$ | $Re_b$ | $Pr_b$ | $k_b$ | $Nu_b$ | $Pr_b^{0.4}$ | $\frac{Nu_b}{Pr_b^{0.4}}$ | $\frac{Nu_b}{Pr_b^{0.4}}$ | $Nu_b$ | $h$ | $\left(\frac{q}{A}\right)_{FC}$ | $\left(\frac{q}{A}\right)_B$ |
| | Btu/hr ft² F | lbm/hr ft² | lb/hr ft | | | Btu/hr ft F | | | | | | Btu/hr ft² F | Btu/hr ft² | |
| | ㉟/㊵ | | | .00[illegible] ㊹/㊺ | | | .00785 ㊸/㊽ | ㊼^0.4 | ㊾/㊿ | from Fig. 25 | (52) × ㊿ | (53) · ㊽/.00785 | ㊵ × (54) | ㉟ − (55) |
| | | ×10⁶ | | | | | | | | | | | ×10⁶ | ×10⁶ |
| 14-1-1-1 | 6454 | 6.23 | 2.88 | 16,940 | 8.50 | .3355 | 150.7 | 2.35 | 64.1 | | | | | |
| 14-1-1-2 | 6698 | | 2.64 | 18,480 | 7.65 | .3397 | 154.4 | 2.25 | 68.6 | | | | | |
| 14-1-2-1 | 6712 | 6.23 | 2.79 | 17,490 | 8.16 | .3370 | 156.0 | 2.31 | 67.5 | | | | | |
| 14-1-2-2 | 6988 | | 2.50 | 19,520 | 7.24 | .3421 | 160.0 | 2.21 | 72.4 | | | | | |
| 14-1-7-1 | 8410 | 6.23 | 2.50 | 19,520 | 7.25 | .3420 | | 2.21 | | 72.2 | 159.6 | 6968 | 1.626 | .537 |
| 14-1-7-2 | 8878 | | 2.13 | 22,910 | 6.04 | .3500 | | 2.05 | | 83.1 | 170.4 | 7614 | 1.685 | .280 |
| 14-1-8-1 | 10,570 | 6.25 | 2.33 | 20,940 | 6.67 | .3456 | | 2.13 | | 76.9 | 163.8 | 7227 | 1.737 | .756 |
| 14-1-8-2 | 11,090 | | 1.95 | 25,280 | 5.37 | .3555 | | 1.96 | | 90.1 | 176.6 | 8010 | 1.800 | .693 |

APPENDIX E

BURNOUT DATA

| Run | D in. | L/D | Po psia | V1 ft/sec | (hs-ho) Btu/lbm | xo | (q/A)BO x $10^{-6}$ Btu/hrft2 | Notes |
|---|---|---|---|---|---|---|---|---|
| 24 | 0.094 | 14.7 | 30.1 | 10 | 79 | | 4.68 | Calming L = 1.6 in. |
| 25 | " | 14.7 | 30.2 | " | 72 | | 4.52 | " |
| 26 | " | 14.6 | 30.2 | " | 70 | | 4.22 | " |
| 27 | " | 15.0 | 30.3 | " | 64 | | 3.68 | " |
| 28 | " | 14.9 | 30.2 | " | 47 | | 3.18 | " |
| 29 | " | 15.0 | 30.2 | " | 22 | | 3.08 | " |
| 30 | " | 15.1 | 30.1 | " | 32 | | 3.04 | " |
| 31 | " | 15.0 | 30.4 | " | 55 | | 3.76 | " |
| 32 | " | 14.9 | 30.1 | " | 40 | | 3.05 | " |
| 34 | " | 14.9 | 30.2 | " | 12 | | 3.20 | " |
| 35 | " | 14.9 | 30.2 | " | 22 | | 2.66 | " |
| 36 | " | 14.6 | 30.0 | " | 2 | | 3.35 | " |
| 37 | " | 15.1 | 30.5 | " | | .0254 | 3.53 | " |
| 40 | " | 14.9 | 31.7 | " | | .0541 | 3.62 | " |
| 41 | " | 14.9 | 31.2 | " | | .0541 | 3.66 | " |
| 42 | " | 14.9 | 33.1 | " | | .1117 | 4.27 | " |

APPENDIX E
(Continued)

| Run | D in. | L/D | Po psia | $V_i$ ft/sec | $(h_s-h_o)$ Btu/lb$_m$ | $x_o$ | $(q/A)_{BO}$ x $10^{-6}$ Btu/hrft2 | Notes |
|---|---|---|---|---|---|---|---|---|
| 4 | 0.1805 | 25.0 | 29.9 | 10 | 38 | | 1.92 | Calming L = 1.6 in. |
| 5 | " | 25.0 | 30.7 | " | 35 | | 1.90 | " |
| 47 | " | 24.7 | 30.6 | 20 | 46 | | 2.66 | " |
| 6 | 0.094 | 24.7 | 29.9 | 10 | 32 | | 2.76 | Calming L = 0.16 in. unless otherwise noted. |
| 7 | " | 24.7 | 30.4 | " | 35 | | 2.68 | |
| 8 | " | 24.7 | 30.5 | 20 | 34 | | 4.13 | |
| 21 | " | 24.7 | 30.1 | " | 31 | | 4.35 | |
| 9 | 0.0465 | 25.0 | 30.6 | 10 | 34 | | 3.60 | |
| 46 | " | 19.8 | 30.6 | " | 32 | | 3.98 | |
| 10 | " | 24.3 | 30.2 | 20 | 39 | | 6.25 | |
| 18 | " | 24.1 | 30.6 | " | 36 | | 6.04 | |
| 12 | 0.023 | 23.5 | 30.1 | 10 | 42 | | 1.87 | Valve upstream, BO in middle |
| 16 | " | 25.0 | 30.7 | " | 33 | | 1.54 | " |
| 19 | " | 24.4 | 29.8 | 20 | 30 | | 4.62 | " |
| 20 | " | 24.0 | 30.5 | " | 35 | | 4.83 | " |
| 45 | " | 17.3 | 29.8 | 10 | 33 | | 4.38 | Valve near TS, no BO |

APPENDIX E
(Continued)

| Run | D in. | L/D | $P_o$ psia | $V_1$ ft/sec | $(h_s-h_o)$ Btu/lb$_m$ | $x_o$ | $(q/A)_{BO}$ x $10^{-6}$ Btu/hr ft$^2$ | Notes |
|-----|-------|------|------|------|------|------|------|-------|
| 45 | 0.023 | 17.3 | 29.8 | 20 | 33 | | 7.97 | Valve near TS |
| 43 | " | 24.4 | 30.1 | " | 36 | | 6.88 | " |
| 44 | " | 21.7 | 30.3 | " | 31 | | 6.35 | " |
| 48 | 0.094 | 34.6 | 29.9 | 10 | 32 | | 2.57 | |
| 49 | " | 34.7 | 29.7 | " | 31 | | 2.57 | |
| 50 | " | 29.6 | 30.6 | " | 32 | | 2.50 | |
| 51 | " | 29.2 | 30.5 | " | 31 | | 2.66 | |
| 53 | " | 20.0 | 30.1 | 10 | 31 | | 2.91 | |
| 54 | " | 21.0 | 29.9 | " | 32 | | 2.88 | |
| 55 | " | 12.3 | 30.1 | " | 32 | | 3.13 | |
| 56 | " | 5.2 | 30.2 | " | 32 | | 4.16 | |
| 57 | " | 4.7 | 30.6 | " | 32 | | 4.19 | |
| 58 | " | 7.6 | 30.6 | " | 34 | | 3.71 | |
| 14 | " | 12.6 | 30.2 | " | 39 | | 3.25 | Calming L = 1.6 in. |
| 15 | " | 12.4 | 30.5 | " | 36 | | 3.05 | " |

APPENDIX E
(Continued)

| Run | D in. | L/D | Po psia | $V_i$ ft/sec | $(h_s-h_o)$ Btu/lb$_m$ | $x_o$ | $(q/A)_{BO}$ x $10^{-6}$ Btu/hrft2 | Notes |
|-----|-------|------|---------|--------------|------------------------|-------|-----------------------------------|-------|
| 22  | 0.094 | 24.7 | 30.6    | 10           | 51                     |       | 3.14                              | Calming L = 1.6 in. |
| 23  | "     | 25.0 | 30.2    | "            | 53                     |       | 3.33                              | " |
| 3   | "     | 50.0 | 30.6    | 20           | 34                     |       | 3.91                              | " |
| 1   | 0.1805| 50.0 | 30.5    | 15           | 30                     |       | 2.53                              | " |
| 2   | "     | 50.0 | 30.2    | "            | 39                     |       | 2.39                              | " |
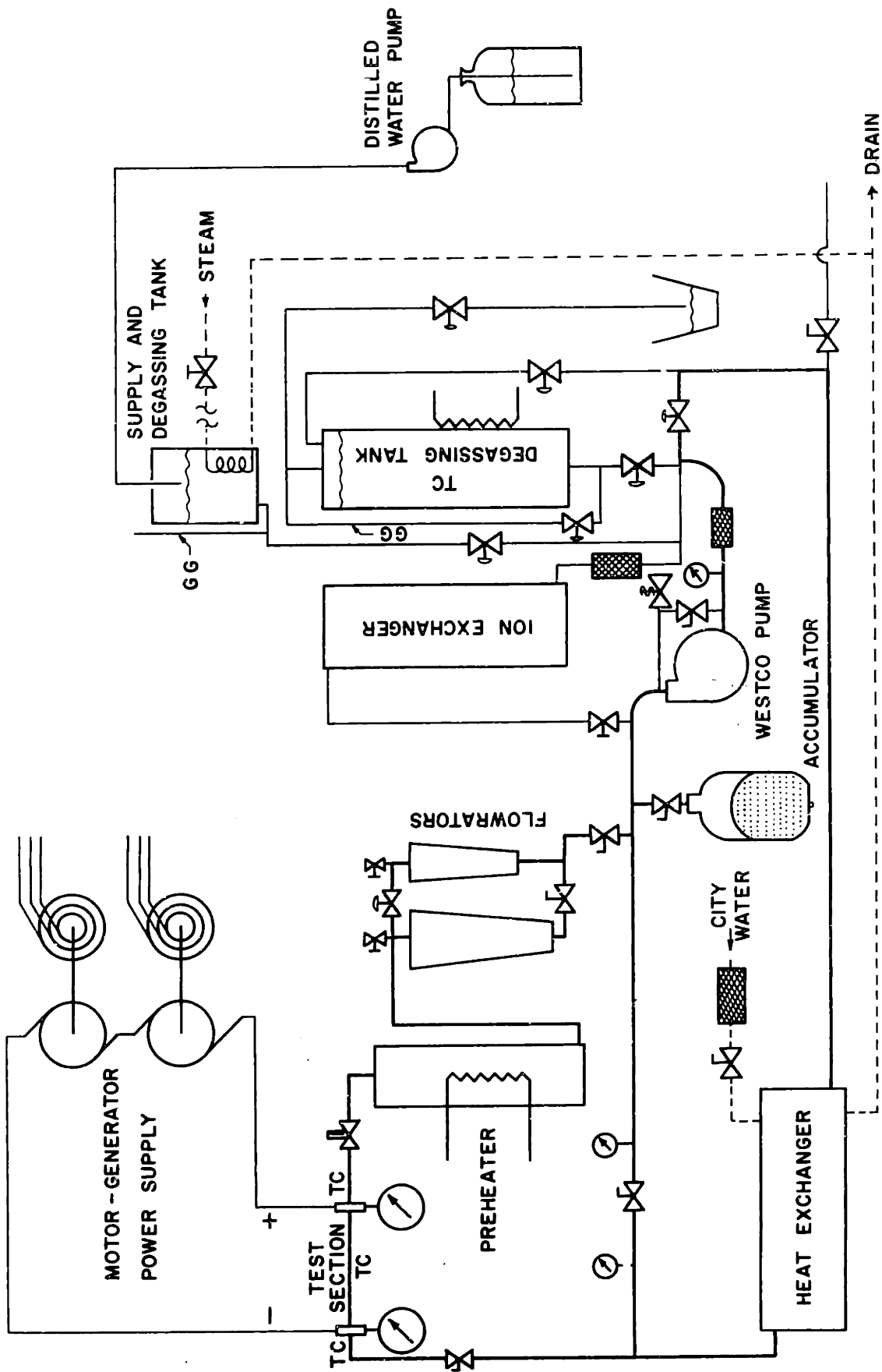
FIG. 1 SCHEMATIC LAYOUT OF HEAT-TRANSFER FACILITY
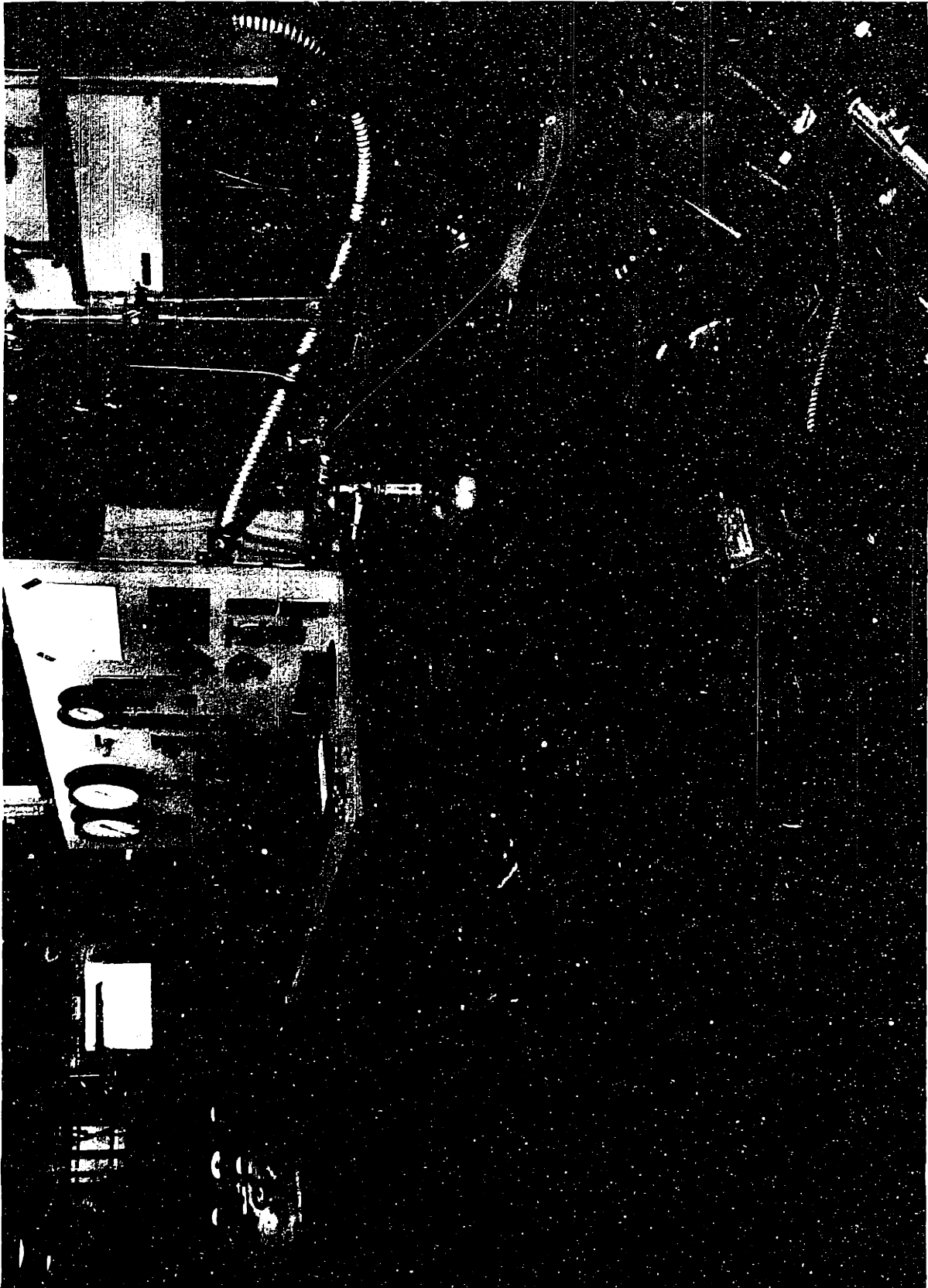
FIG. 2 GENERAL VIEW OF HEAT-TRANSFER FACILITY
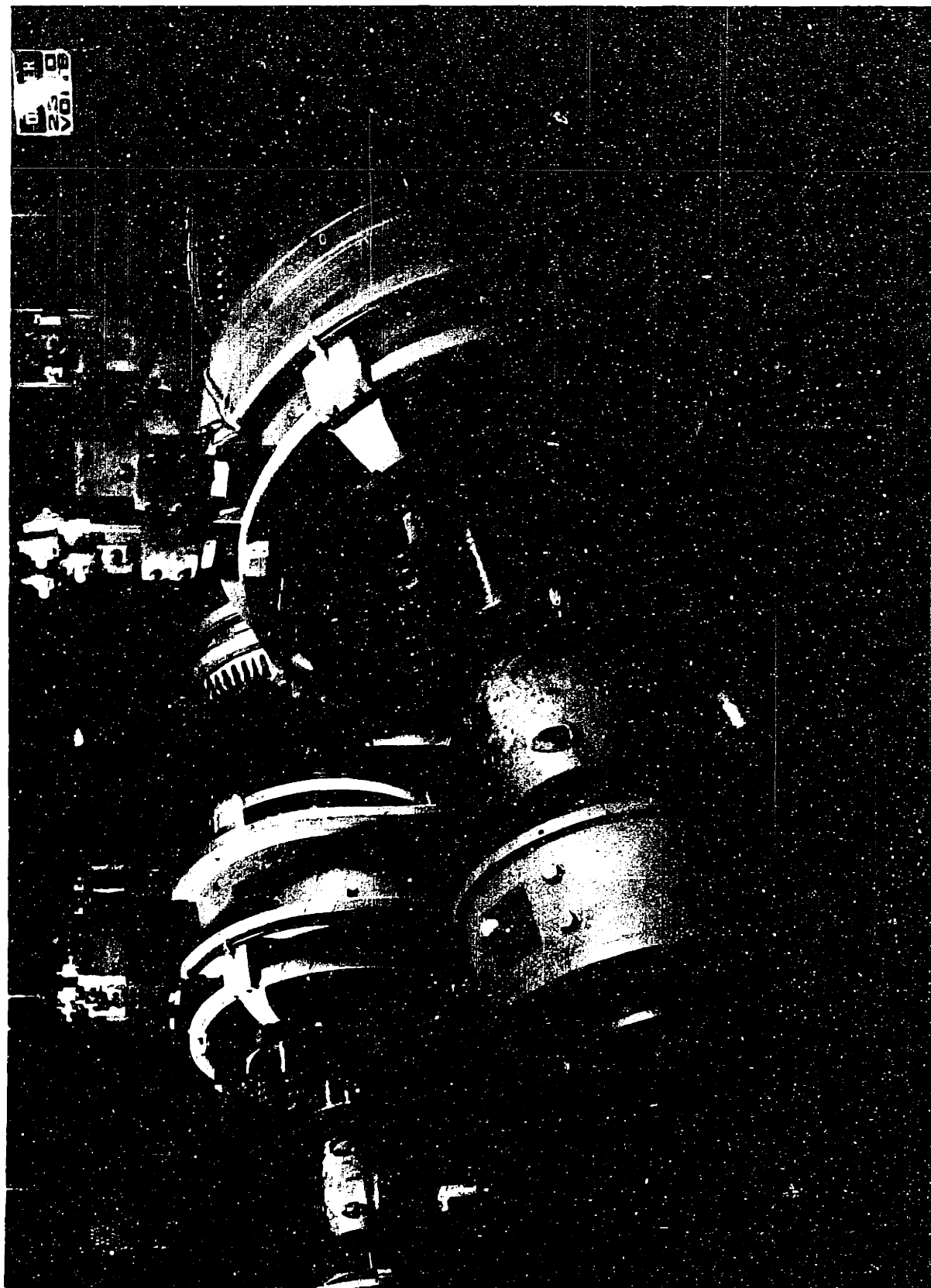
FIG. 3   MOTOR-GENERATOR INSTALLATION
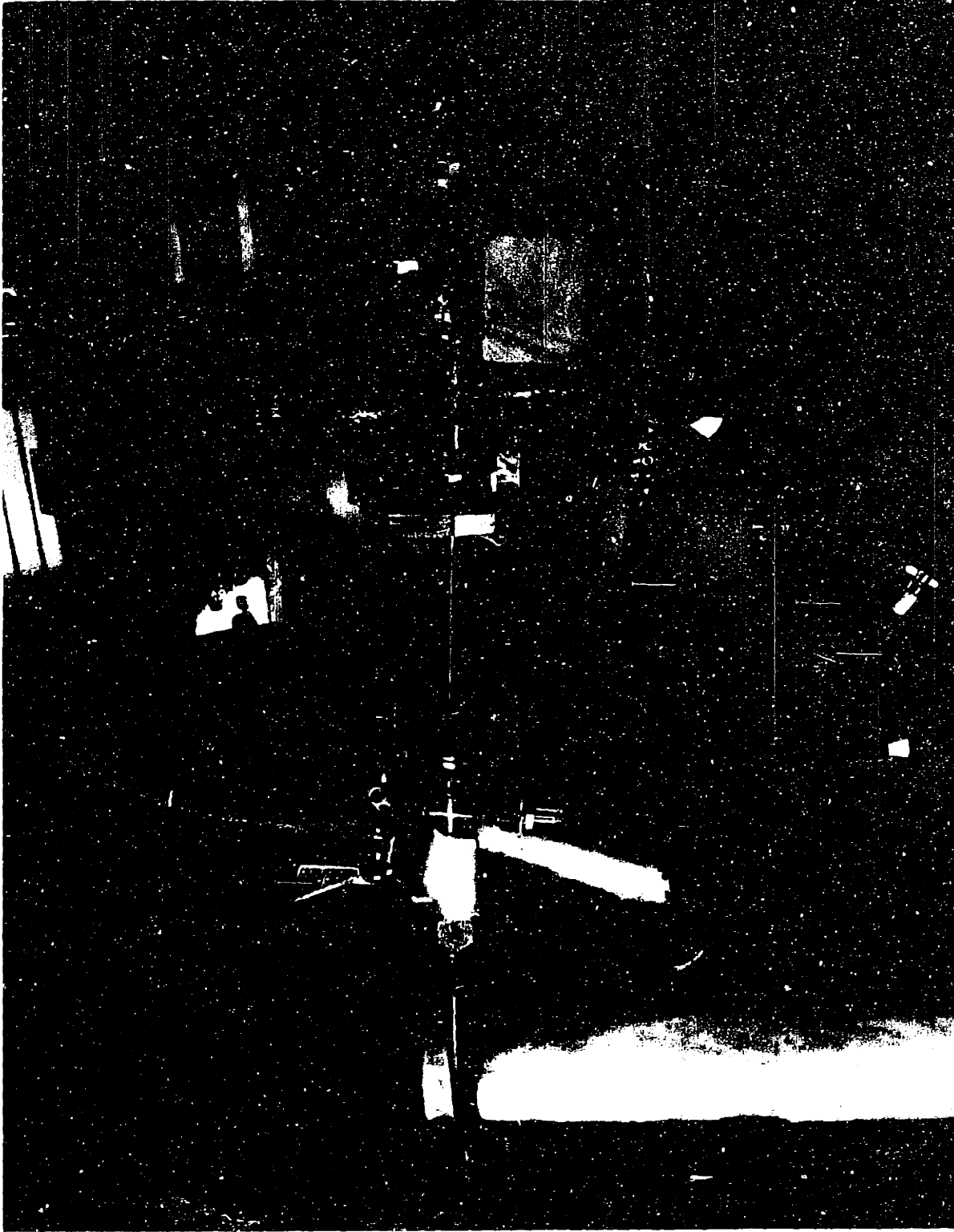
FIG. 4. DETAILS OF TEST-SECTION INSTALLATION
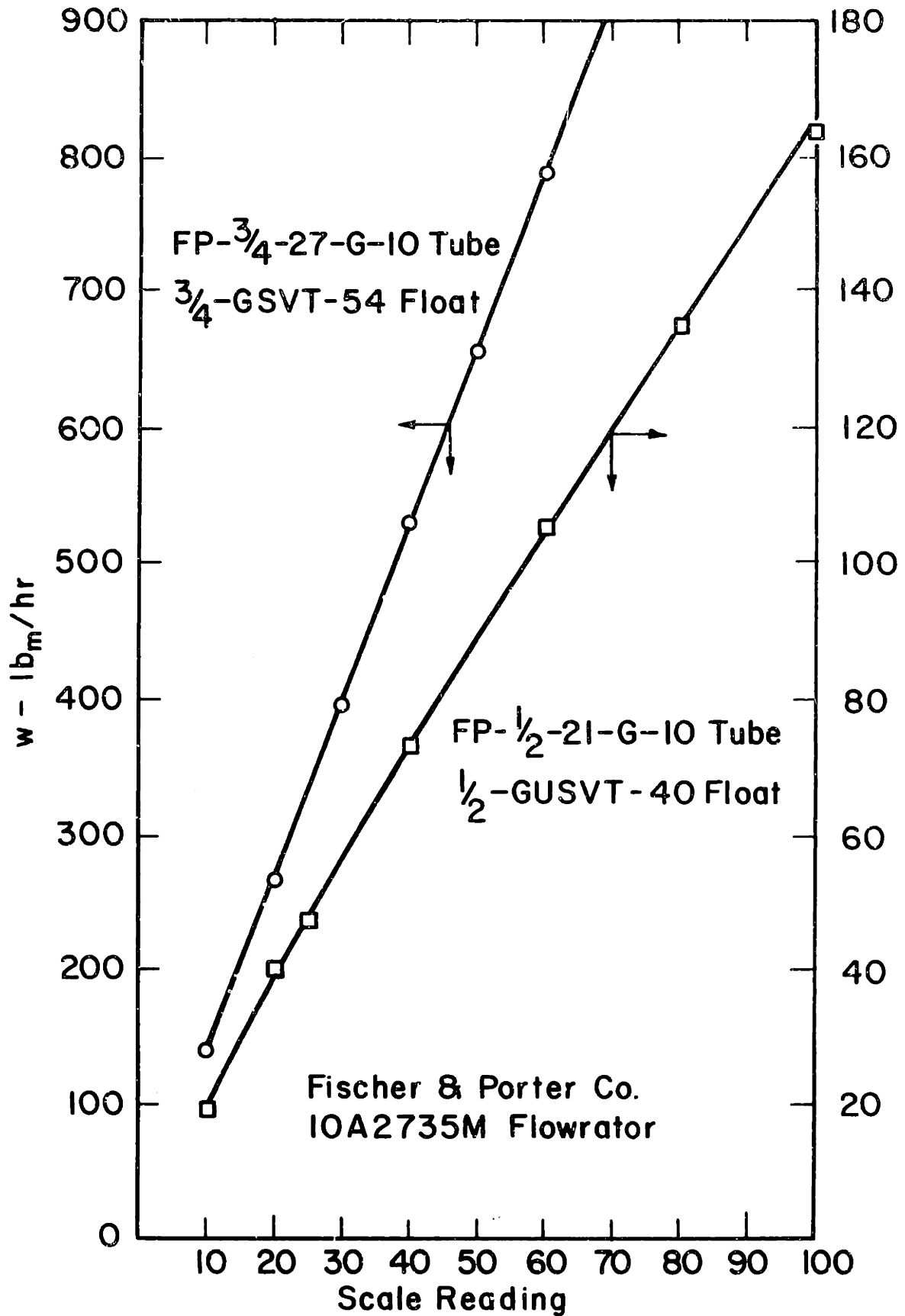
FIG. 5 FLOWRATOR CALIBRATION CURVES

$$k = 8.46 \left[ 1 + 0.526 \times 10^{-3} \, t \right]$$

o  Reference 5

□  Reference 6

$t - °F$

$k - $ Btu/hr ft °F
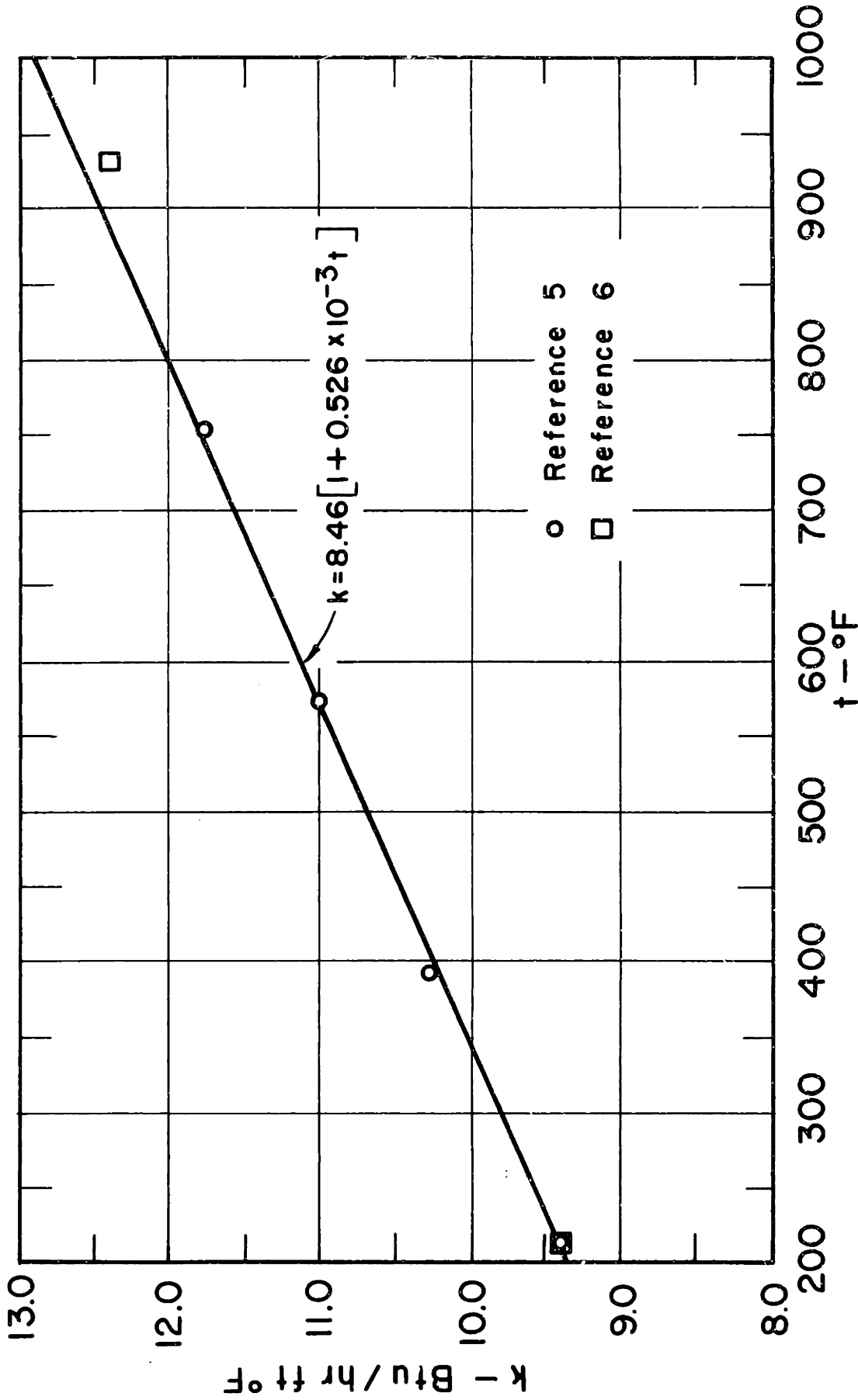
FIG. 6  TEMPERATURE DEPENDENCE OF THERMAL CONDUCTIVITY FOR 304 STAINLESS STEEL
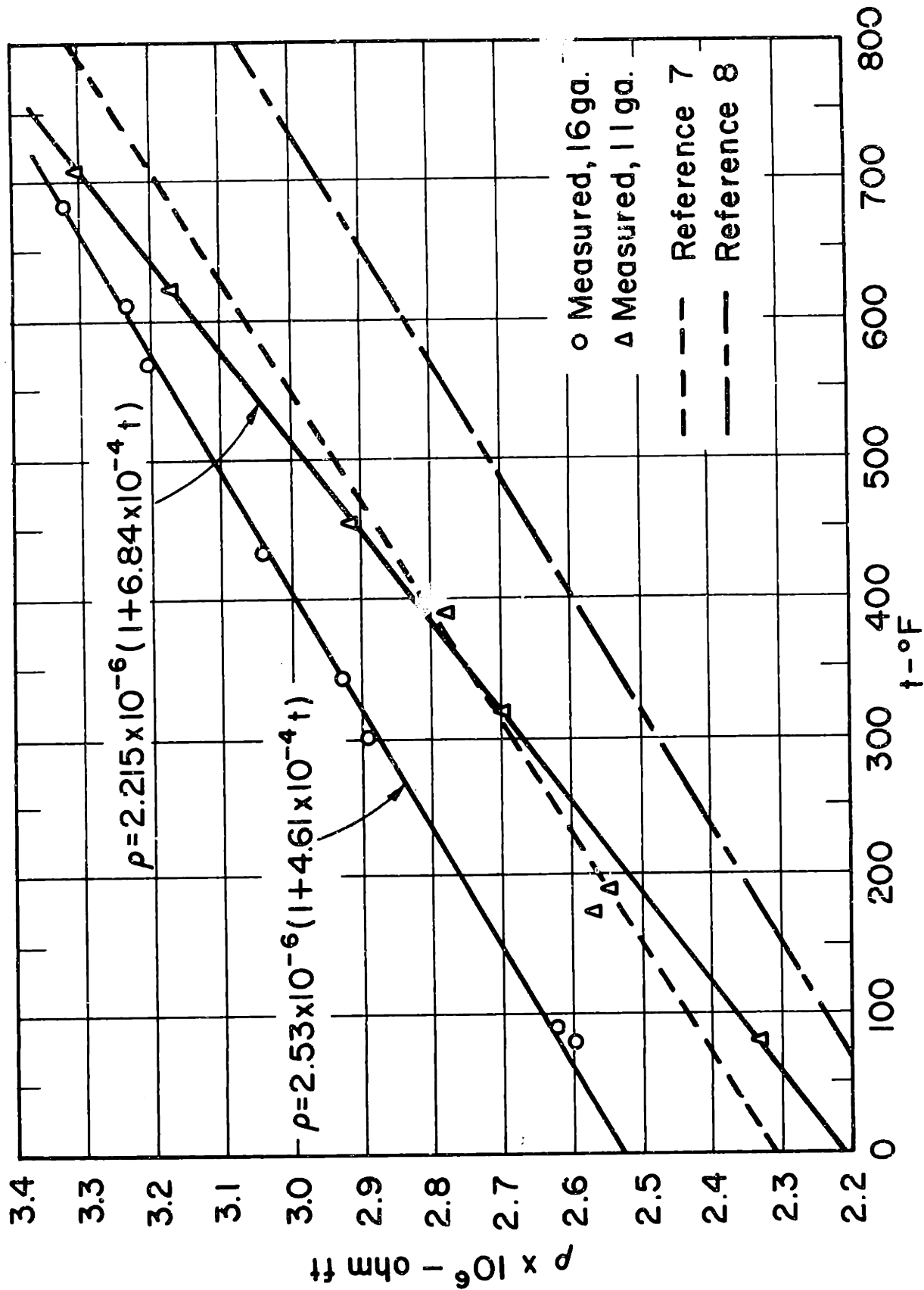
FIG. 7  TEMPERATURE DEPENDENCE OF RESISTIVITY FOR 304 STAINLESS
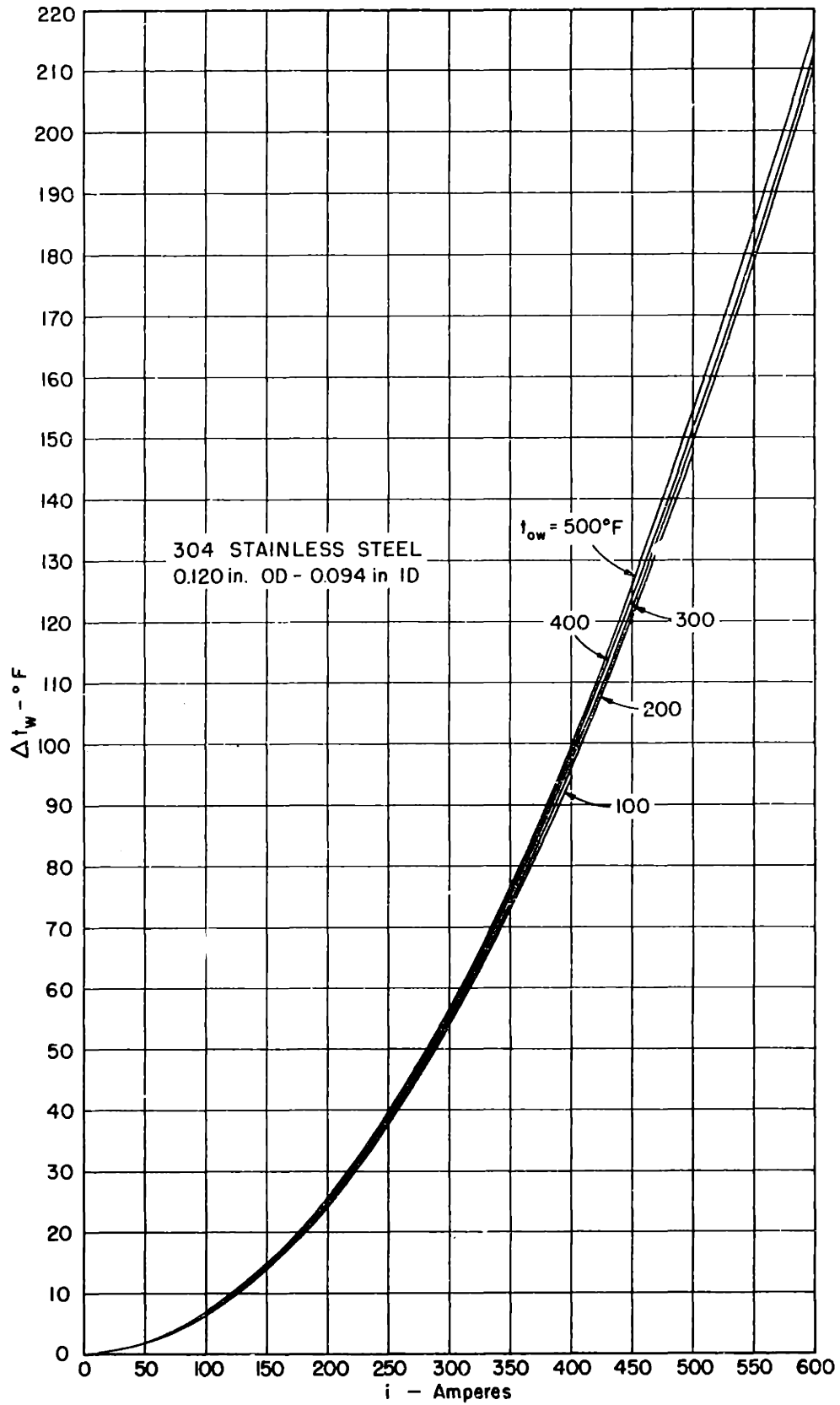
FIG. 8  WALL–TEMPERATURE  CORRECTION  CHART FOR 11 GAGE
STAINLESS–STEEL TUBE
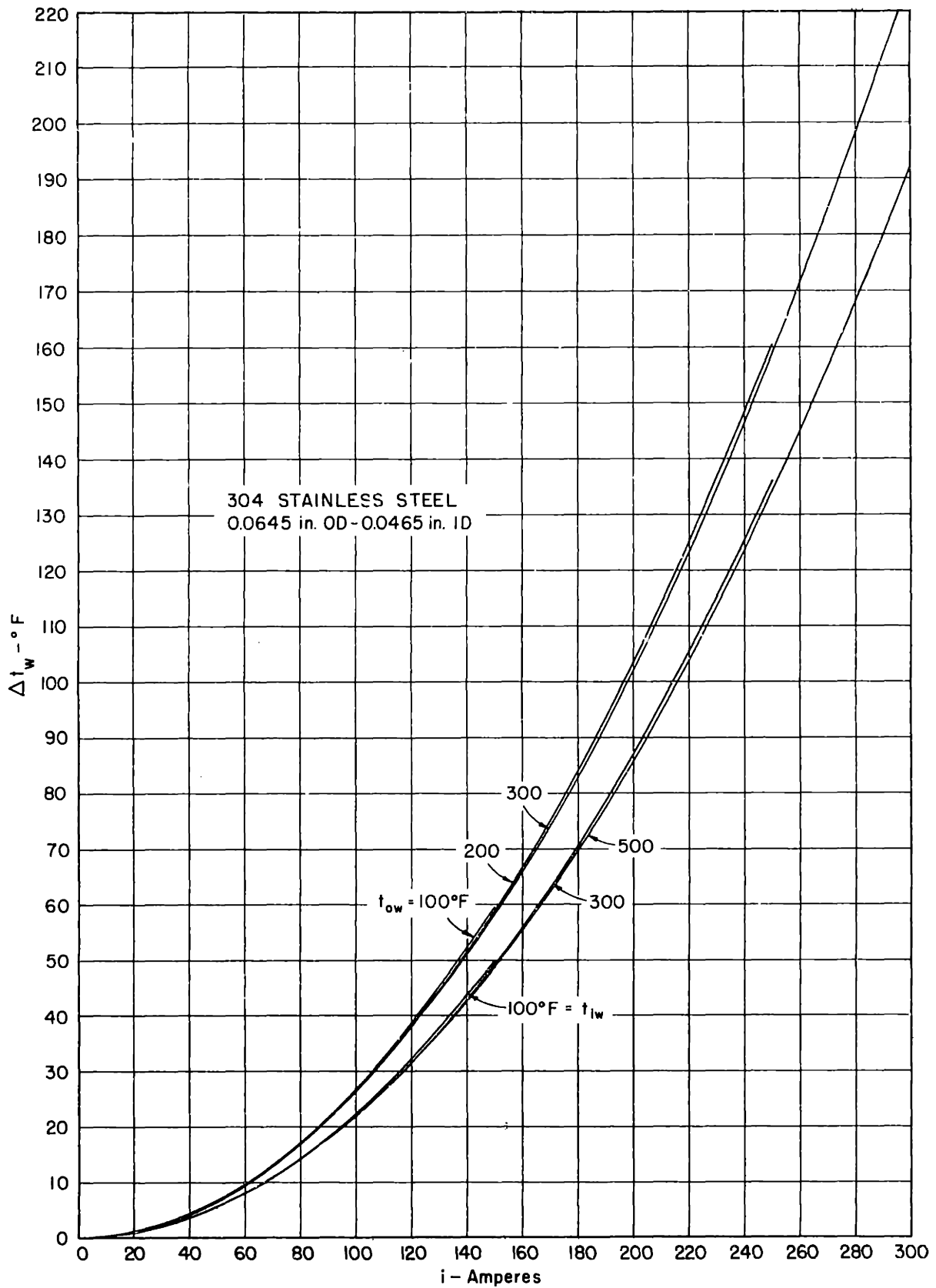
FIG. 9   WALL-TEMPERATURE  CORRECTION  CHART  FOR  16 GAGE
STAINLESS-STEEL TUBE
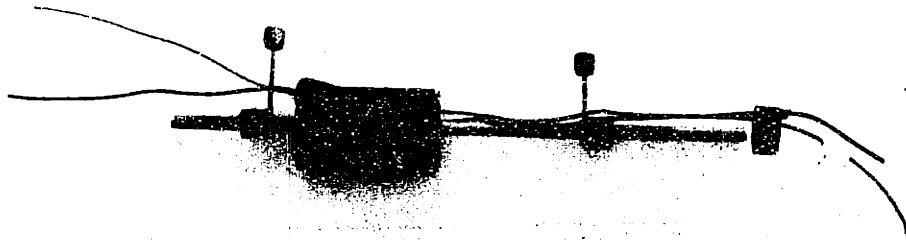
TS 16 FORCED—CONVECTION
SURFACE BOILING IN TUBE
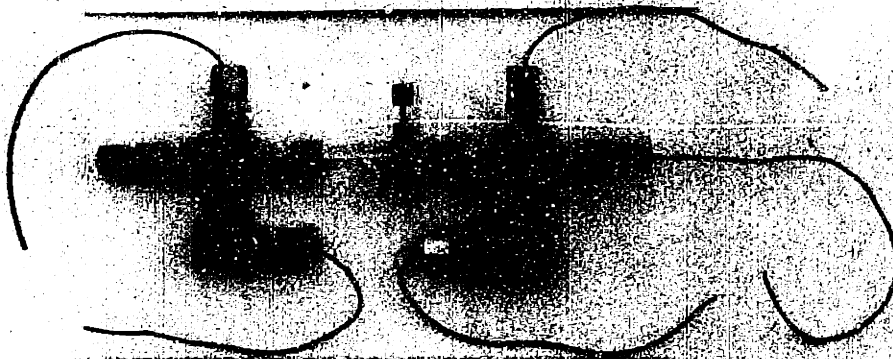
VI 4 FORCED—CONVECTION
SURFACE BOILING IN ANNULUS

BO 50 BURNOUT IN
FORCED—CONVECTION BULK BOILING
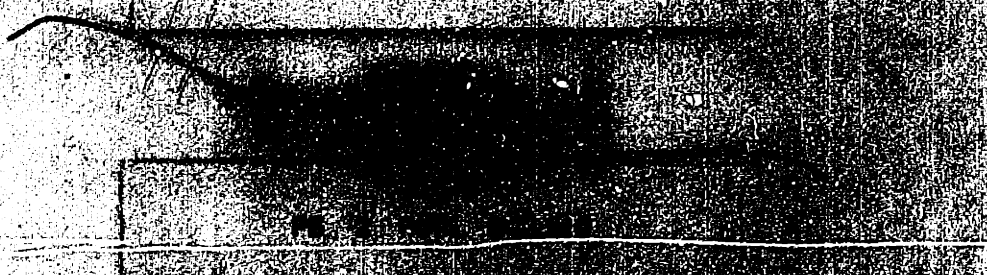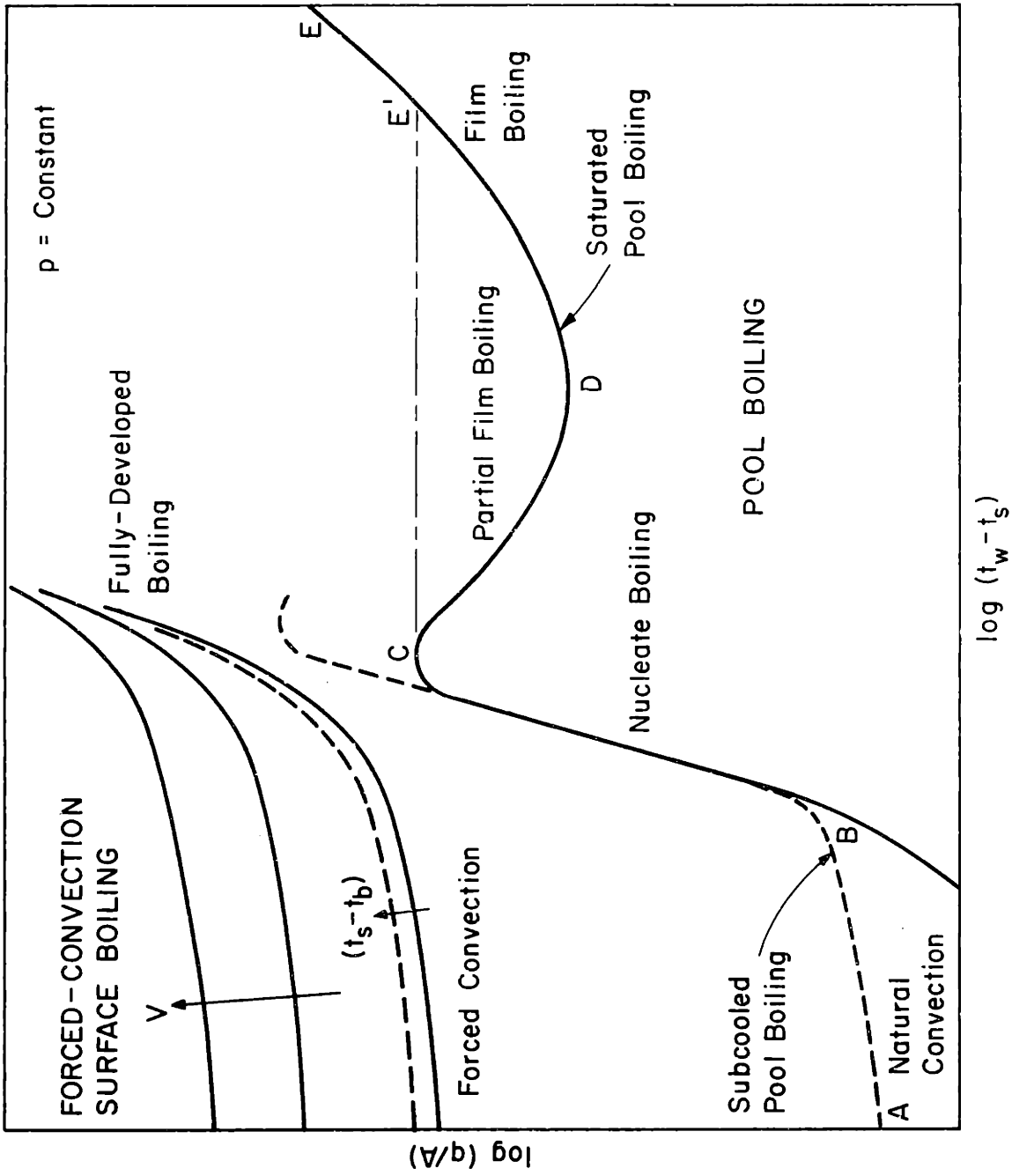
FIG. II  REGIMES IN BOILING HEAT TRANSFER
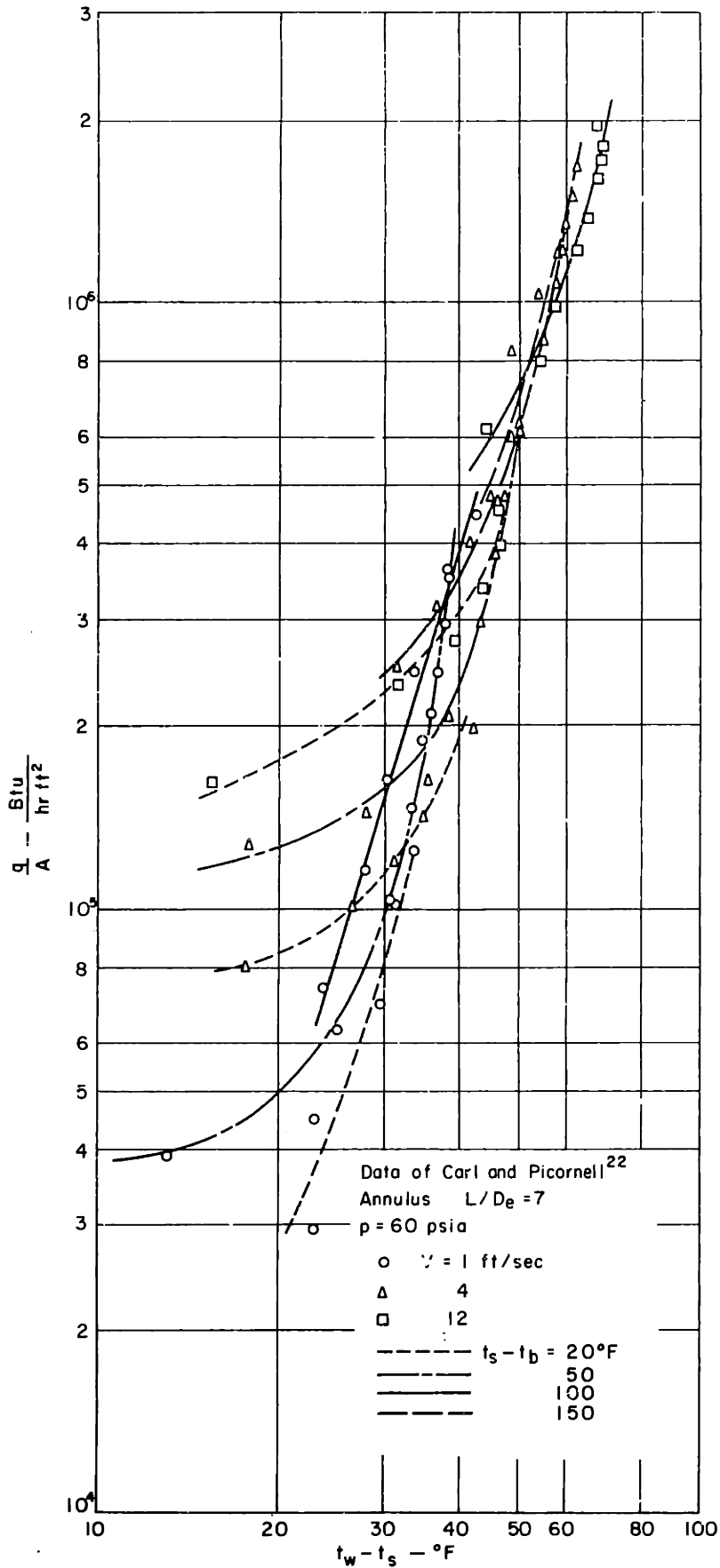
FIG. 12 FORCED-CONVECTION SURFACE-BOILING DATA
OF McADAMS' PROJECT
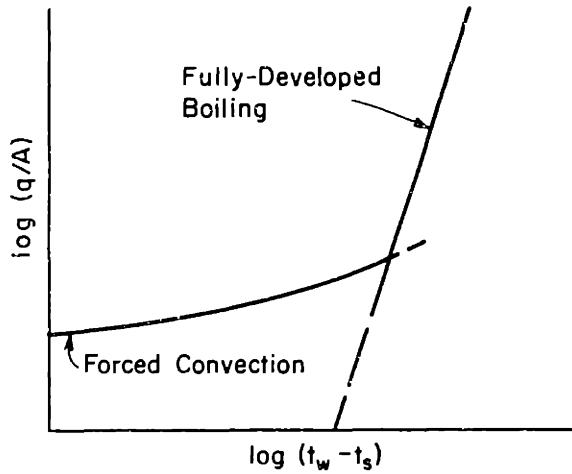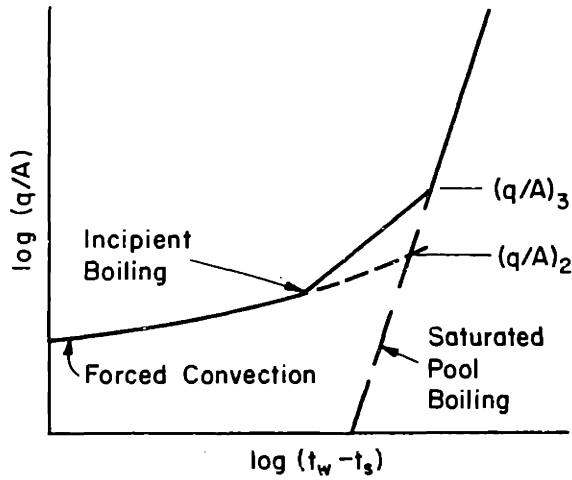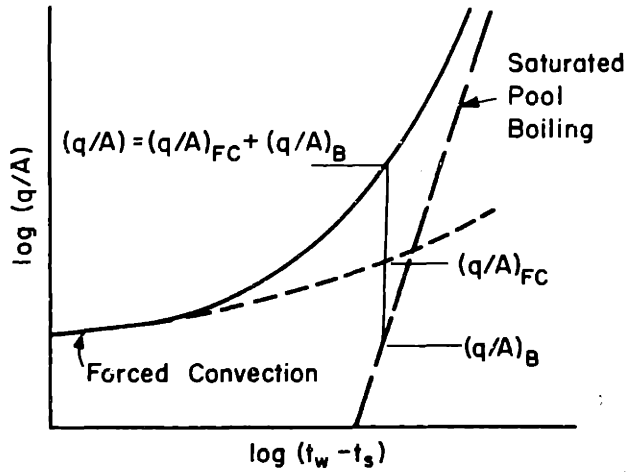
FIG. 13 DESIGN PROCEDURES FOR PREDICTION OF FORCED-CONVECTION
SURFACE-BOILING CURVE
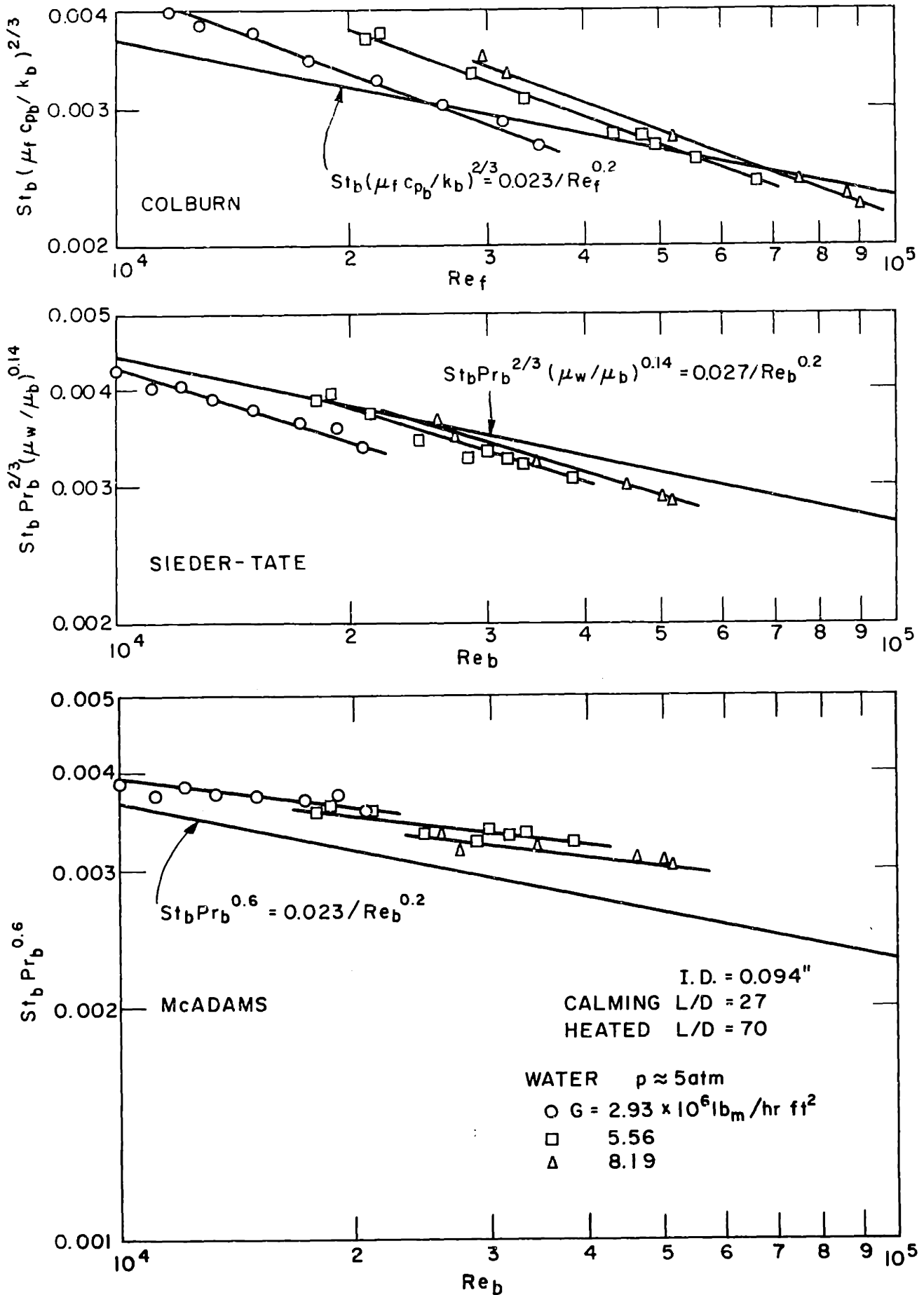
FIG. 14  COMPARISON OF FORCED-CONVECTION WATER
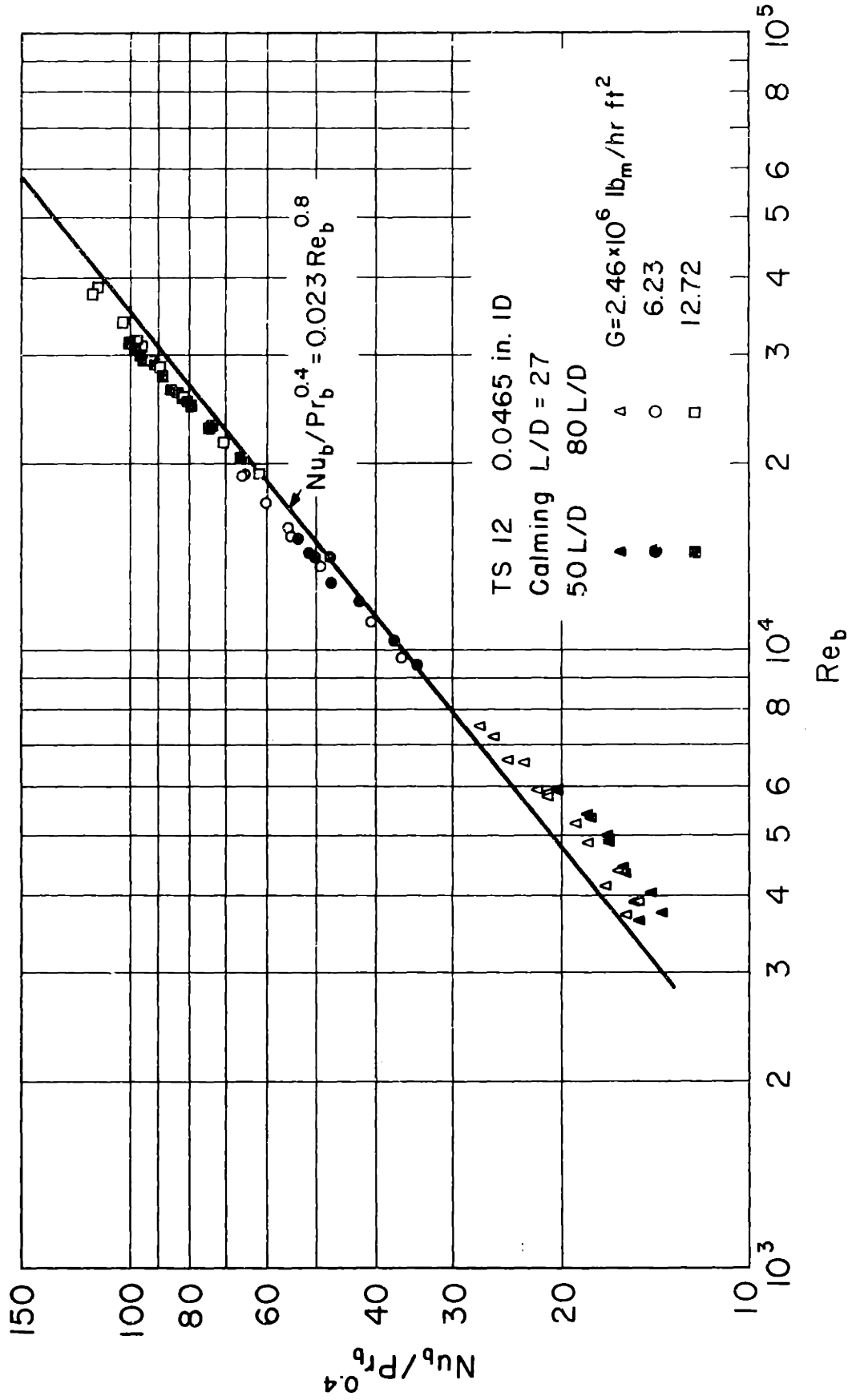
FIG. 15  CORRELATION OF FORCED-CONVECTION DATA FOR TEST
SECTION 12
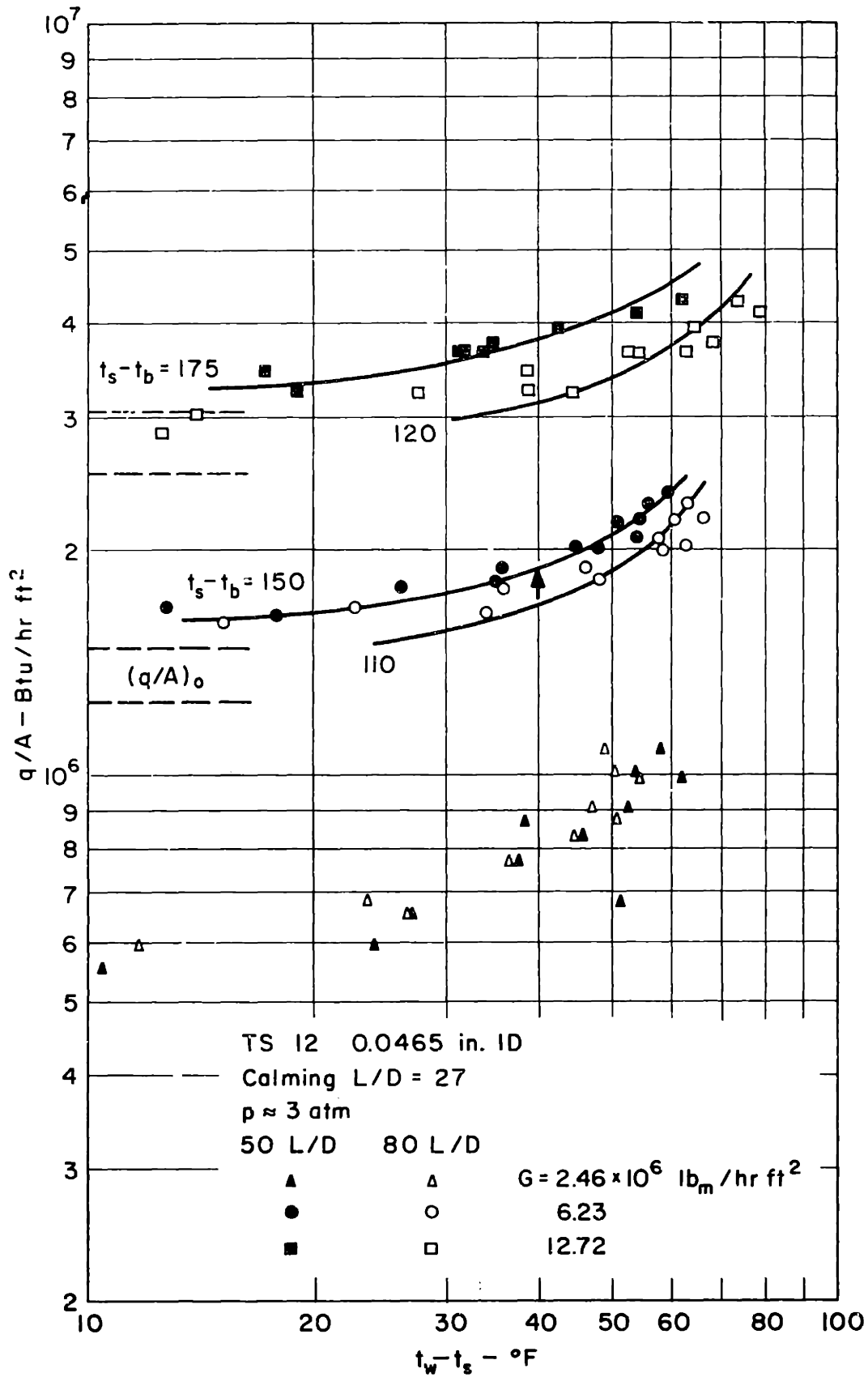
FIG. 16 FORCED-CONVECTION SURFACE BOILING OF WATER
IN A TUBE AT LOW WALL SUPERHEAT
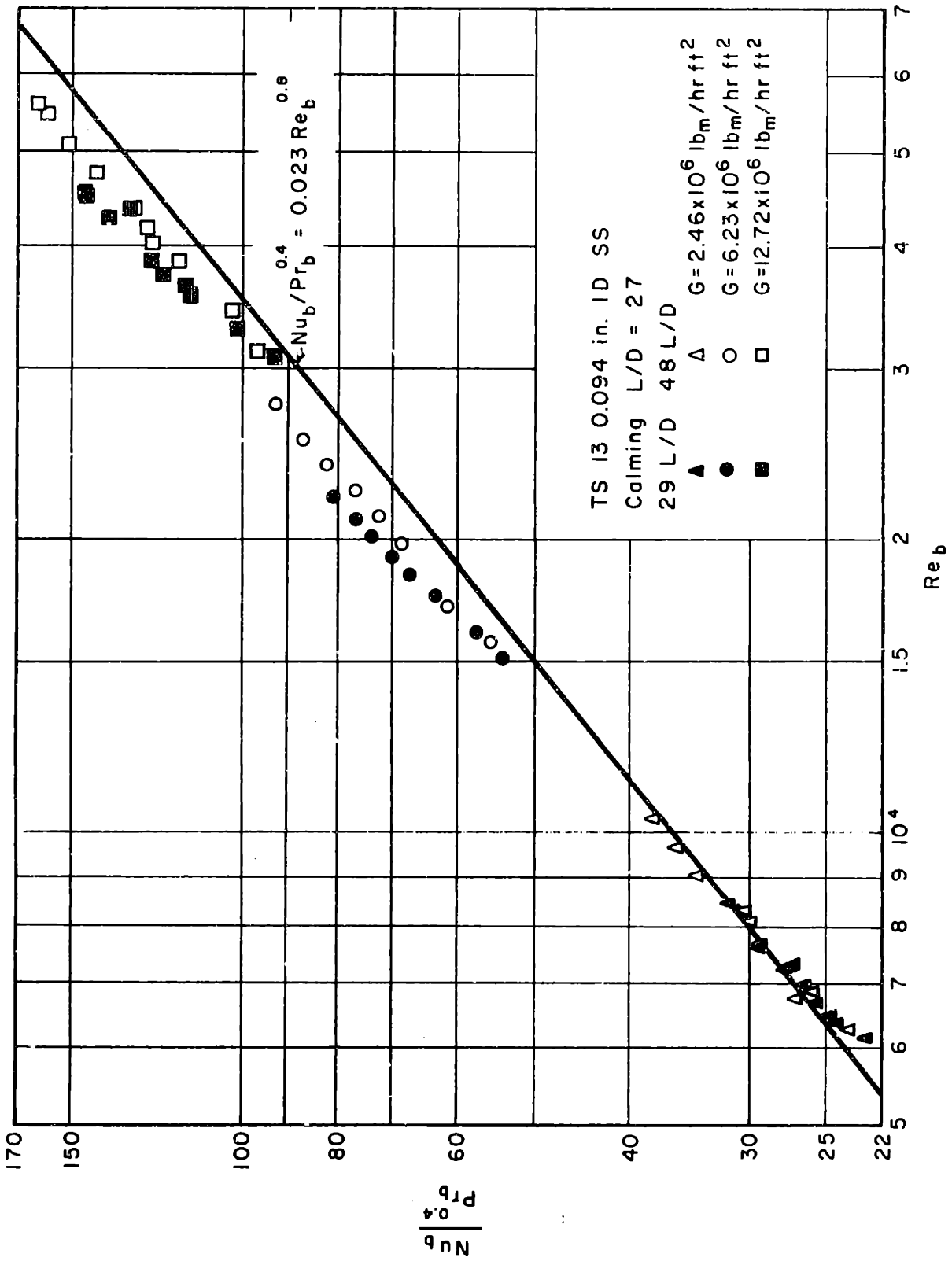
FIG. 17 CORRELATION OF FORCED—CONVECTION DATA FOR TEST SECTION 13
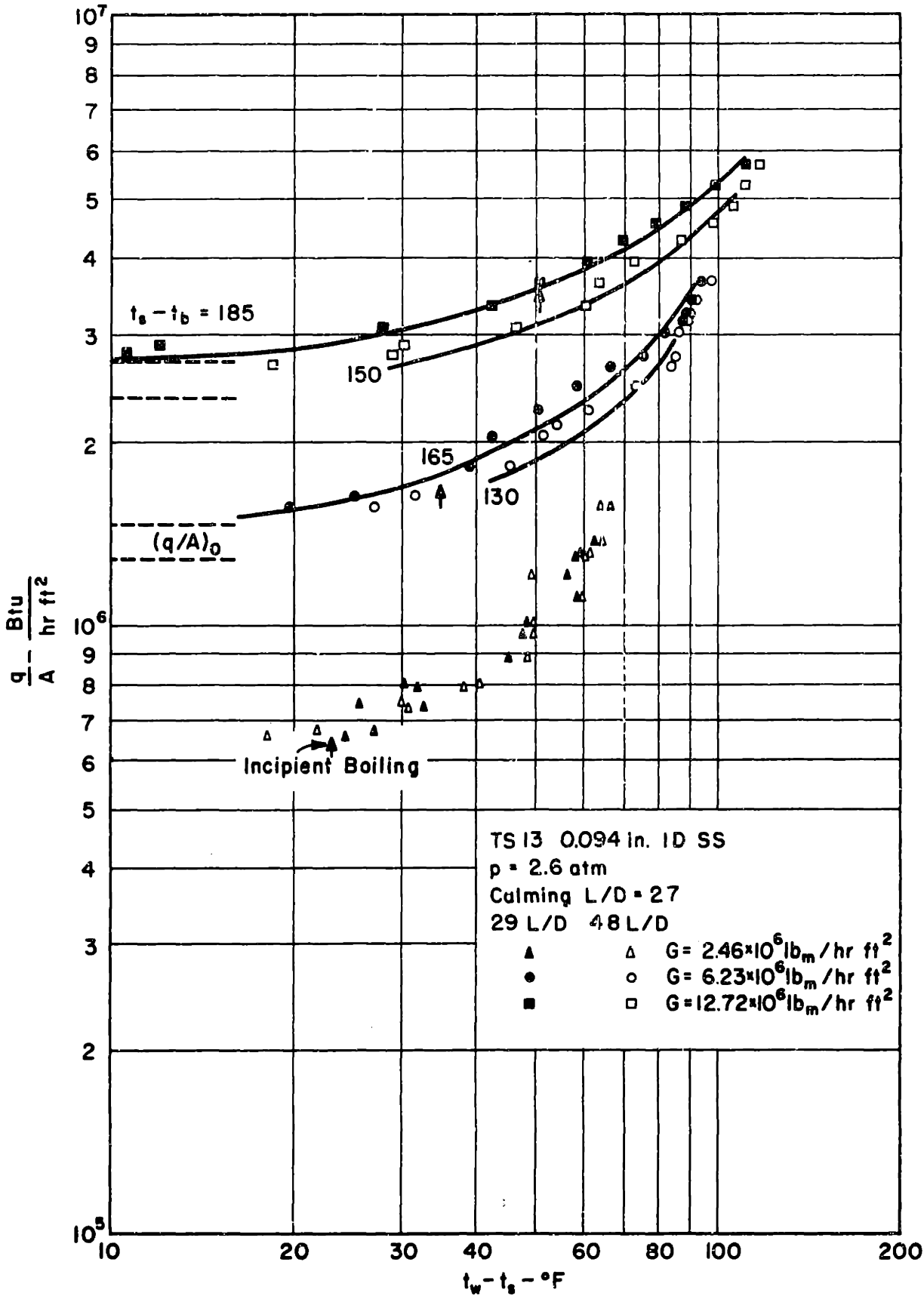
FIG. 18  FORCED-CONVECTION SURFACE BOILING OF WATER IN
         A TUBE
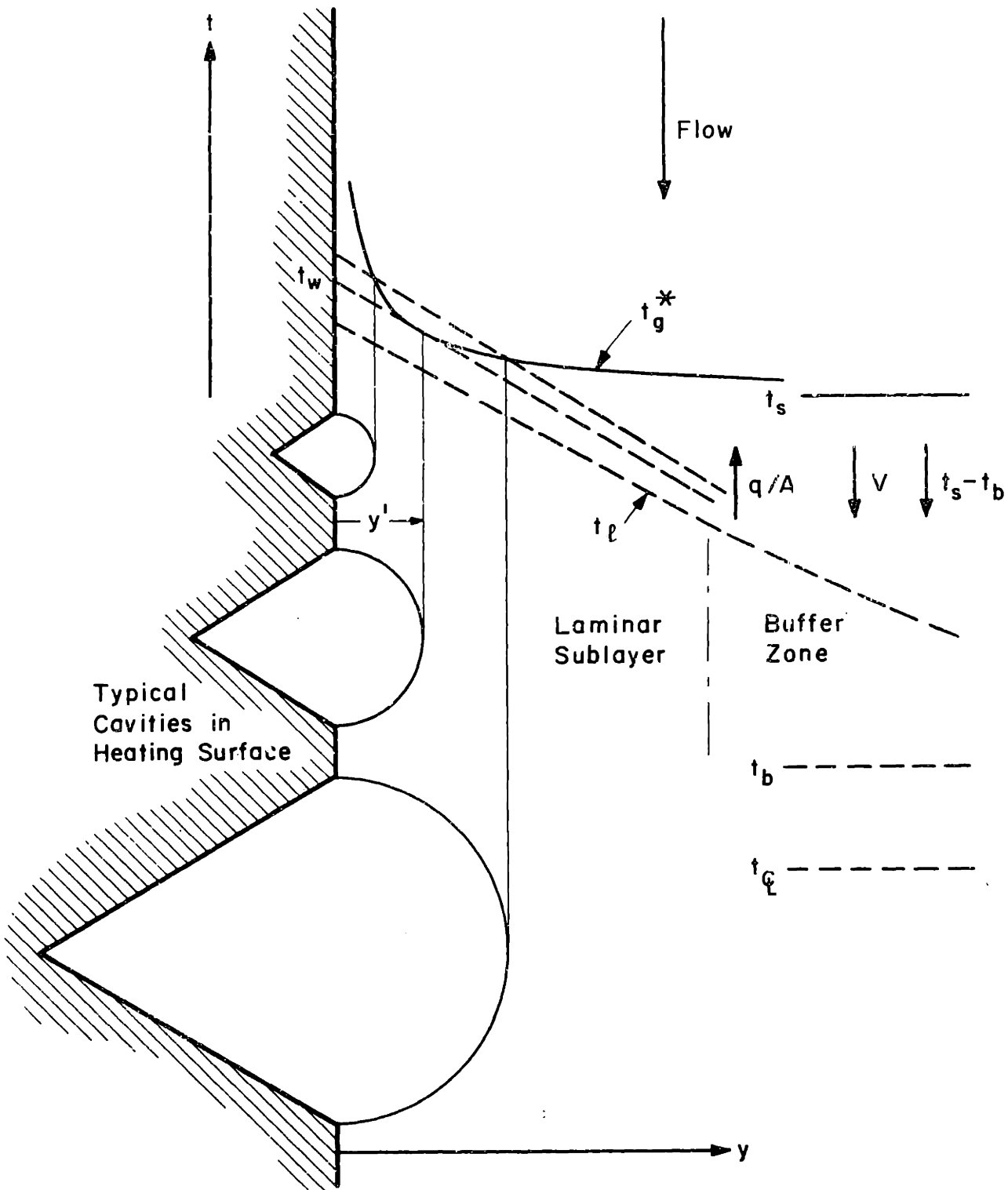
FIG. 19 INITIATION OF BUBBLE GROWTH IN FORCED-CONVECTION
SURFACE BOILING
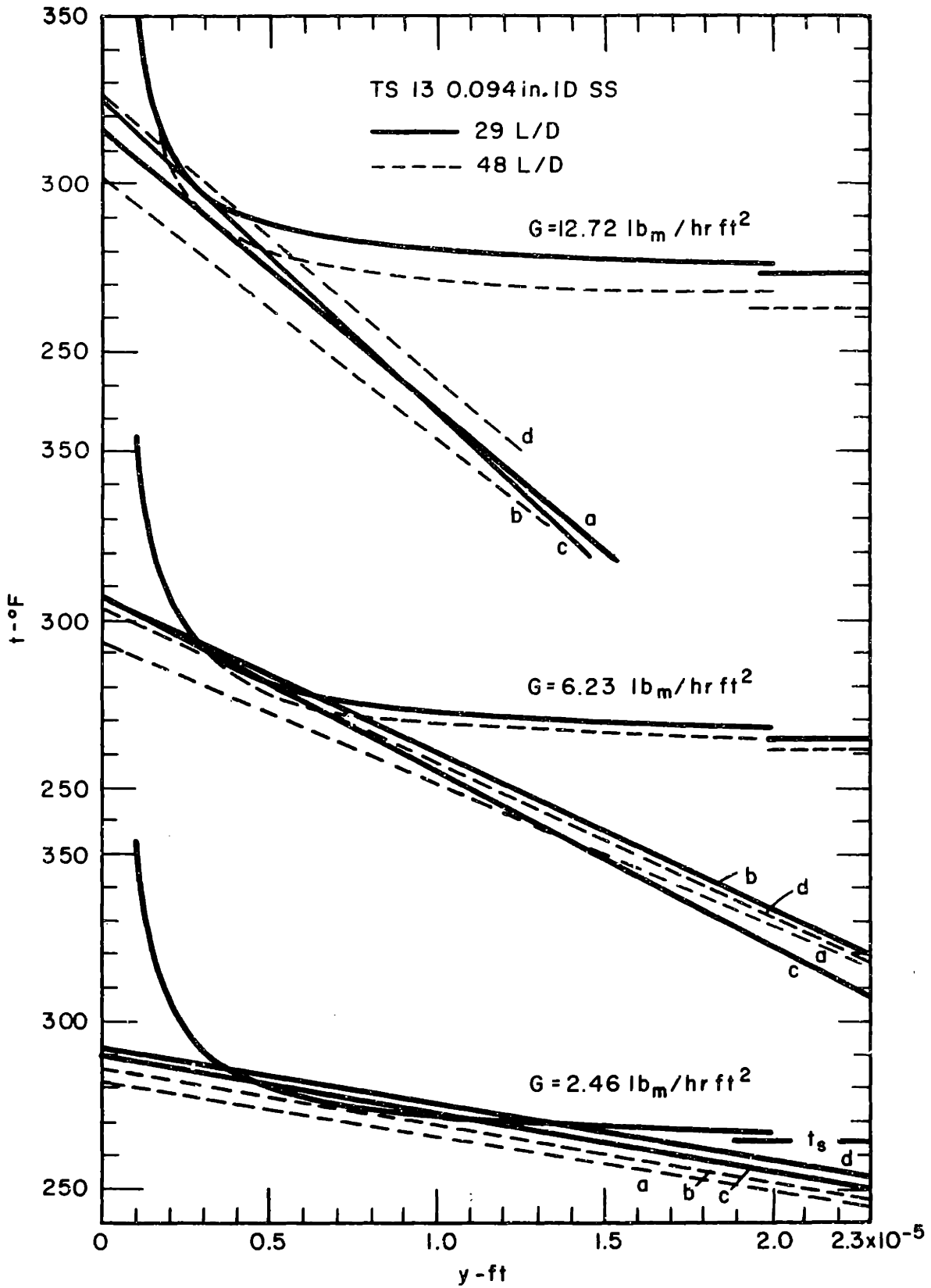
FIG. 20 ANALYTICAL DETERMINATION OF INCIPIENT BOILING
WITH FORCED CONVECTION
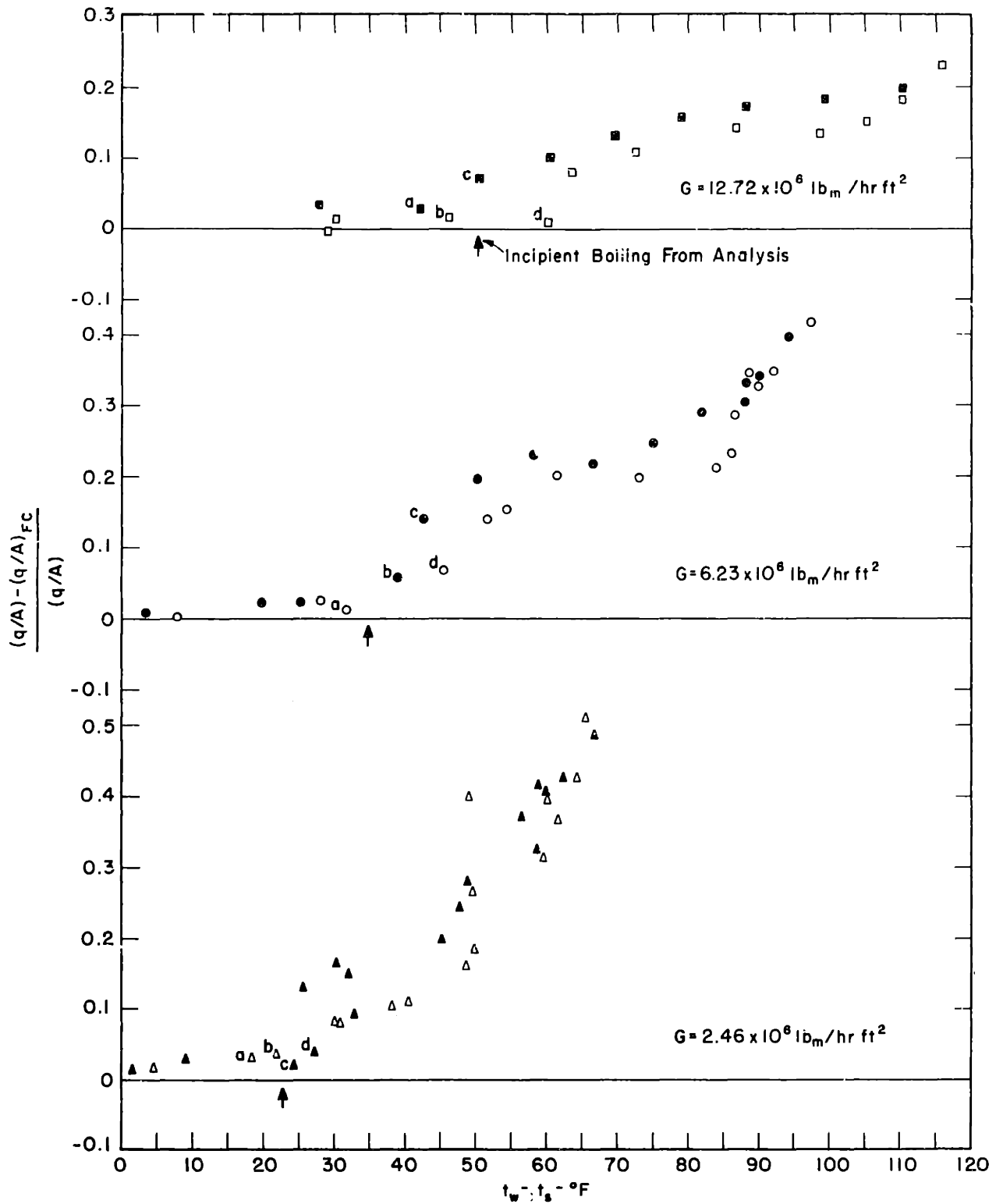
FIG. 21 EXPERIMENTAL DETERMINATION OF INCIPIENT BOILING WITH FORCED CONVECTION
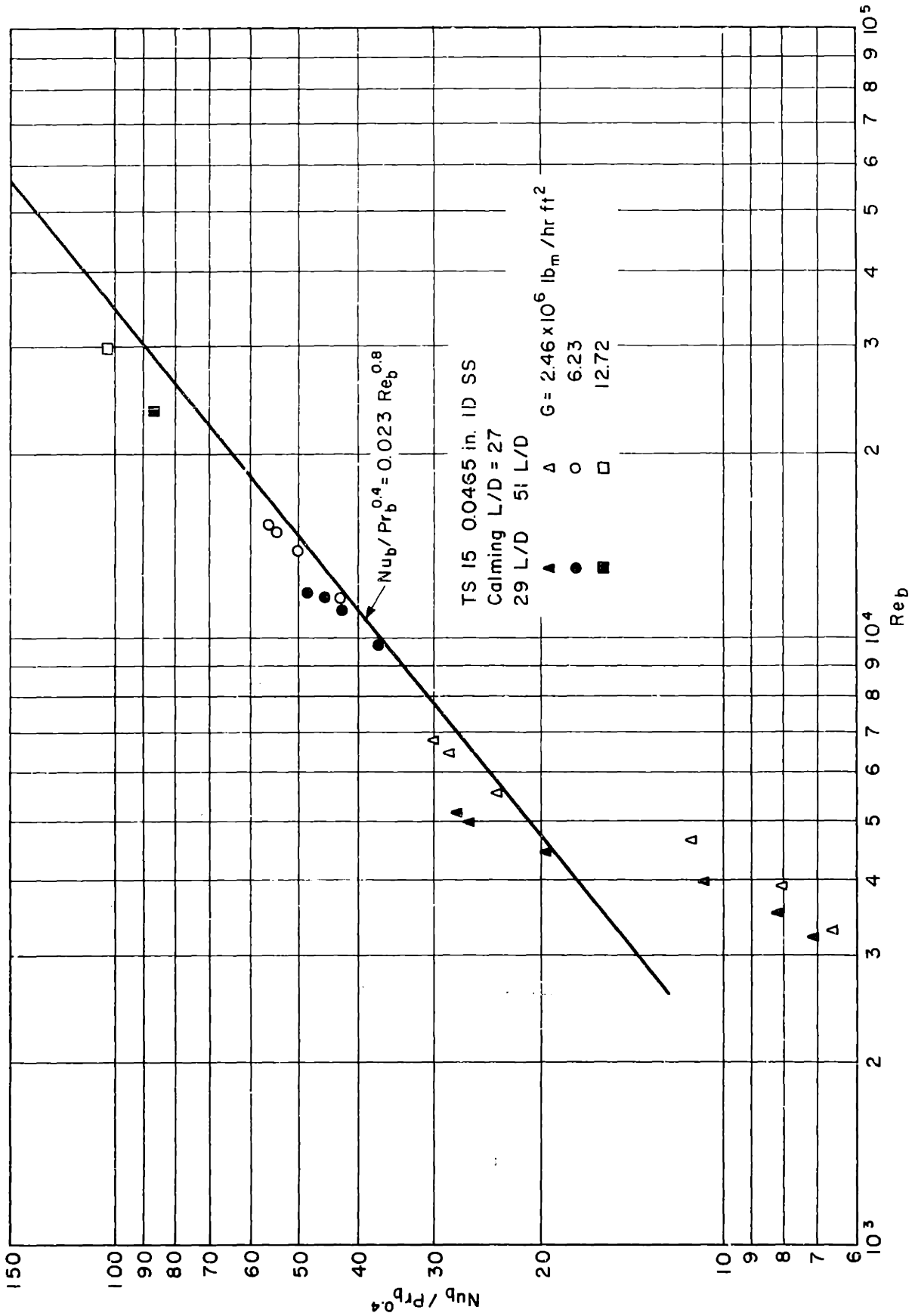
FIG. 22 CORRELATION OF FORCED-CONVECTION DATA FOR TEST SECTION 15
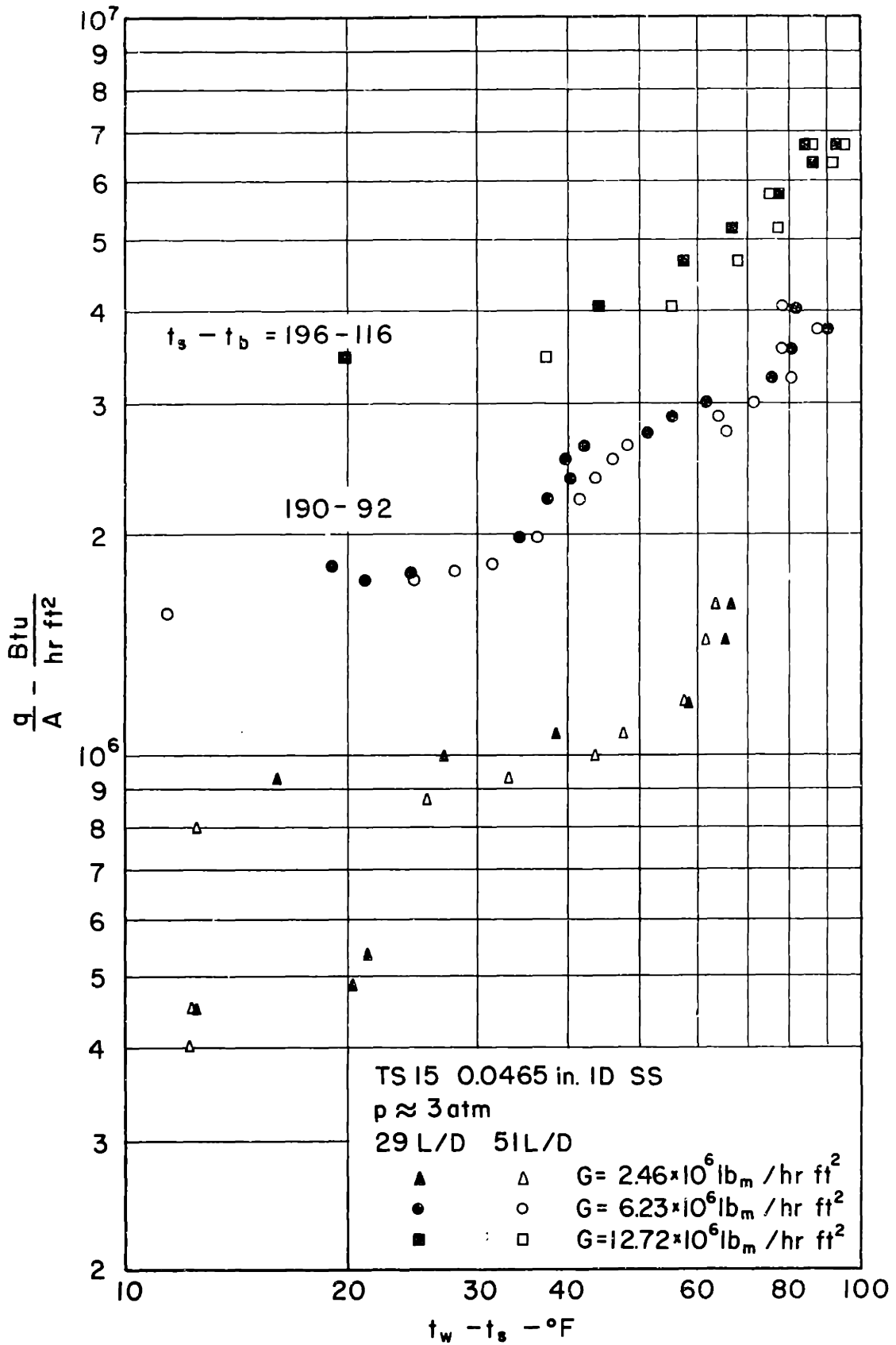
FIG. 23 FORCED-CONVECTION SURFACE BOILING OF
WATER IN A SMALL-DIAMETER TUBE
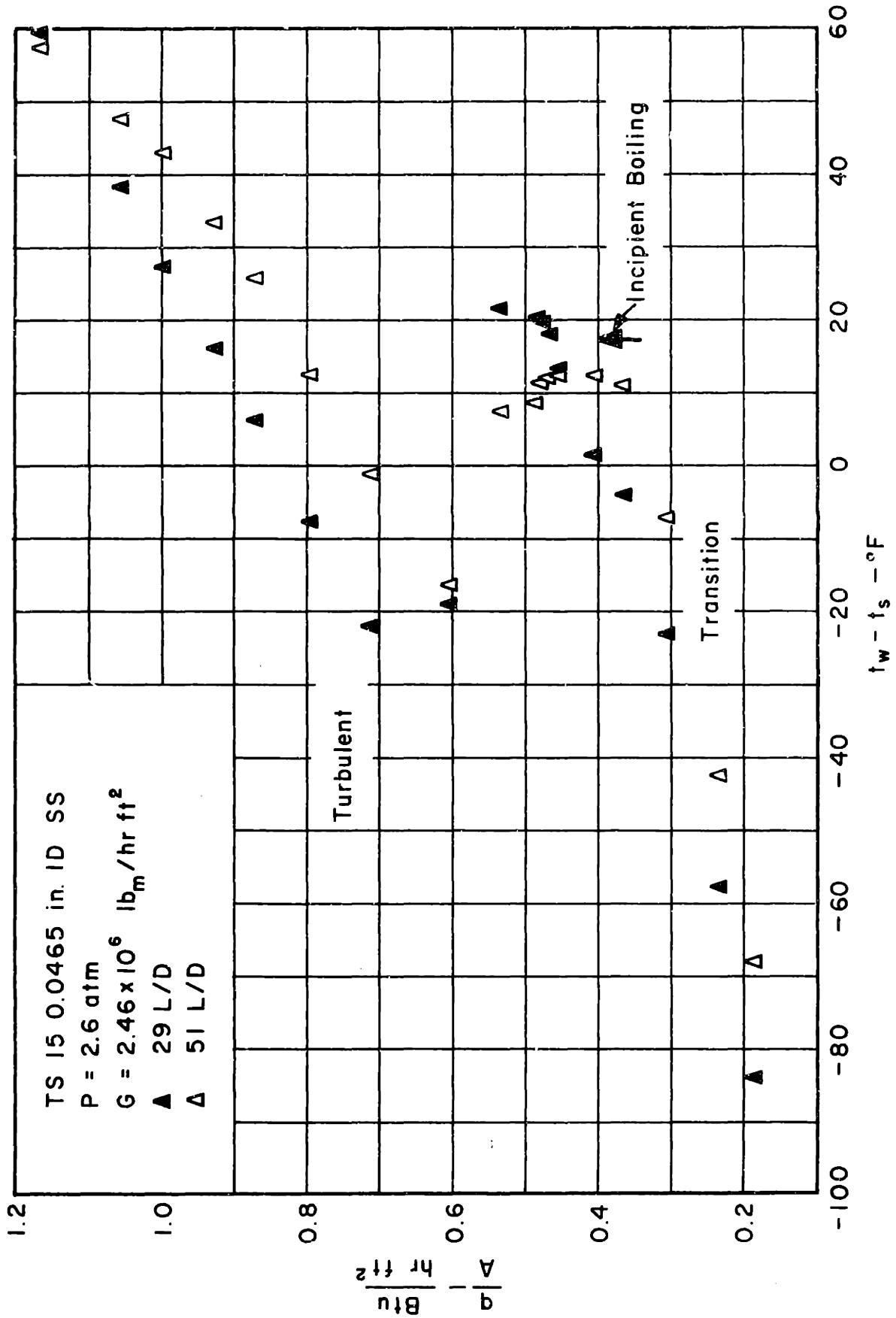
FIG. 24   TRIPPING OF BOUNDARY LAYER BY SURFACE BOILING
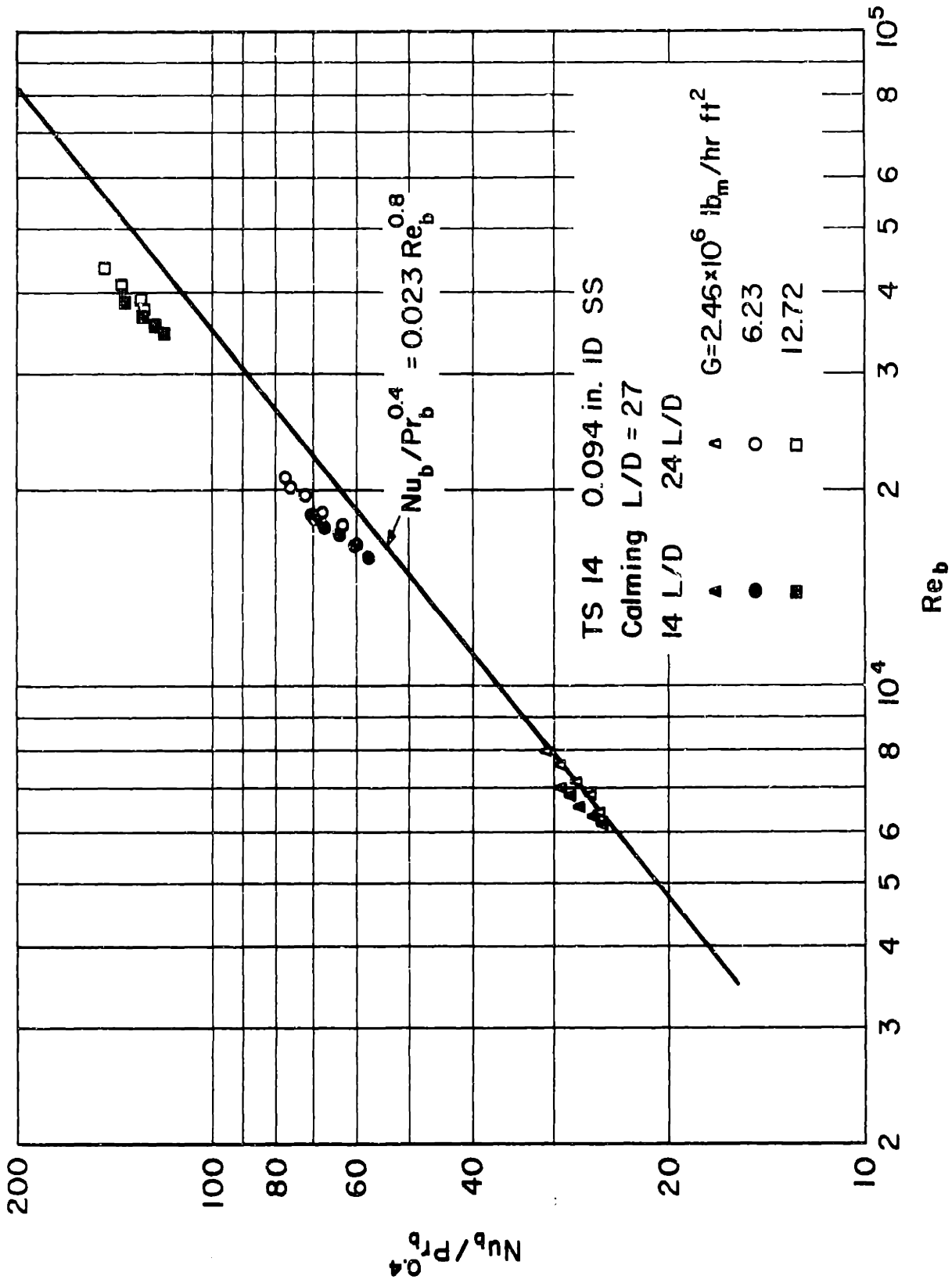
FIG. 25 CORRELATION OF FORCED-CONVECTION DATA FOR TEST SECTION 14
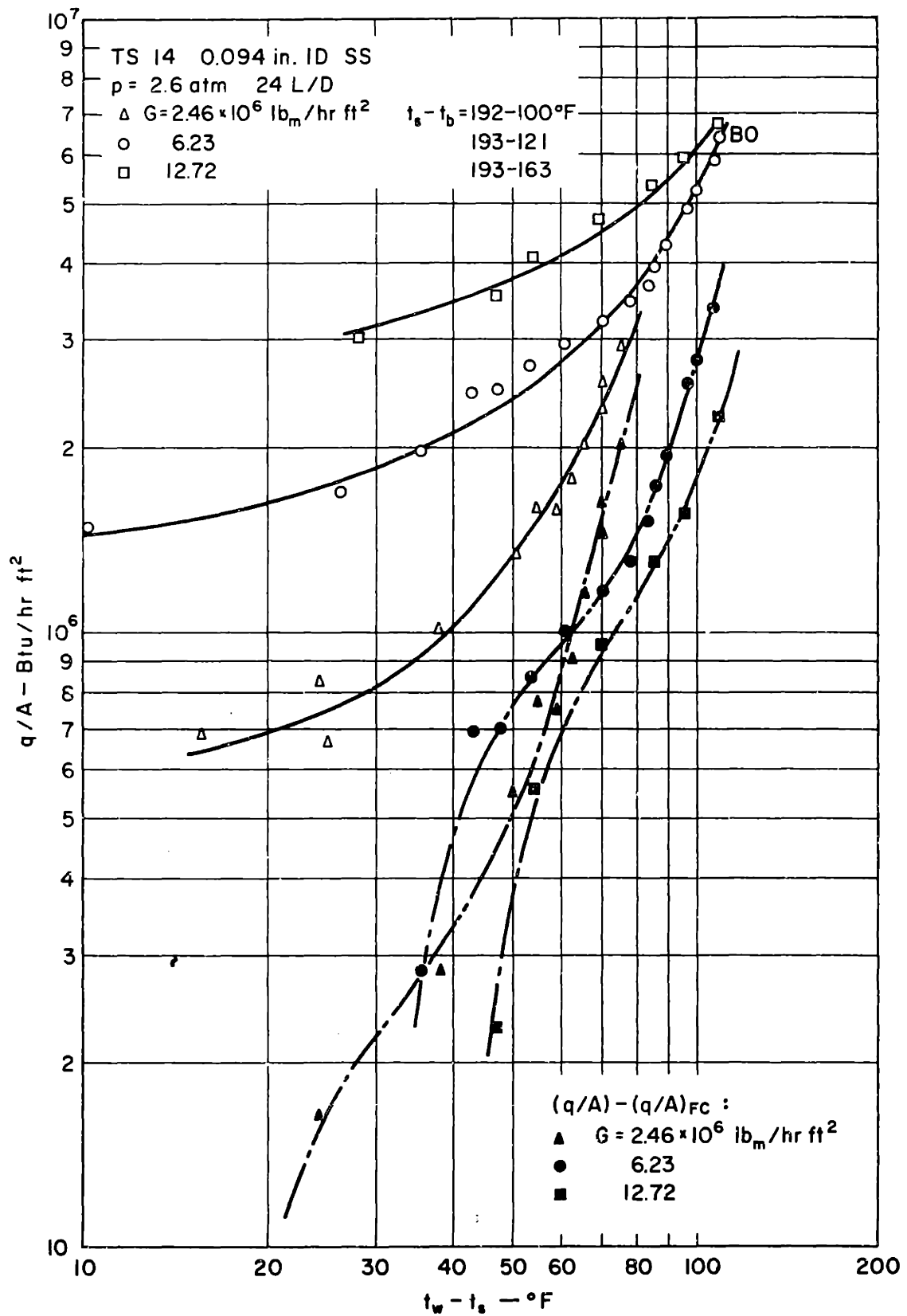
FIG. 26 FORCED-CONVECTION SURFACE-BOILING DATA INCLUDING
RESULTS OBTAINED BY SUBTRACTING FORCED-CONVECTION
q/A FROM TOTAL q/A
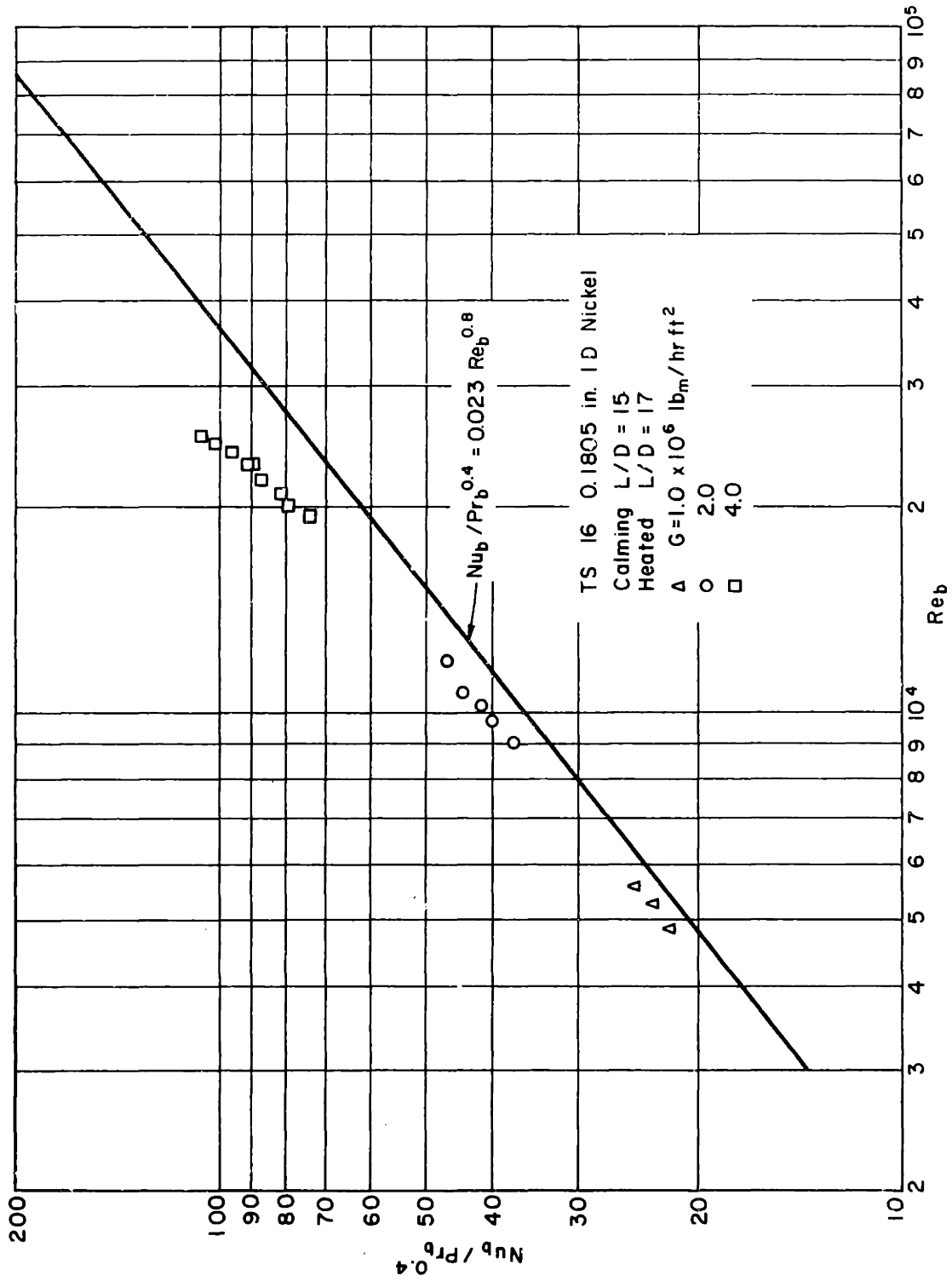
FIG.27 CORRELATION OF FORCED-CONVECTION DATA FOR TEST SECTION 16
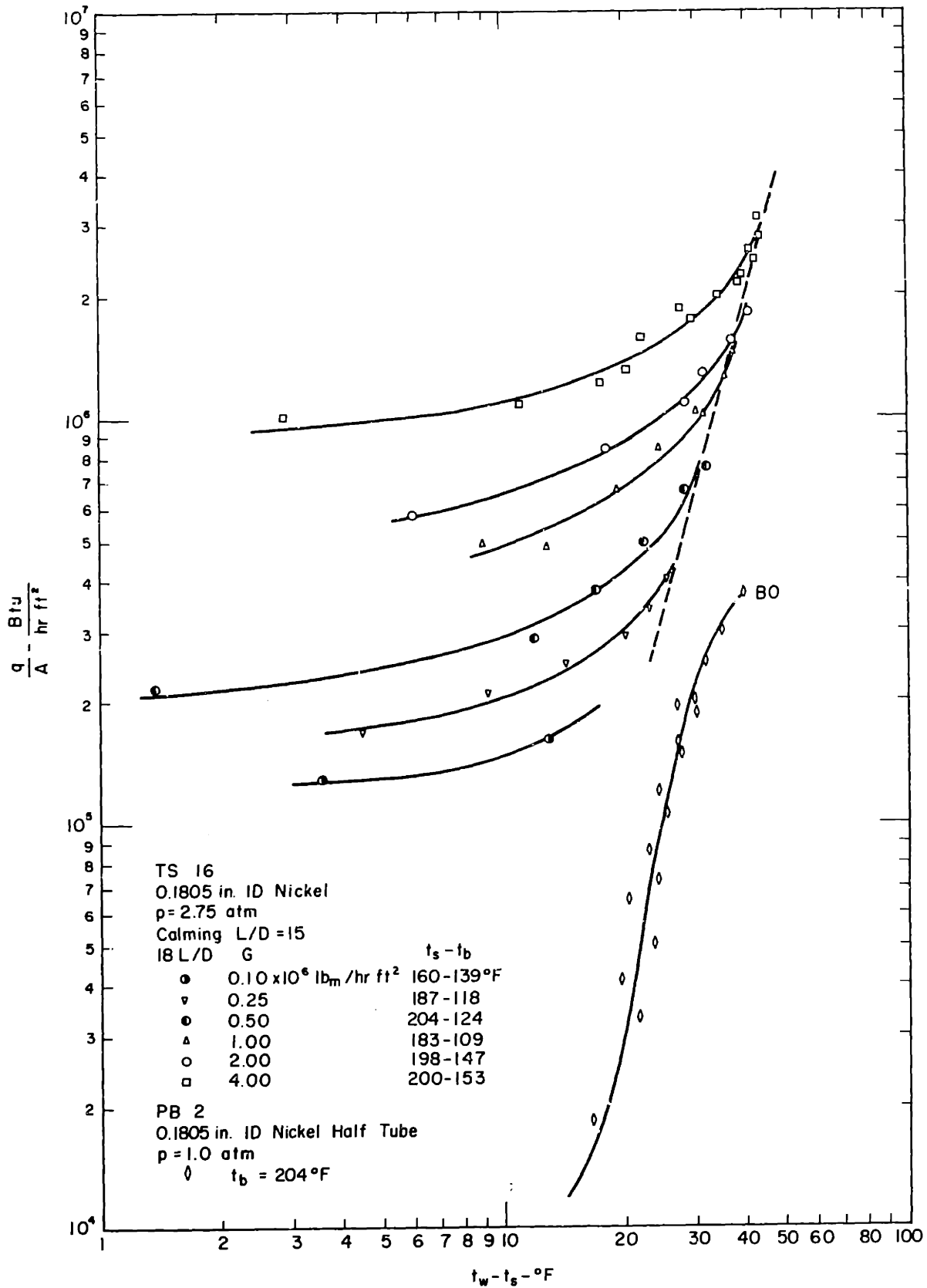
FIG. 28 COMPARISON OF FORCED - CONVECTION SURFACE BOILING AND POOL BOILING FOR NICKEL TUBE
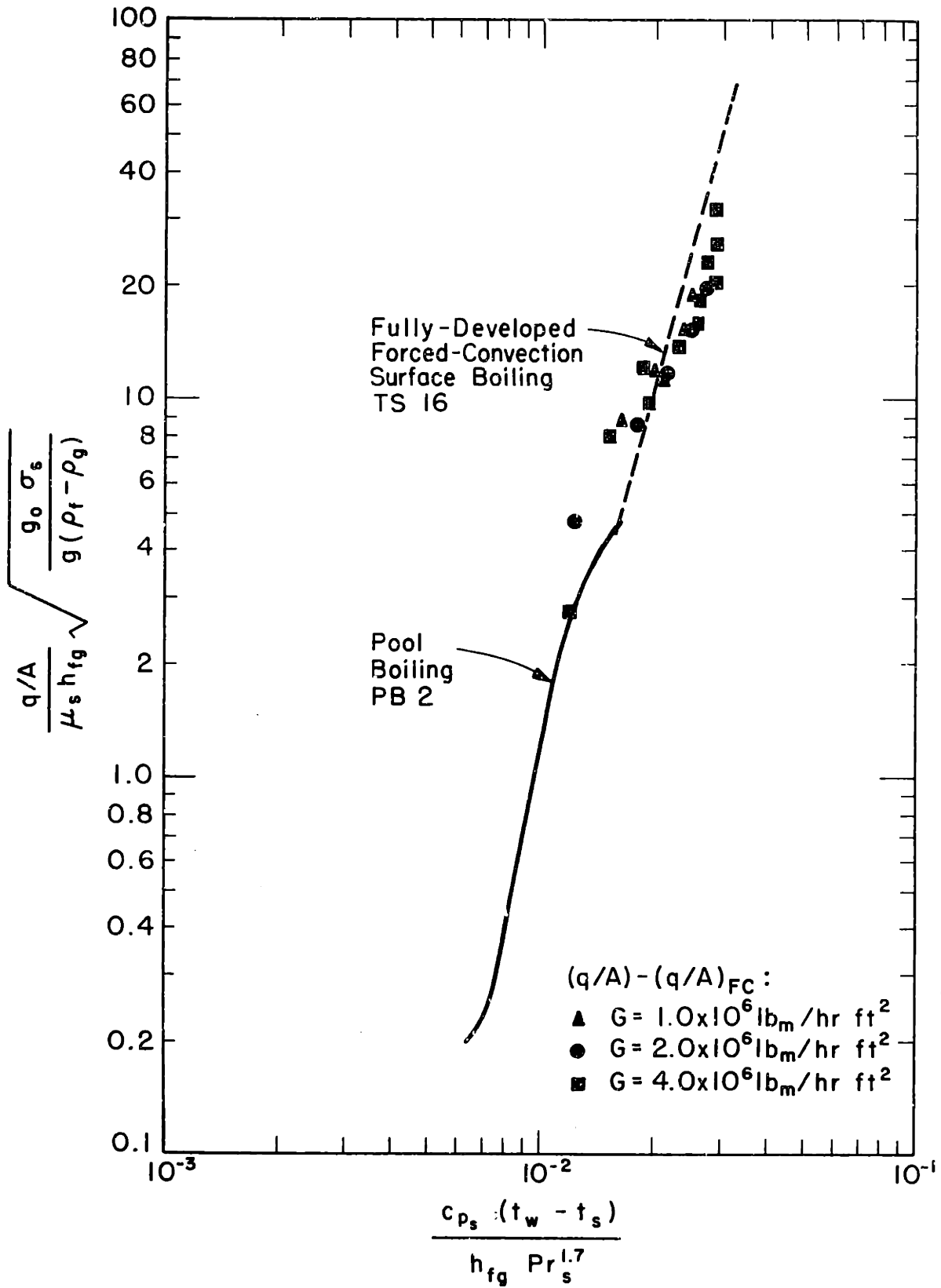
FIG. 29 CORRELATION OF PRESSURE EFFECT IN FORCED-CONVECTION SURFACE BOILING AND POOL BOILING
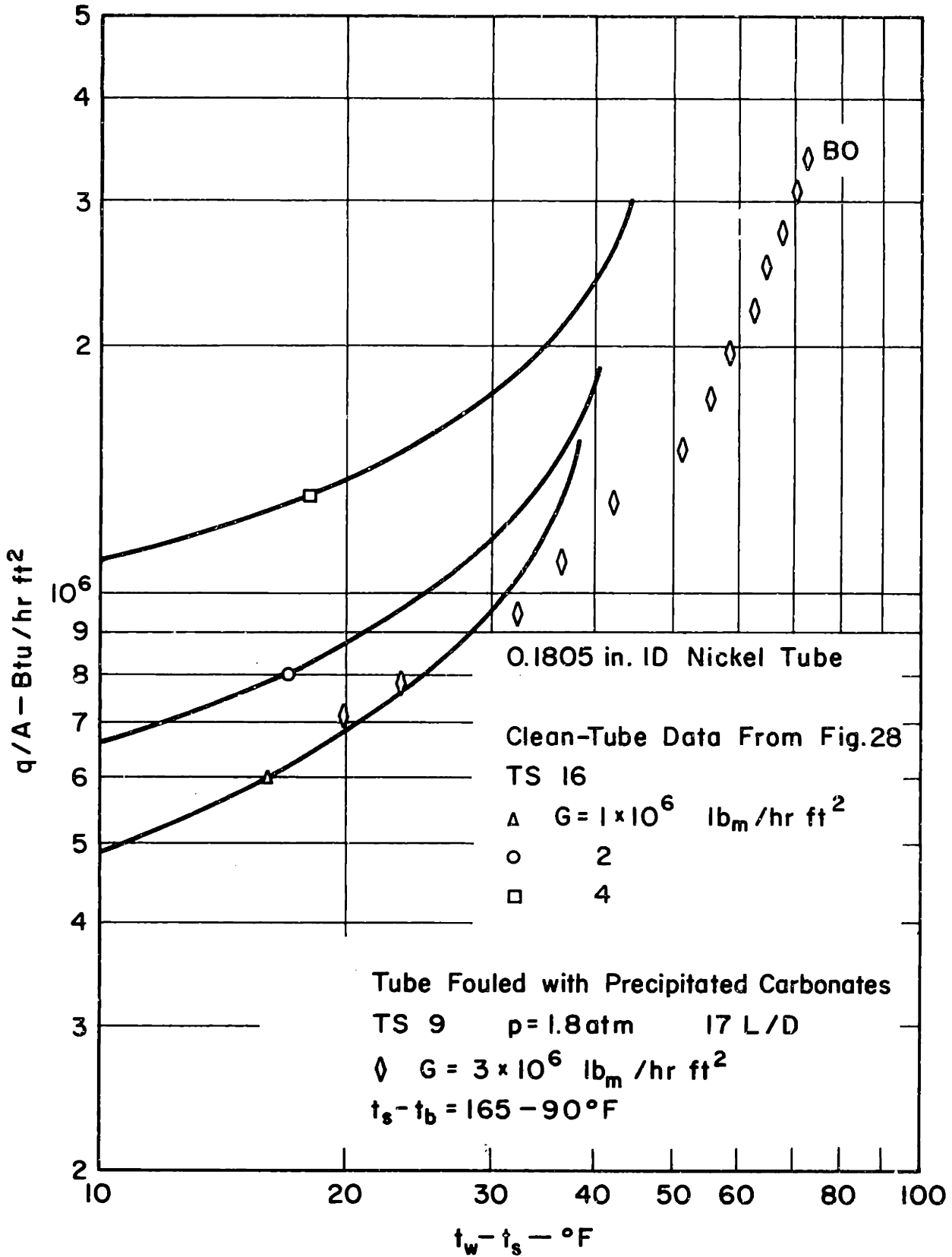
FIG. 30 COMPARISON OF CLEAN- AND FOULED-TUBE DATA
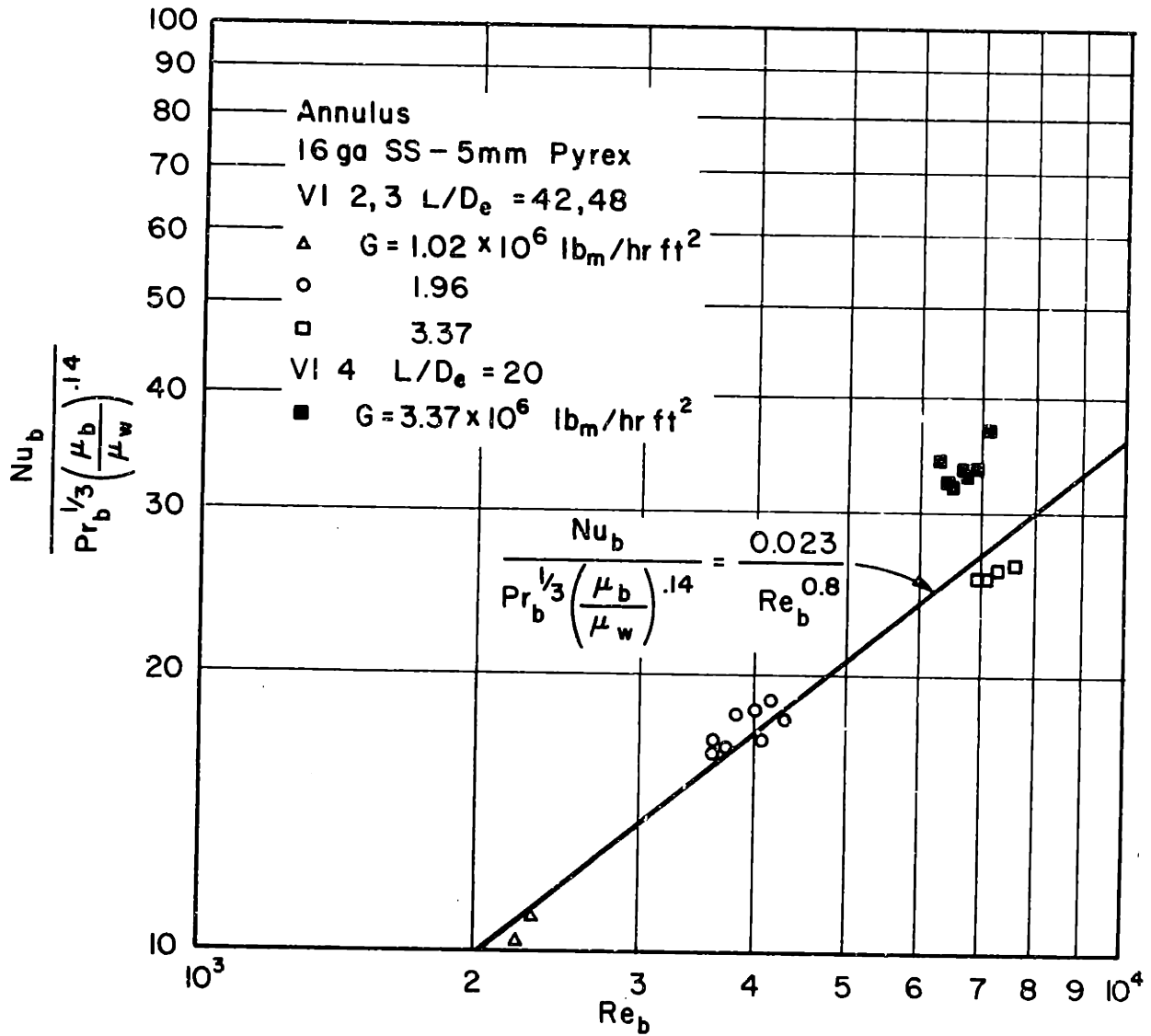
FIG. 31 CORRELATION OF ANNULAR FORCED-CONVECTION DATA
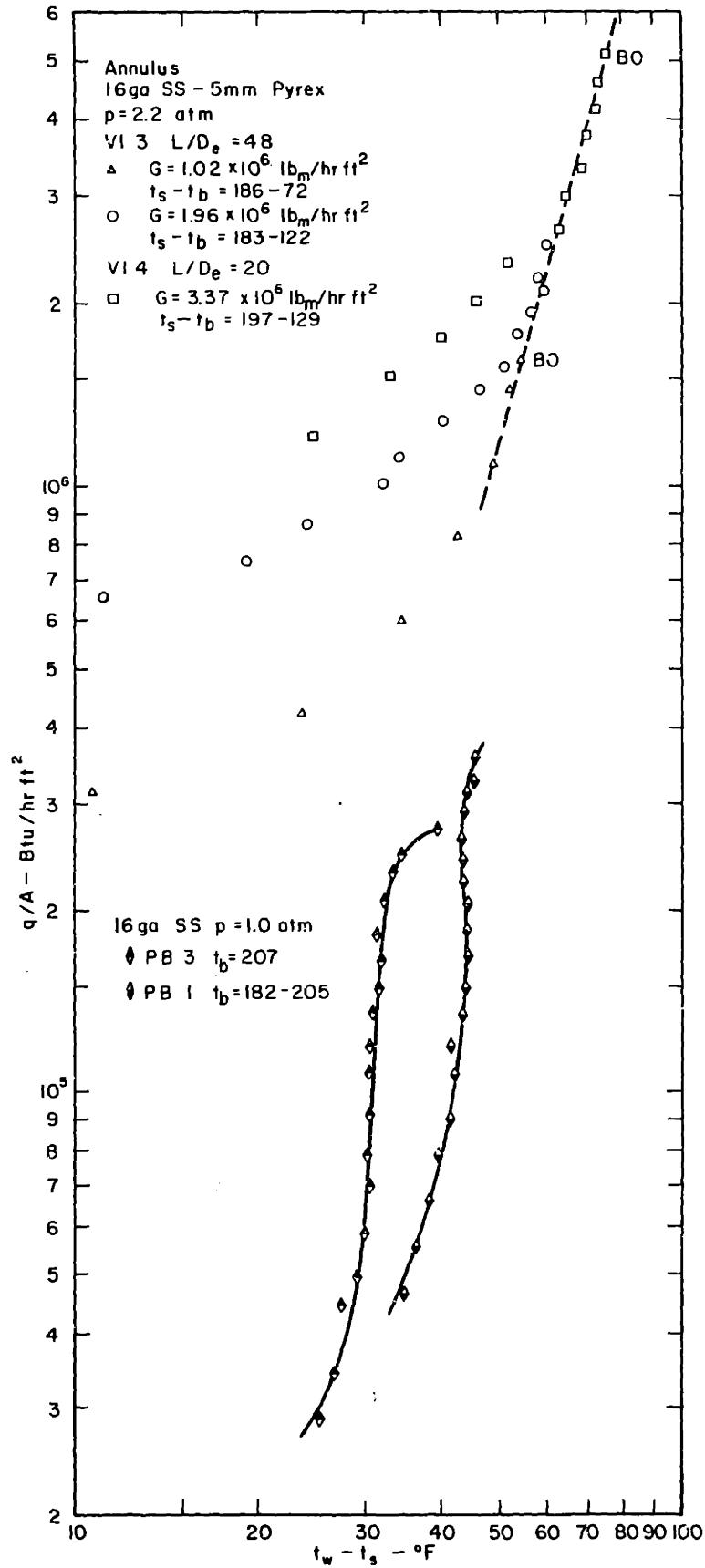
FIG. 32 FORCED - CONVECTION SURFACE - BOILING DATA AND
POOL - BOILING DATA FOR ANNULUS AND TUBE
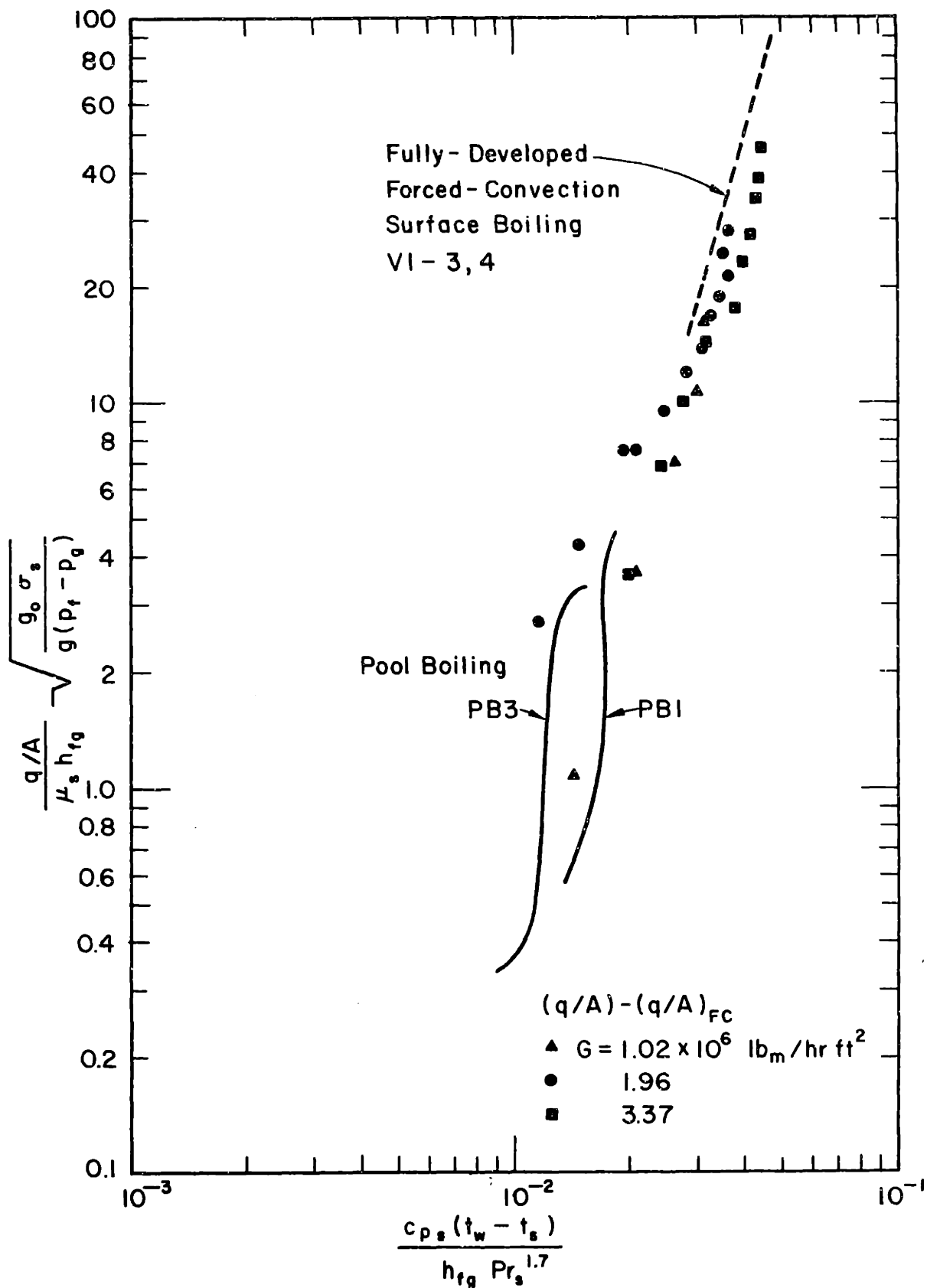
FIG. 33 CORRELATION OF PRESSURE EFFECT IN FORCED-CONVECTION SURFACE BOILING AND POOL BOILING
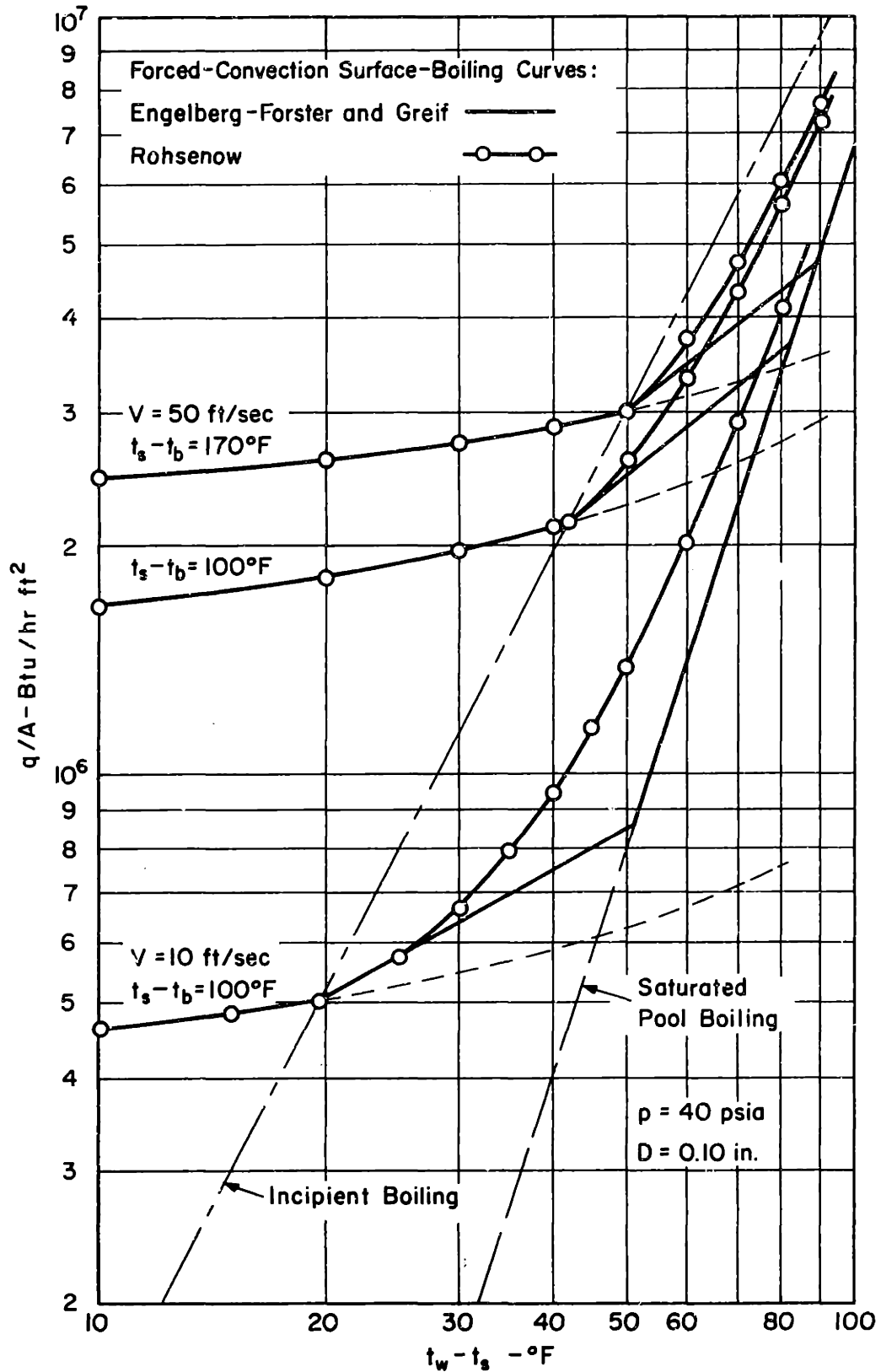
FIG. 34 CONSTRUCTION OF CURVES FOR FORCED-
CONVECTION SURFACE BOILING OF WATER
IN A TUBE
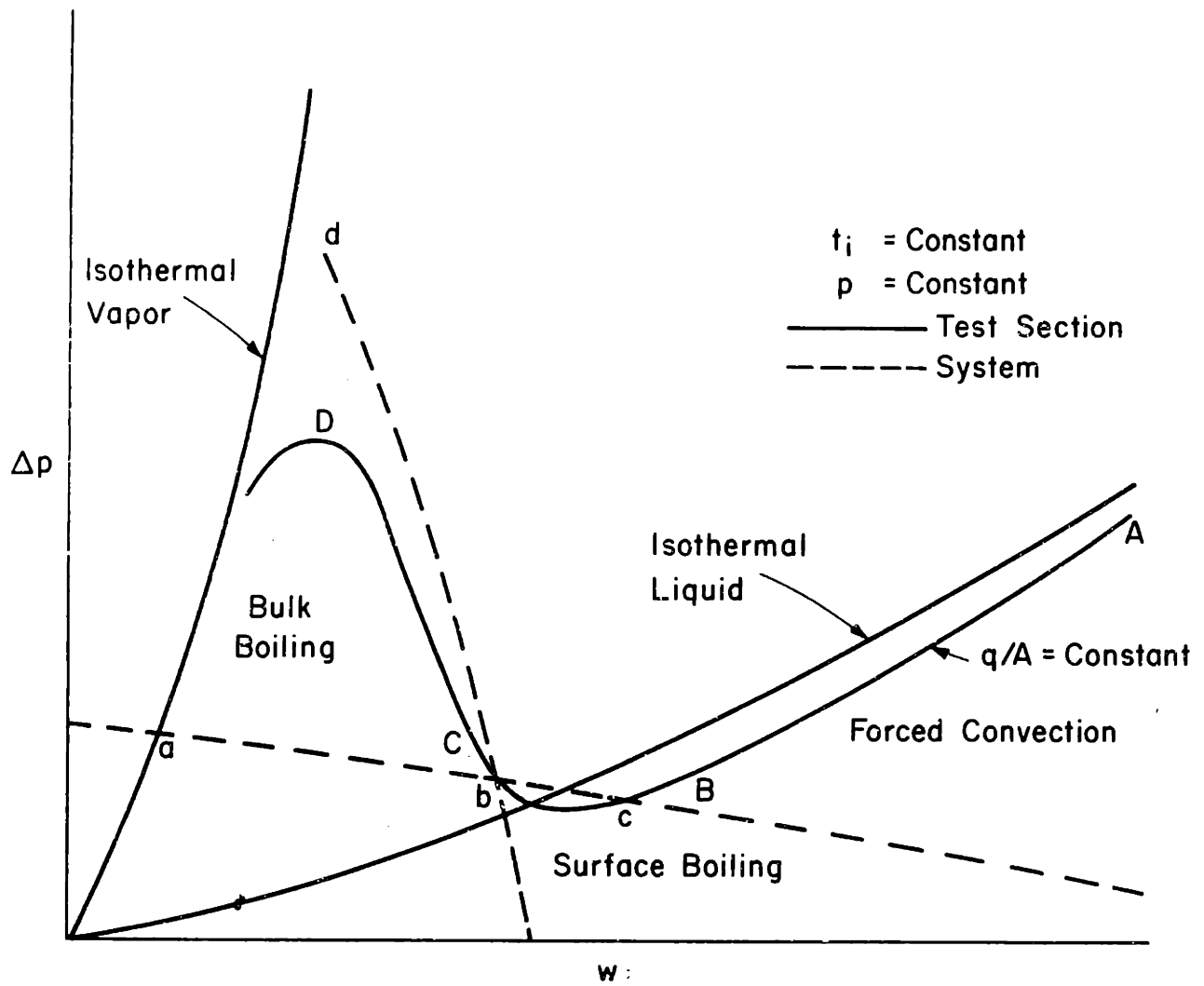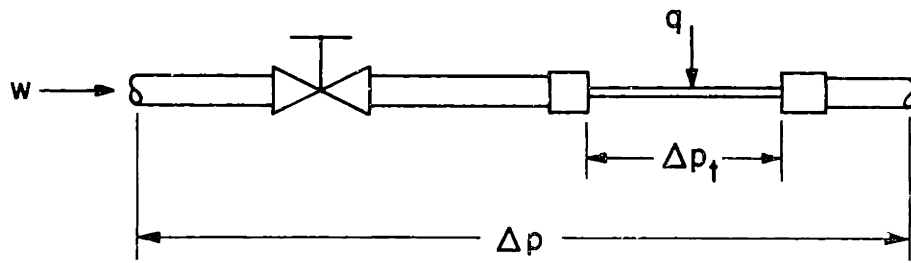
FIG. 35 INSTABILITY DUE TO FLOW EXCURSION

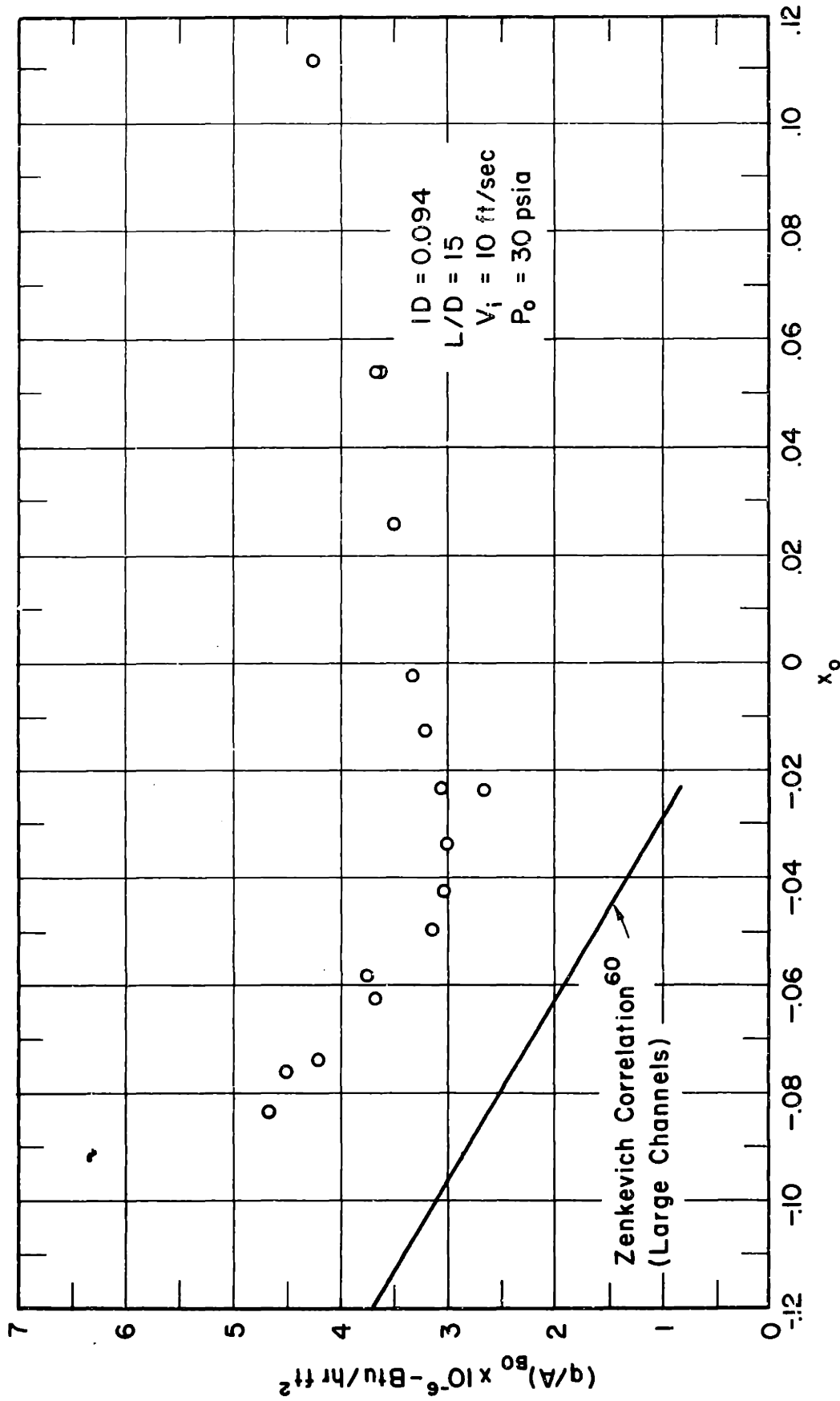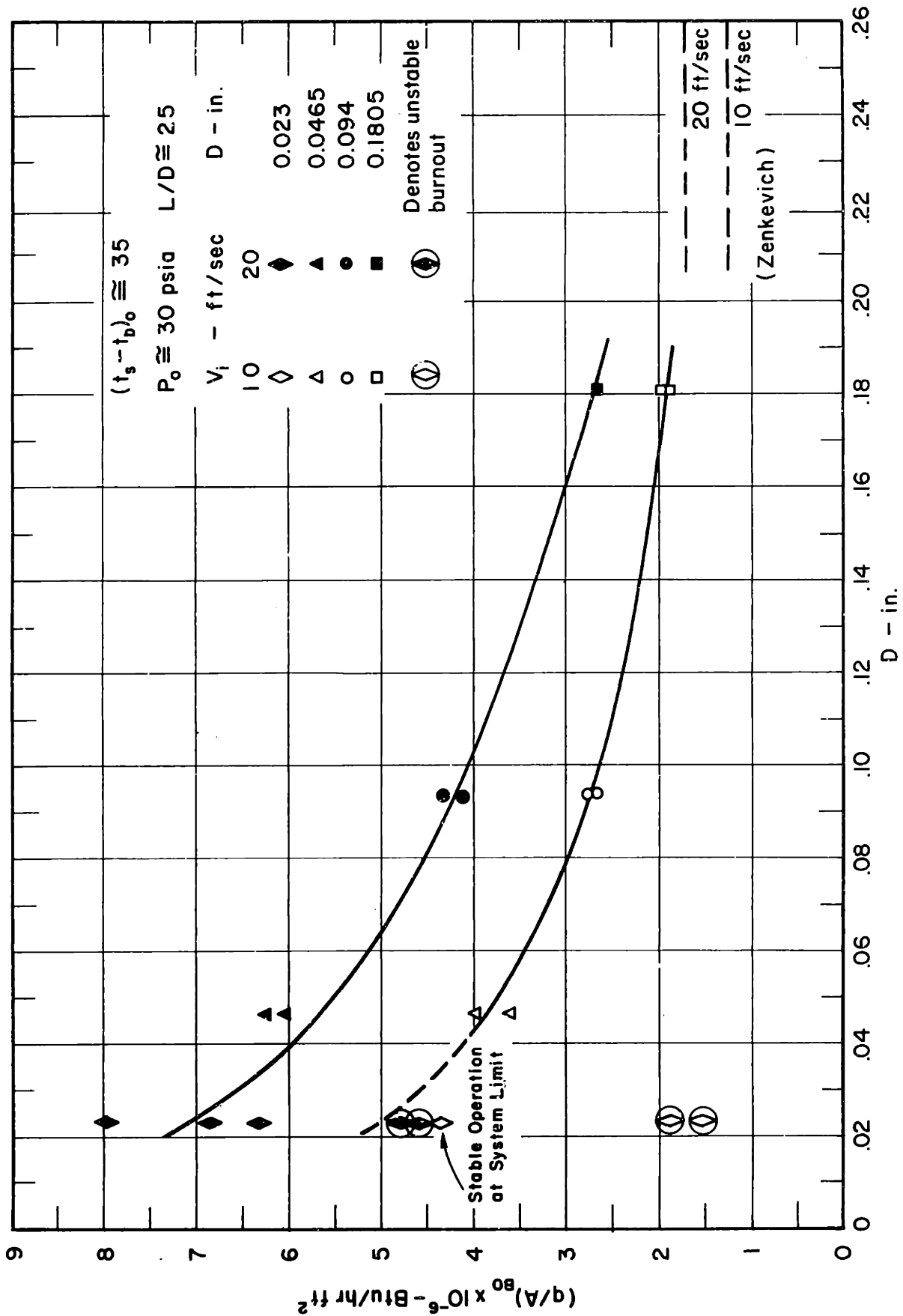FIG. 36 DEPENDENCE OF BURNOUT HEAT FLUX ON EXIT QUALITY FOR SMALL-DIAMETER TUBE

FIG.37 DEPENDENCE OF BURNOUT HEAT FLUX ON TUBE DIAMETER AND VELOCITY FOR SURFACE BOILING
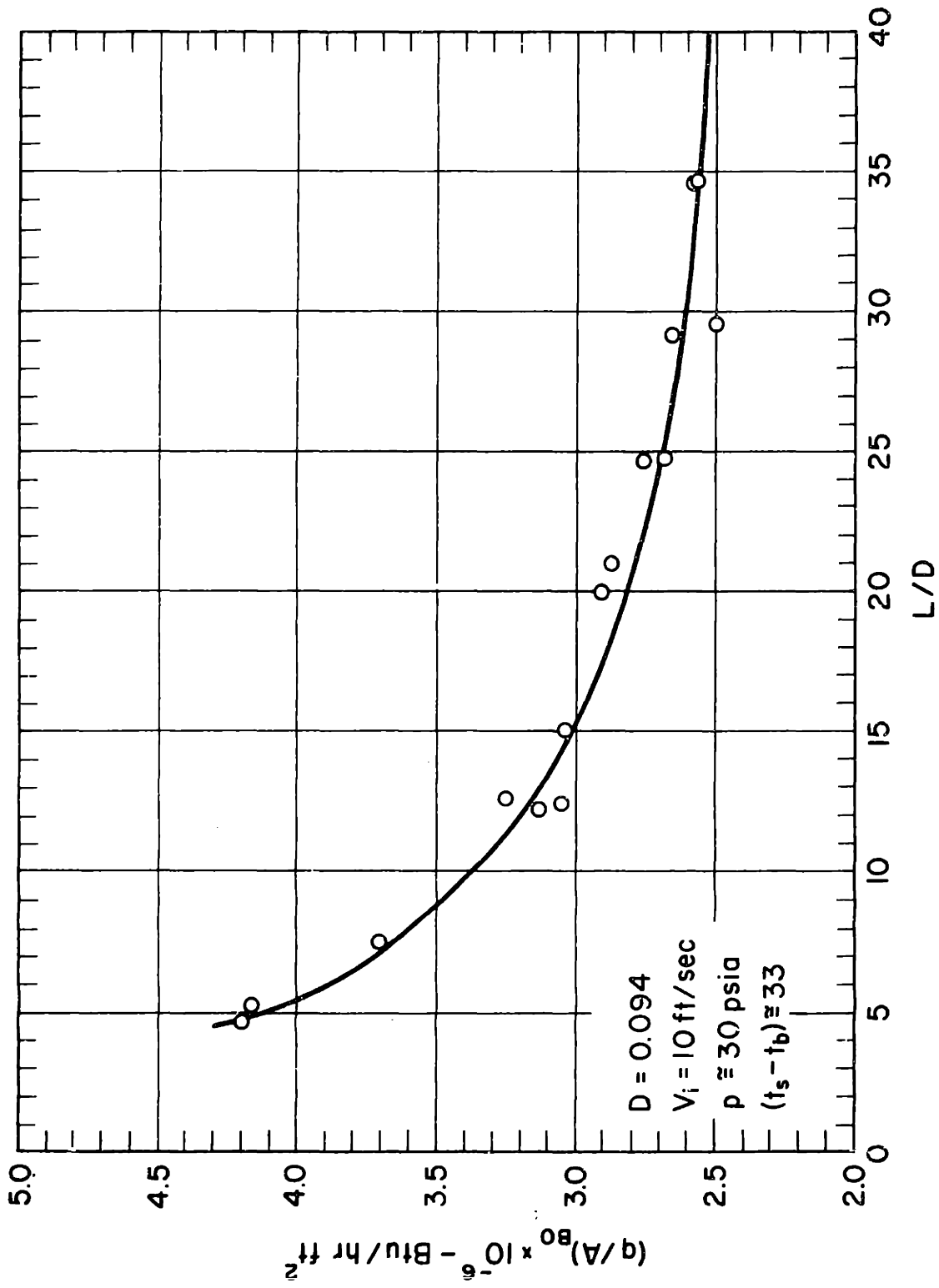
FIG. 38 DEPENDENCE OF BURNOUT HEAT FLUX ON LENGTH–
DIAMETER RATIO

## BIOGRAPHICAL NOTE

Arthur E. Bergles was born August 9, 1935, the son of Edward and Victoria Bergles of New York City. He attended primary and secondary schools in Rhinebeck, New York, and graduated from Rhinebeck Central School in June, 1953.

He entered the Massachusetts Institute of Technology as a freshman in September, 1953. He was a member of the Honors Group in the Department of Mechanical Engineering and received the Visking Fellowship for his year of graduate study. He was elected to Pi Tau Sigma, Tau Beta Pi, and Sigma Xi. He received his Bachelor and Master of Science Degrees in June, 1958. As a Fulbright grantee, he spent the following year doing research in heat transfer at the Technische Hochschule in Munich, Germany.

In September, 1959, he was appointed a Research Assistant in Mechanical Engineering at M.I.T., a position he has held since then with the exception of one summer as a D.S.R. Staff Member. He has worked on research projects in transient heat conduction, heat transfer between rotating cylinders, low-density wind-tunnel design, and boiling heat transfer.

He has held positions with United States Steel Corporation, Stone & Webster Engineering Corporation, Joseph Kaye & Company, and Dynatech Corporation. He has also done work for the Martin Company, Baltimore, and Digital Equipment Corporation. He will join the M.I.T. National Magnet Laboratory as a D.S.R. Research Staff Member in the near future.

His professional associations include Associate Membership in the American Society of Mechanical Engineers.

He married the former Priscilla L. Maule of Taunton in June, 1960.